Glucocorticoid Action in the Mediobasal Hypothalamus Regulates Glucose Production *In Vivo*

by

Emilie Beaulieu-Bayne

A thesis submitted in partial fulfillment of the requirements for the degree of

Master of Science

Department of Physiology
University of Alberta

ABSTRACT

Background: Diabetes is characterized by dysregulated glucose homeostasis that leads to hyperglycemia, due in part to increased hepatic glucose production (GP) and insulin resistance. Excessive levels and/or action of glucocorticoids (GCs) are associated with obesity, insulin resistance, and hyperglycemia. Whereas the peripheral effect of GCs to elevate glycemia is well known, less is known about the brain effect of GCs to modulate metabolism. The brain senses nutrients and hormones to regulate glucose homeostasis. This study aims to delineate a mechanism of GC action in the mediobasal hypothalamus (MBH) that modulates GP in normal and pre-obese rodents. I hypothesize that GC action in the brain alters glucose metabolism.

Methods: Male SD rats underwent stereotaxic MBH bilateral cannulation and intravenous (iv) and intraarterial catheterization to enable simultaneous direct infusions into the MBH, iv infusions, and blood sampling, respectively. Mildly hyperinsulinemic-euglycemic clamps with tracer dilution methodology combined with MBH GC infusion ± GC receptor (GR) inhibition enabled measurement of GP and utilization while assessing MBH GC interaction with its MBH receptors independent of changes in plasma insulin, glucagon, and glucose levels.

Results: In healthy regular-chow (RC) fed rats, MBH GC infusion potently stimulates GP and lowers the requirement for exogenous glucose infusion without altering glucose utilization. This effect is mediated via GRs since co-infusion of GR antagonist mifepristone (MIF), or a Hsp90 inhibitor, as well as chronic MBH GR or Hsp90 inhibition with MBH

GR shRNA or MBH Hsp90 shRNA negates the ability of MBH GCs to increase GP. MBH GCs similarly increased glucose excursions during iv glucose tolerance tests (ivGTT), which were reversed with concomitant MBH MIF infusion. Rats fed with high fat diet (HFD) for 3 days had altered glucose kinetics and increased basal plasma corticosterone, insulin, and blood glucose levels without changes in body weight. MBH MIF infusion or chronic MBH GR inhibition with MBH GR shRNA lowered GP compared to MBH vehicle and mismatch control HFD rats with MBH saline infusions, suggesting that blocking excessive MBH GC action in a model of pre-obesity with hypercorticosteronemia resulting from HFD feeding attenuates GP to improve glucose homeostasis.

Conclusion: This study provides novel evidence that MBH GC action modulates GP in healthy and pre-obese rats. Importantly, targeted inhibition of MBH GC action may help improve glucose regulation in obesity-related metabolic disease.

PREFACE

This thesis is an original work by Emilie Beaulieu-Bayne (EBB). The research project, of which this thesis is a part, received research ethics approval from the University of Alberta Research Ethics Board, Project Name “CNS regulation of metabolic homeostasis”, № 1604. This project was funded by the Natural Sciences Research Council of Canada (NSERC), Diabetes Canada Scholar Award and Alberta Diabetes Institute (ADI) Pilot Project grant. EBB was funded by the Canada Graduate Scholarships – Master’s Program (CGS-M) from the Canadian Institutes of Health Research (CIHR) during the execution of this project, as well as by the Faculty of Graduate Studies and Research (FGSR), the Graduate Students' Association (GSA), the ADI, and the Department of Physiology from the University of Alberta for conference travel funding.

ACKNOWLEDGEMENTS

I would firstly like to thank my supervisor, Dr. Jessica Yue, for the generous guidance and support provided to me throughout these two years of research. Thank you for offering me the opportunities to travel and deepen my knowledge in neurometabolic and diabetes research. Your passion for brain regulation of metabolism is contagious and you have taught me how to be a critical thinker in science, not only helping me develop in a lab setting but also on a personal level. I must thank our animal technician Bryan Lum, for performing all the MBH cannulation surgeries and vascular catherization surgeries (with the help of Dr. Yue), and Carrie-Lynn Soltys our molecular technician for helping with western blotting and for performing my qRT-PCR analysis. Your contributions to this project are not unrecognized. Thank you to all of the Yue lab members for offering endless laughs and off topic conversations. A special thank you to the past and present students of the lab who have directly contributed to this project, Miguel Cardoso, Shuling Yang, Hyejun Kim and Aleesha Amjad Hafeez. I would also like to thank my committee members Dr. Catherine Chan and Dr. Rene Jacobs for their contributions and time spent being part of this process. Thank you to my parents who have always encouraged me to peruse graduate studies and who have supported me in my move across the country on such a short notice, and for my family at lululemon for accepting receiving me with open arms in Edmonton and allowing me to endlessly crush goals. Lastly, I would like to thank Spencer Sharpe for his endless love and encouragements throughout this process, especially when lack of sleep got the best of me.

TABLE OF CONTENTS

LIST OF TABLES

LIST OF FIGURES

LIST OF ABBREVIATIONS

11DHC – 11-Dehydrocorticosterone

11β-HSD – 11β-Hydroxysteroid Dehydrogenases

ACTH – Adrenocorticotrophic Hormone

AgRP – Agouti-Related Peptide

ARC – Arcuate Nucleus

B_0 – Reference

$Ba(OH)_2$ – Barium Hydroxide

CNS – Central Nervous System

CORT – Corticosterone

CRH – Corticotropin-Releasing Hormone

CVD – Cardiovascular Disease

DVC – Dorsal Vagal Complex

FA – Fatty Acid

FFA – Free Fatty Acid

G6Pase – Glucose-6-Phosphatase

GC – Glucocorticoid

GIR – Glucose Infusion Rate

GLUT4 – Glucose Transporter

GP – Glucose Production

GR – Glucocorticoid Receptor

GU – Glucose Uptake

HFD – High-Fat Diet

HPA – Hypothalamic-Pituitary-Adrenal

Hsp – Heat-Shock Protein

HXK – Hexokinase

ICV – Intra-Cerebral Ventricle

iv – Intravenous

ivGTT – Intravenous Glucose Tolerance Test

LV – Lenti Virus

MBH – Medial Basal Hypothalamus

mGR – Membrane-Bound Glucocorticoid Receptor

MR – Mineralocorticoid Receptors

NPY – Neuropeptide Y

NSB – Non-Specific Binding

PC – Pyruvate Carboxylase

PDH – Pyruvate Dehydrogenase

PDK – Pyruvate Dehydrogenase Kinase

PDP – Pyruvate Dehydrogenase Phosphatase

PE-50 – Polyethylene Tubing

PEPCK – Phosphoenolpyruvate Carboxykinase

POMC – Pro-Opiomelanocortin

pPDH – Phosphorylated Pyruvate Dehydrogenase

PR – Progesterone Receptor

PVN – Paraventricular Nucleus

RC – Regular-Chow

RIA – Radioimmunoassay

SAT – Subcutaneous Adipose Tissue

SCN – Suprachiasmatic Nucleus

SD – Sprague Dawley

shRNA – Short Hairpin RNA

T2D – Type 2 Diabetes

TC – Total Counts

Tub – Tubulin

VAT – Visceral Adipose Tissue

VMH – Ventromedial Hypothalamus

WAT – White Adipose Tissue

$ZnSO_4$ – Zinc Sulfate

Chapter 1: BACKGROUND

1.1 – Diabetes and Obesity

1.1.1 – Diabetes and Obesity Overview

The prevalence of diabetes and obesity is growing and has become a worldwide epidemic. Type 2 diabetes (T2D) is classified as a chronic disease in which the body is unable to adequately utilize the insulin it makes or is unable to produce enough insulin in more advanced stages of the disease[1]. Globally, 422 million individuals were diabetic in 2014 compared to 108 million in 1980[2]. Historically, T2D has been referred to adult-onset diabetes but its diagnosis in children has also been on the rise[2]. Earlier onset of T2D increases the chance of experiencing severe and chronic complications later in adulthood due to the longer duration of exposure to the disease[3]. The increased prevalence of T2D in both adults and children is highly correlated with the increasing incidence of obesity across a wide span of age groups.

Adults who are obese have abnormal fat accumulation and have a Body Mass Index (BMI) of 30kg/m^2 or geater[4]. Last year (2018) over 7.3 million Canadian adults were classified as obese and its occurrence has more than doubled worldwide since 1980 highly due to the increased consumption of energy-dense foods and sedentary lifestyle[5–7]. In the U.S., food processing had become the largest industry by 1920, and carbonated sweetened drinks, fast food and frozen dinners rich in saturated fats were in highly popular by the 1950s[8]. In addition, time spent watching television significantly increased since the 1970s, and physical education in schools has been declining in developed countries[8]. Given this lifestyle shift in the last few decades, the current worldwide epidemic of obesity should come as no surprise.

Both obese and diabetic individuals are at high risk for developing life-ending comorbidities such as cardiovascular disease (CVD). In addition, T2D increases the risk for developing foot ulcers and infection as a consequence from reduced blood flow and neuropathy, blindness subsequent to retinopathy, and kidney failure[2,7,9]. T2D and obesity impose a large economic burden on the global health-care system, but they are often preventable conditions through lifestyle modifications[10]. Although T2D and obesity are tightly related, they are not exclusive to one another and can occur independently.

1.1.2 – Metabolic Characteristics of Diabetes and Obesity

T2D is characterized by a dysregulation in glucose homeostasis that leads to hyperglycemia, due in part to increased hepatic glucose production (GP), triglyceride-rich very low-density lipoprotein secretion and insulin resistance[11,12]. Insulin resistance often develops following chronic states of energy surplus, and the action of insulin on nutrient flux in target tissues consequently becomes impaired. In addition to being a contributing cause for insulin resistance, energy surplus can stimulate accumulation of excess adipose tissue and lead to the onset of obesity, highlighting the relationship between BMI, T2D and insulin resistance.

The development of insulin resistance in obesity can be attributed in part to chronic low-grade inflammation in adipose tissue induced by metabolic overload [13]. Adipocyte hypertrophy provokes a local inflammatory response and pro-inflammatory cytokines such as IL-6 and TNFα are subsequently secreted from adipose tissue and released into circulation causing systemic inflammation[13,14]. Inflammation can alter insulin signalling in adipocytes through more than one mechanism. It can inhibit the insulin receptor and the

insulin signalling pathway, inhibit PPARγ function which plays a role in driving lipid synthesis and storage into cells, as well as increase plasma free fatty acid (FFA) concentration by increasing the rate of lipolysis and decreasing triglyceride synthesis[14]. Individuals that are abdominally obese are more susceptible to insulin resistance as visceral adipose tissue is highly metabolically active. In fact, visceral fat is more susceptible to lipolysis[15] and secretes greater amounts of pro-inflammatory cytokines than subcutaneous adipose tissue[16,17].

In states of insulin resistance, glucose uptake (GU) in muscle as well as glucose and fatty acid uptake in adipose tissue is reduced. Whereas skeletal muscle is the main tissue responsible for insulin-mediated glucose clearance from the circulation in the post-prandial state[18], the liver is the key organ responsible for releasing glucose into the circulation[19]. In addition, insulin fails to reduce hepatic gluconeogenesis and glycogenolysis[20]. In an attempt to maintain homeostasis and decrease plasma glucose levels, insulin secretion is initially upregulated. Over time, pancreatic β-cell exhaustion occurs and β-cell function becomes impaired and fails to secrete sufficient insulin in response to a rise in glucose levels[21].

Although T2D and obesity are both associated with insulin resistance, not all obese individuals develop dysregulated glucose homeostasis. In contrast to individuals with T2D, insulin secretion from β-cells in obese insulin resistant individuals is usually adequate in order to fully compensate for reduced insulin sensitivity and plasma glucose levels remain normal[22,23].

1.2 – Glucocorticoids

Excessive plasma concentrations and/or action of glucocorticoids (GC) are associated with T2D, obesity, insulin resistance, and hyperglycemia[24,25]. GCs are key regulators in energy flux and their metabolic actions will later be discussed. In addition to GC production and turnover being increased in obesity[26], GC activity is locally increased in visceral adiposity by local enzymatic conversion and further enhances the risk for metabolic disorders[27]. In fact, GC sensitivity has also been shown to fluctuate in a wide span of disease[28].

1.2.1 – Glucocorticoid Synthesis and Intracellular Action

GCs, which include cortisol in humans and corticosterone (CORT) in rodents, are steroid hormones released by the adrenal cortex upon stressor-induced activation of the hypothalamic-pituitary-adrenal (HPA) axis[29,30]. Steroid hormones are synthesized from cholesterol in process known as steroidogenesis, an enzymatic process that occurs in mitochondria[31]. In the zona fasciculata of the adrenal gland, cholesterol is transported from the outer to the inner mitochondrial membrane via the transport protein StAR (steroidogenic acute regulatory protein). Cholesterol is then converted to the common steroid precursor pregnenolone by the enzyme P450scc (side chain cleavage enzyme), which constitutes of the rate-limiting step in steroid hormone biosynthesis[32,33]. A variety of mitochondrial cytochrome P450 enzymes then catalyze the next series of chemical reactions involved in the synthesis of CORT[34,35].

After their secretion from the adrenal cortex, circulating GCs can enter cells through passive diffusion, and their bioavailability not only depends on circulating levels in the

blood stream but also on cellular-specific level and/or activity of 11β-hydroxysteroid dehydrogenases (11β-HSDs), enzymes located in the endoplasmic reticulum[36]. 11β-HSD2 is involved in oxidizing CORT, but not most synthetic GCs, into its inactive form 11-dehydrocorticosterone (11DHC), whereas 11β-HSD1 has the reverse effect and allows for 11DHC to be converted to active CORT[37,38]. 11β-HSD1 is principally expressed in the liver, adipose tissue, kidneys and brain, whereas 11β-HSD2 is mainly found in the kidneys and salivary glands[39]. Inflammatory signals such as IL-1β and TNFα can alter tissue sensitivity to GCs through an upregulation in the expression of 11β-HSD1[36,40].

GC receptors (GR) are found in the majority of cells of the body and are involved in a wide span of physiological processes[37]. In the hypothalamus, GRs are highly expressed in both the paraventricular nucleus (PVN) and the arcuate nucleus (ARC) of the hypothalamus[41–45]. In the absence of the steroid hormone, GRs are found principally in the cell cytoplasm as part of a large multi-protein complex[46,47]. This complex includes chaperone proteins such as heat-shock protein (Hsp) 90 and Hsp70, as well as a multitude of other proteins, which help maintain the receptor in a transcriptionally inactive conformation while favoring high affinity ligand binding[37]. Hsp70 is thought to have an essential role of holding the GR inactive through partial unfolding, whereas Hsp90 reverses this process. In order for ligand binding to occur and for the GR to become active, Hsp90 is required and allows in an ATP-dependent manner for the activation of various other client proteins involved in the translation of the GR inside the nucleus and subsequent gene transcription and *de novo* protein synthesis[48,49]. These nuclear receptors belong to the family of ligand-dependent transcription factors[50].

1.2.2 – Glucocorticoid Regulation: The Hypothalamic-Pituitary-Adrenal Axis

The HPA stress response is a neuronally driven adaptation response that affects numerous organ systems. It helps mobilize energy stores to ensure that the body has a sufficient energy supply if faced with a physical demand[51]. When the body perceives a stressor (psychological or physical), hypothalamic PVN neurons release corticotropin-releasing hormone (CRH), which then stimulate the release of adrenocorticotrophic hormone (ACTH) from the anterior pituitary. ACTH then acts on its receptors in the adrenal cortex and stimulates the synthesis and release of GCs into the systemic circulation[52]. Typically, negative feedback terminates the HPA stress response where GCs act on GRs at the level of the PVN of the hypothalamus and anterior pituitary to inhibit further HPA activity (figure 1.2.1)[29,53], but disruption in metabolic homeostasis may lead to a hyperactivation of the HPA axis[54,55]. HPA axis hyperactivity occurs in both diabetes and obesity[24,56]. It has been proposed that hyperactivity is part of a vicious cycle where excess energy intake, hyperglycemia and body weight gain act as chronic stressors and further increases GC secretion through HPA hyperactivity, which in turn also stimulates hunger to increase energy intake[57].

The HPA axis is not only regulated by the stimulatory input of stress, but also by rhythmic inputs from the suprachiasmatic nucleus (SCN) of the hypothalamus, the hippocampus and diet composition[58–61]. The SCN is strategically located above the optic chiasm and receives afferent light/dark inputs from the eyes. This allows the SCN to act as a master circadian pacemaker in mammals and coordinate circadian rhythms in other tissues and brain areas[62]. In humans, light activates the central clock and inputs are sent from the SCN to neurons of the PVN, allowing for diurnal GC secretion patterns where GC

levels are at peak in the morning and at nadir at night[58,63,64]. Mineralocorticoid receptors (MR) in the hippocampus play an important role in regulating GC-mediated feedback control of the HPA axis. In the hippocampus, MRs bind with GCs with a greater affinity than GRs and are saturated even when basal GC levels are low at trough of the circadian rhythm[59]. This allows for tonic inhibition of the HPA axis through inhibitory projections mediated by GABAergic neurons to the PVN[59,65]. In addition to regulating the secretion of GCs and other hormones, it has been shown that metabolism and energy balance in peripheral tissues can also be regulated by the circadian clock[66]. In fact, studies have shown that high-fat diet (HFD) feeding disrupts clock gene expression in various tissues such as the hypothalamus, liver and adipose tissue, and affects glucose homeostasis by altering circadian variation in glucose tolerance and insulin sensitivity[67]. Moreover, long term HFD feeding is associated with HPA hyperactivity and increased basal plasma GC levels[60,61]. In addition, disruption of the circadian rhythm through shift work has been strongly associated with obesity and diabetes[68]. Given the strong relationship between dysregulated circadian rhythmicity and metabolic disturbances, GC rhythmicity plays without a doubt an important role in regulating glucose homeostasis[69].

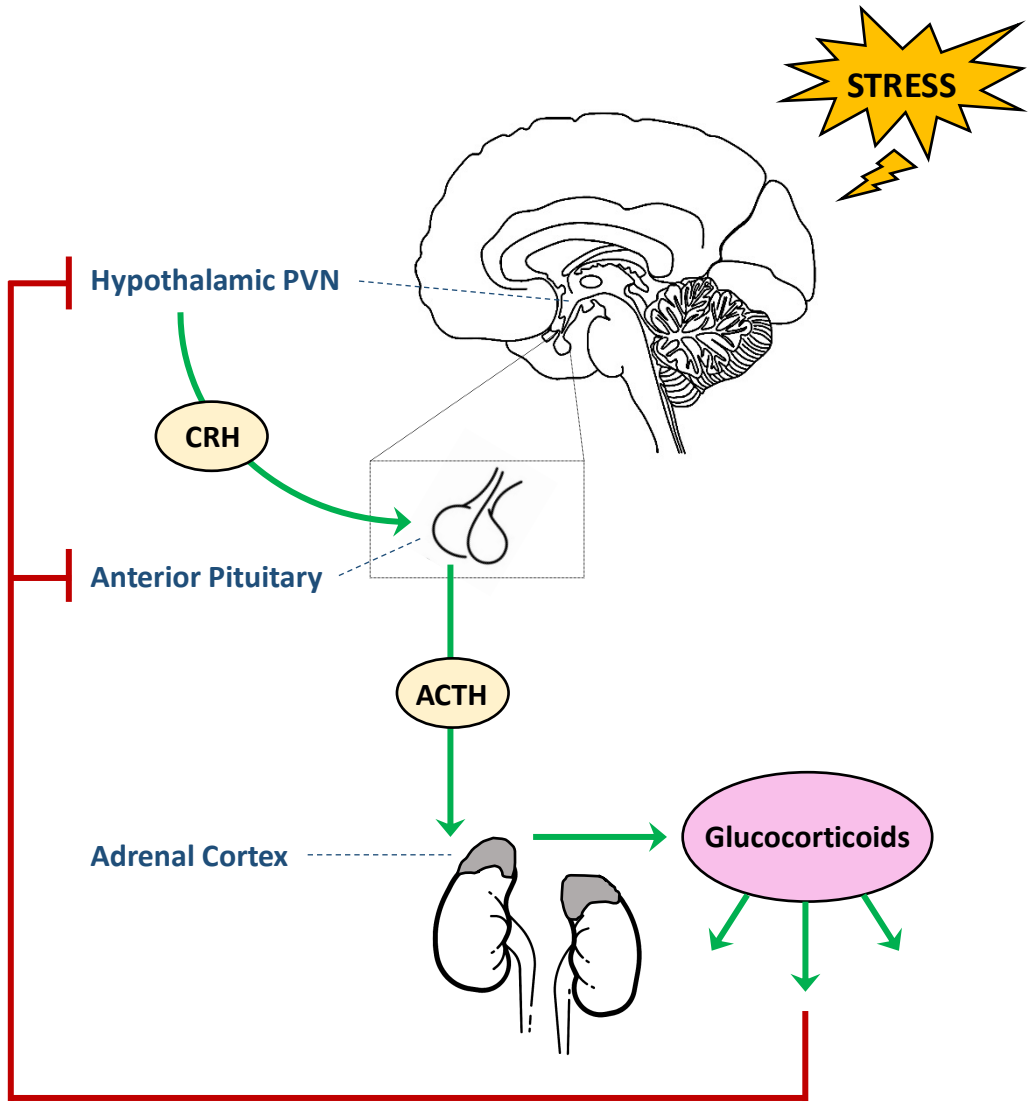

Figure 1.2.1 – Diagram of the HPA axis. Upon the presence of a stressor, CRH is released from the PVN of the hypothalamus, which stimulates the release of ACTH from the anterior pituitary, which then stimulates the release of GCs from the adrenal cortex. GCs act on GRs at the level of the PVN and anterior pituitary to inhibit further HPA activity. ACTH: adrenocorticotrophic hormone; CRH: corticotropin-releasing hormone; PVN: paraventricular nucleus.

1.2.3 – Peripheral Actions of Glucocorticoids: Non-Metabolic Actions

GCs are involved in many physiological processes in both health and disease. GCs are involved in the regulation of immune function, cardiovascular system, central nervous system (CNS), skeletal growth, reproductive system, cell proliferation and more[70]. GCs have powerful anti-inflammatory and immunosuppressive properties and they are widely used in clinical settings to help treat inflammatory and autoimmune diseases[70].

GCs affect most immune cells and help to prevent hyperactivation of the immune system and combat systemic infections. GC action on classical GRs can modulate the activation of signalling pathways such as PI3K, JNK and T cell receptor signalling complex and subsequently modulate pro-inflammatory gene expression[71]. GR activation can downregulate the activity of numerous DNA-bound transcription factors such as for example NF-κB, STAT3 and AP-1, and successively downregulate pro-inflammatory cytokine genes via transrepression such as IL-1β, IL-2, IL-4, IL-5, IL-6, IL-8, IL-12, IL-18 and TNFα[72]. In addition to modulating pro-inflammatory cytokine release, GCs can upregulate the release of anti-inflammatory cytokine IL-10, enhance M2-like macrophage phenotype (anti-inflammatory), consequently promoting the removal of apoptotic cells and enhancing tissue healing[73]. Given the anti-inflammatory properties of GC action, GC therapy is widely used for the treatment of rheumatoid arthritis, asthma, COPD, psoriasis and eczema[49].

GCs also play a vital role in maintaining proper cardiac function. In cardiac cells, GCs exert both antiapoptotic and anti-inflammatory actions[74]. GCs have also been shown to regulate cardiomyocyte size[75] as well as play a role in maintaining blood pressure

homeostasis by inhibiting the secretion of vasodilators[49]. Although GCs are cardioprotective, excessive levels resulting from either upregulated endogenous production or exogenous administration is correlated with a greater risk of developing CVD[76]. Chronic GC therapy has also been associated with bone mass regression. GC action on bone supresses osteoblast formation, as well as enhances osteoblast apoptosis. Consequently, the risk for GC induced osteoporosis and bone fractures is elevated in individuals undergoing chronic GC therapy[77].

In addition to regulating the HPA axis, disruption in GC homeostasis has been widely associated with CNS related disorders. For example, elevated GC levels and aberrant GR signalling has been linked with schizophrenia, substance abuse, post-traumatic stress disorder and mood disorders[49,78,79]. In addition, GR overexpression in specific brain regions like the forebrain and amygdala has been linked to anxiety behaviours[80,81]. Although the use of GCs is highly effective and beneficial for the treatment of inflammatory and autoimmune disorders, long-term GC exposure is clearly associated with undesirable outcomes and the adverse effects on health may outweigh the benefits. These pleiotropic effects explain why obesity-related insulin resistance following low-grade inflammation in adipose tissue cannot be treated with GC therapy. Taken together, the development of GC-based therapeutic strategies that target distinct physiological processes may reduce the undesired off-target metabolic effects[82].

1.2.4 – Peripheral Actions of Glucocorticoids: Metabolic Actions

As aforementioned, GCs are key regulators in energy flux and help mobilize energy stores to provide sufficient substrate supply to the body under conditions of stress.

Consequently, GCs affect substrate output from adipocytes and the liver and suppress insulin-stimulated GU in peripheral tissues (figure 1.2.2)[20].

In white adipose tissue (WAT), physiological increases in plasma GCs promote lipolysis and impair the ability of insulin to suppress lipolysis[83]. Consequently, GC-mediated adipose tissue lipolysis leads to the release of FFAs into the systemic circulation and increased plasma FFA concentration in turn can induce insulin resistance in adipocytes[84,85]. In addition to promoting lipolysis, GC action also paradoxically promotes lipogenesis in the fed state. Acting synergistically with insulin, GCs promote fat storage and variations in fat distribution in obesity can be attributed to the varying sensitivity of different fat depots to GCs[52,86–88]. Whereas subcutaneous adipose tissue (SAT) is more susceptible to lipolysis, visceral adipose tissue (VAT) is more prone to lipogenesis[20]. GCs can also modulate adipokine secretion by WAT. For example, adiponectin, which acts to enhance insulin sensitivity, is found at lower concentrations in obesity and diabetes and GCs can directly suppress its gene expression in adipocytes[89,90]. In addition, GC action in adipocytes locally upregulates leptin mRNA and increases plasma leptin levels through the enhancement of leptin production[91]. Leptin is an adipokine that relays information regarding energy status of WAT to the CNS to help regulate energy homeostasis by inhibiting hunger. In obesity and diabetes, leptin secretion is upregulated but hunger is not suppressed as a result of leptin resistance in the ARC of the hypothalamus[92]. In addition, GCs inhibit insulin-stimulated GU in WAT by decreasing insulin receptor affinity, reducing insulin receptor expression, as well as decreasing the translocation of glucose transporter (GLUT4)[93–95].

In skeletal muscle, GC action attenuates insulin-stimulated muscle GU. Similarly to WAT, GCs impairs GLUT4 translocation to the cell membrane, but also suppresses glycogen synthase activity[96–98]. The GC-mediated increase in plasma FFA concentration resulting from GC action on WAT can also affect insulin sensitivity in muscle tissue. In fact, a strong correlation exists between plasma FFA levels, skeletal muscle insulin resistance, hyperglycemia and T2D[99]. It was initially hypothesized that FFAs compete with glucose for mitochondrial oxidation and as a result muscle GU is downregulated in the presence of increased plasma lipid levels[100]. This glucose-fatty acid cycle, also known as the Randle hypothesis, was postulated following experiments performed on isolated rat hearts and diaphragms. Follow-up human *in vivo* studies suggest that this glucose-fatty acid cycle is not the mechanism underlying FFA-mediated insulin resistance in skeletal muscle[101]. It has now been demonstrated that increases in plasma FFA concentrations reduce insulin-stimulated glucose storage in muscles through mechanisms that reduce glucose transport and phosphorylation[102–104].

Elevated circulating levels of FFAs can also stimulate the hepatic gluconeogenesis pathway (figure 1.2.3[105]). Following the reduction of FFAs into acetyl-CoA during β-oxidation, pyruvate carboxylase (PC) is allosterically activated and the pyruvate dehydrogenase (PDH) complex is inhibited, thereby reducing oxidative metabolism[106]. PC irreversibly carboxylates pyruvate, which promotes hepatic gluconeogenesis through an increased pyruvate flux[107]. Furthermore, adipose tissue lipolysis provides glycerol as a substrate for hepatic GP. GC action in the liver also directly increases the gene transcription of PC[108]. Ligand-bound GRs also activate the transcription of the two rate limiting gluconeogenic enzymes phosphoenolpyruvate carboxykinase (PEPCK) and glucose-6-

phosphatase (G6Pase)[109,110]. In addition to enhancing glucose output, GC-action downregulates glucose oxidation in the liver by stimulating the expression of pyruvate dehydrogenase kinase (PDK)[111]. PDK phosphorylates and inhibits the PDH complex that catalyzes the conversion of pyruvate to acetyl-CoA for the citric acid cycle[112]. Elevated mRNA and protein levels of PDK are also observed in fasted states and in the livers of diabetic and insulin resistant animals[113,114]. In contrast to skeletal muscle, GC action stimulates hepatic glycogenesis by upregulating glycogen synthase activity[115,116]. GCs can also increase hepatic ceramide synthesis which promotes resistance to the suppressive effect of insulin on GP[117]. The mechanism by which ceramides antagonize hepatic insulin signalling is suggested to be through the inhibition of Akt/PKB, a downstream target of insulin receptor signalling[117–119]. Given the catabolic effect of this stress hormone to elevate circulating glucose levels, it can be surmised without a doubt that chronic elevation of GCs leads to metabolic deterioration.

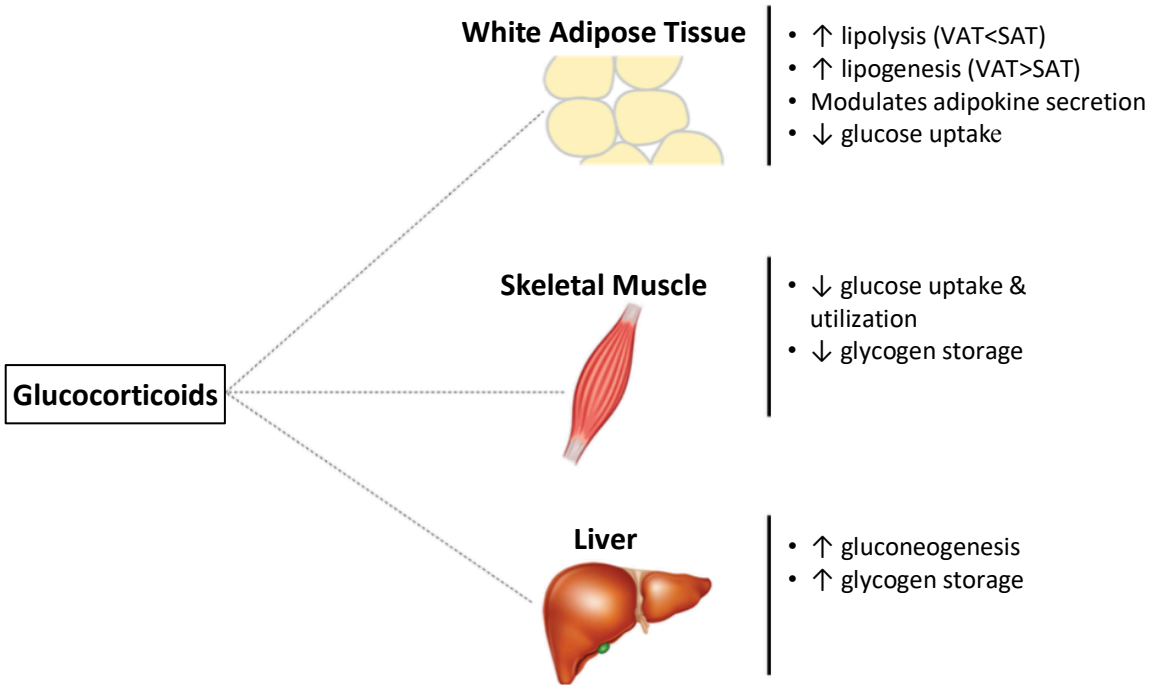

Figure 1.2.2 – Schematic representation of the direct role of GCs on energy homeostasis in peripheral tissues. GCs regulate energy flux and help mobilize energy stores to provide sufficient substrate supply to the body under conditions of stress. SAT: subcutaneous adipose tissue; VAT: visceral adipose tissue.

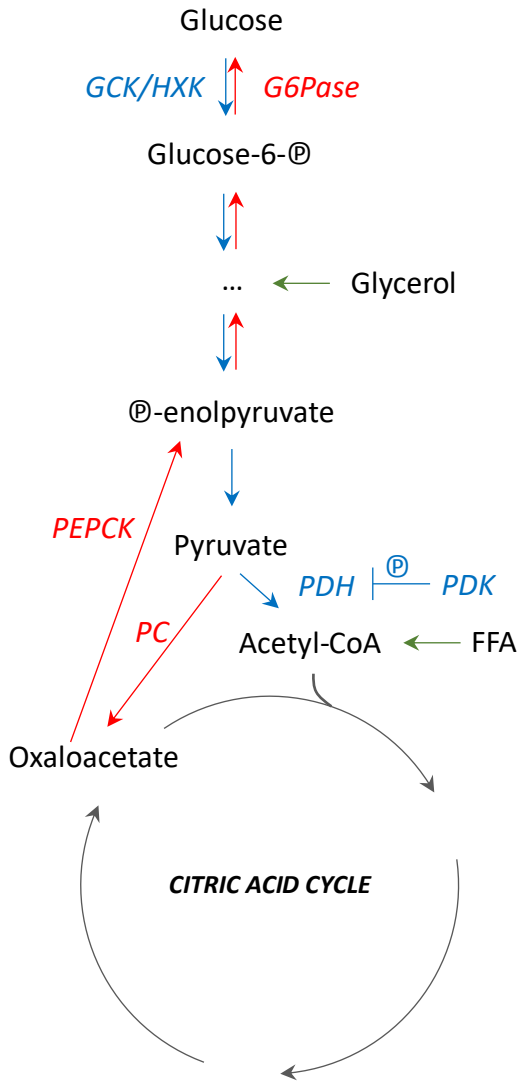

Figure 1.2.3 – Simplified glucose metabolism pathway. Reactions specific to gluconeogenesis are shown in red, and glycolysis is shown in blue. GCK/HXK: glucokinase/hexokinase; G6Pase: glucose-6-phosphatase; PC: pyruvate carbolylase; PDH: pyruvate dehydrogenase complex; PDK: pyruvate dehydrogenase kinase; PEPCK: phosphoenolpyruvate carboxykinase. Adapted from: Palmer, M. *Gluconeogenesis.*

1.2.5 – Glucocorticoid Receptor Isoforms and Polymorphisms

GRs are molecular proteins that are composed of an N-terminal transactivation domain, a DNA-binding domain and a C-terminal ligand-binding domain[70]. The two major nuclear GR isoforms GRα and GRβ differ only in their C-terminal regions and are generated from alternative splicing of the ninth exon of the GR gene (NR3C1 gene in humans, Nr3c1 in rats). While GRα is functional when activated by GCs, GRβ does not bind GCs and acts as a dominant-negative inhibitor of GRα and modulates cell sensitivity to GCs. GRα is usually expressed at higher levels than GRβ, but increases in the ratio of GRβ to GRα can lead to GC resistance[28,49,70].

Mutations of the GR gene and subsequent modulation of tissue-specific GR sensitivity to GCs have been associated with the development of metabolic disturbances such as elevated fasting insulin and glucose levels, increased body weight and BMI, and abdominal obesity [120–122]. For example, GR gene polymorphism *Bcl*I (rs41423247) has shown to increase HPA axis sensitivity to GCs while also leading to increased body fat mass and insulin resistance in homozygous carriers[123]. On the other hand, ER22/23EK polymorphism has been associated with relative GC resistance but has been reported to be linked with favourable metabolic profiles[124]. In addition, it has been reported that GRβ expression is increased in visceral fat and GRα expression is decreased in subcutaneous abdominal adipose tissue of obese individuals and in metabolic syndrome[125–127]. Therefore, tissue-specific variations in GR expression can impact CG sensitivity and can contribute to the pathogenesis of metabolic disturbances.

In addition to classical nuclear GR signalling, GC action on cytosolic GRs or membrane-bound GR (mGR) can lead to rapid nongenomic effects[128,129]. GCs have shown to be capable of triggering rapid cellular responses that occur too quickly to be regulated at the transcriptional level. These rapid nongenomic effects may ensue via GC action on either cytosolic or the novel non-classical mGR to activate yet to be fully defined signalling pathways[128,129]. Evidence that points towards the existence of mGRs emerges from high-sensitivity immunofluorescence staining. This technique has allowed researchers to confirm the physiological presence of mGRs on human immune cells and it has been observed that their frequency is upregulated with immunostimulation[130]. In addition, mGRs have been shown to exist in amphibian neuronal membranes[131]. Other nuclear receptors, such as the estrogen receptor, has recently been shown to also mediate signalling events through membrane receptors and seems to have an involvement in mediating glucose and liver metabolism[132–134].

1.3 – Hypothalamic Nutrient and Hormone Sensing and Regulation of Hepatic Glucose Production

The medial basal hypothalamus (MBH) brain region, which includes the ARC and minor medial aspects of the ventromedial hypothalamus (VMH), is an important region of the brain involved in mediating a wide span of neuroendocrine and physiological functions. Located next to the third ventricle and adjacent to the median eminence, the ARC is a circumventricular organ characterized by its close proximity to a leaky blood-brain barrier (figure 1.3.1)[135,136]. This optimal placement allows neurons in the ARC to sense fluctuations in hormones and nutrients in the blood and control metabolic homeostasis[137]. In response to metabolic cues from the periphery that relay to the brain the nutritional status of the body, the hypothalamus acts accordingly to modulate food intake, energy expenditure, as well as lipid and glucose metabolism[137].

1.3.1 – Nutrient sensing

Considering that the brain's metabolic energy relies almost mainly on glucose and glucose metabolites, the brain possesses nutrient-sensing abilities to help regulate and maintain peripheral glucose homeostasis and subsequently prevent large swings in glycemia. Therefore, circulating plasma glucose not only serves as a nutritive substrate for the brain, but plays a crucial role in providing the central nervous system with vital information regarding the body's nutritional status. Evidence suggesting a role for the brain in whole-body glucose regulation dates back to the 19th century when it was observed that lesioning the floor of the fourth ventricle induced altered glucose homeostasis resulting in hyperglycemia[138]. It is now generally understood that an increase or decrease in extracellular glucose can be sensed by neurons within various areas of the brain[139,140]. The

mechanism by which hypothalamic glucose sensing helps maintain peripheral glucose homeostasis seems to involve modulating hepatic glucose output in a negative feedback fashion rather than affecting GU by peripheral tissues. In a set of experiments, infusing glucose through the intra-cerebral ventricle (ICV) route inhibited both gluconeogenesis and glycogenolysis which together contribute to net hepatic GP. This down regulation of hepatic glucose output was demonstrated by significant inhibition of hepatic G6Pase and decreased G6pc gene expression independent of changes in GU by metabolically active tissues[141].

Amino acids and fatty acids (FA) can also cross the blood-brain barrier and rapidly access the brain to relay nutritional status to the CNS. Infusing the amino acid leucine into the MBH lowers plasma glucose levels while also leads to decreased plasma insulin levels. As previously reported, MBH leucine decreased circulating glucose concentrations by supressing hepatic GP[142]. Similarly, ICV infusion of oleic acid, a monounsaturated long-chain FA commonly found in vegetable and animal fats from a human diet, was demonstrated to decrease plasma glucose levels, increase hepatic insulin sensitivity and induce an anorectic effect[143]. Simultaneous ICV infusion of oleic acid and tolbutamide or glybenclamide, potent K_{ATP} blockers, blunts the metabolic effects of ICV oleic acid indicating that the metabolic effects following central action of oleic acid involve the activation of K_{ATP} channels[143]. In contrast to the glucose lowering effects of hypothalamic FA sensing, elevated systemic levels of FFAs can stimulate gluconeogenesis without affecting net hepatic glucose output[144]. However, a set of experiments demonstrated that increasing plasma FFA levels while simultaneously inhibiting hypothalamic FA action disrupts glucoregulation by decreasing glycogenolysis and subsequently increasing hepatic

GP. Therefore, hypothalamic lipid sensing is necessary for hepatic autoregulation and the prevention of dysregulated glucose metabolism[145].

1.3.2 – Hormone sensing

In addition to sensing extracellular nutrient levels with the goal of maintaining whole body glucose homeostasis, the hypothalamus is equipped with hormone sensing mechanisms that also contribute to regulating peripheral glucose. Insulin delivers to the brain peripheral information regarding energy status and has been hypothesized to provide negative feedback for chronic regulation of energy balance[146–148]. Studying the effects of hypothalamic insulin sensing has allowed for consideration the use of intranasal insulin as an agent to correct for hyperglycemia in T2D diabetes[149]. Within the ARC of the hypothalamus, insulin receptors are localized in anorexigenic pro-opiomelanocortin (POMC) and orexigenic neuropeptide Y (NPY)/agouti-related peptide (AgRP) neurons[150] and specific deletions of the insulin receptor in either of these neuron populations has been shown to negatively affect glucose metabolism[151]. When insulin receptors in AgRP neurons are intact but specifically removed in POMC neurons, hypothalamic insulin action suppresses hepatic GP. When insulin receptors are strictly expressed in POMC neurons but not AgRP neurons, central insulin action fails to suppress hepatic GP and induces hyperglycemia, suggesting that insulin sensing mechanisms in AgRP neurons are necessary for the maintenance of whole body glucose homeostasis[152,153]. The glucoregulatory effects of hypothalamic insulin action have been shown to be mediated by a decrease in the firing rate of both POMC and AgRP neurons through the opening of K_{ATP} channels and consequent cellular hyperpolarization[152,154]. ICV administration of potent K_{ATP} blockers has been shown to prevent the decrease in hepatic GP following hypothalamic insulin action in

a similar fashion as central lipid sensing previously discussed[154,155]. The actions of hypothalamic insulin signalling on peripheral glucose regulation seem to be mediated through autonomic neural modulation of hepatic gluconeogenesis. ICV infusions of insulin are shown to decrease hepatic expression of G6Pase and PEPCK[152,155,156] whereas selectively vagotomizing the hepatic branch prevents the decrease in liver gluconeogenic enzymes in response to ICV insulin[155].

In addition to sensing extracellular rises in insulin, the hypothalamus can also respond to rises in glucagon in order to help maintain peripheral glucose homeostasis. Glucagon receptors have been identified in the hypothalamic region of the brain[157,158] and paradoxically, centrally acting glucagon lowers hepatic GP whereas it is systemically known elicit a rise in blood glucose[158]. Hypothalamic glucagon, signalling via its G-protein coupled receptor, activates adenylate cyclase and increases levels of cAMP which allows for intracellular signal transduction within the hypothalamus via PKA signalling[157,158]. Infusing glucagon directly into the MBH has been shown to lower hepatic GP during basal pancreatic euglycemic clamps and improve glucose tolerance in response to a glucose bolus during an intravenous glucose tolerance test independently of changes in GU and changes in circulating insulin and glucagon levels. Not only does the MBH sense glucagon that is directly infused into the hypothalamus[158] but an increase in circulating glucagon can also cross the blood-brain-barrier and activate neuronal activity[159] and glucagon signalling targets like PKA within the MBH[158]. Moreover, a modest physiological rise in circulating glucagon levels signals via glucagon receptors in the MBH to regulate hepatic GP[158]. Hypothalamic glucagon sensing is proposed to be a physiological mechanisms in place that allows to counter regulate the stimulatory effect of elevated plasma glucagon levels on the

liver and prevent hyperglycemia when hyperglucagonemia is sustained[158]. Taken together, the ability of the brain to respond to hormones to trigger neural signalling pathways and to regulate peripheral glucose metabolism can be assessed via direct hormone infusions into targeted brain regions like the MBH, and it is also important to highlight that the brain can sense increases in circulating hormones to affect glucose metabolism as well.

It has been established that hypothalamic nutrient and hormone sensing is defective in animal models of HFD feeding and obesity. This sensing impairment has been demonstrated to disrupt metabolic homeostasis by promoting aberrant glucose regulation and further promoting the development of obesity[160,161]. Importantly, restoring hypothalamic nutrient and hormone sensing is shown to normalize energy balance and glucose homeostasis in overfed rodents[162]. Given these findings, hypothalamic nutrient and hormone sensing undoubtedly plays a physiological role in regulating whole body energy homeostasis and is clearly involved in the development of metabolic disturbances observed in obesity and diabetes.

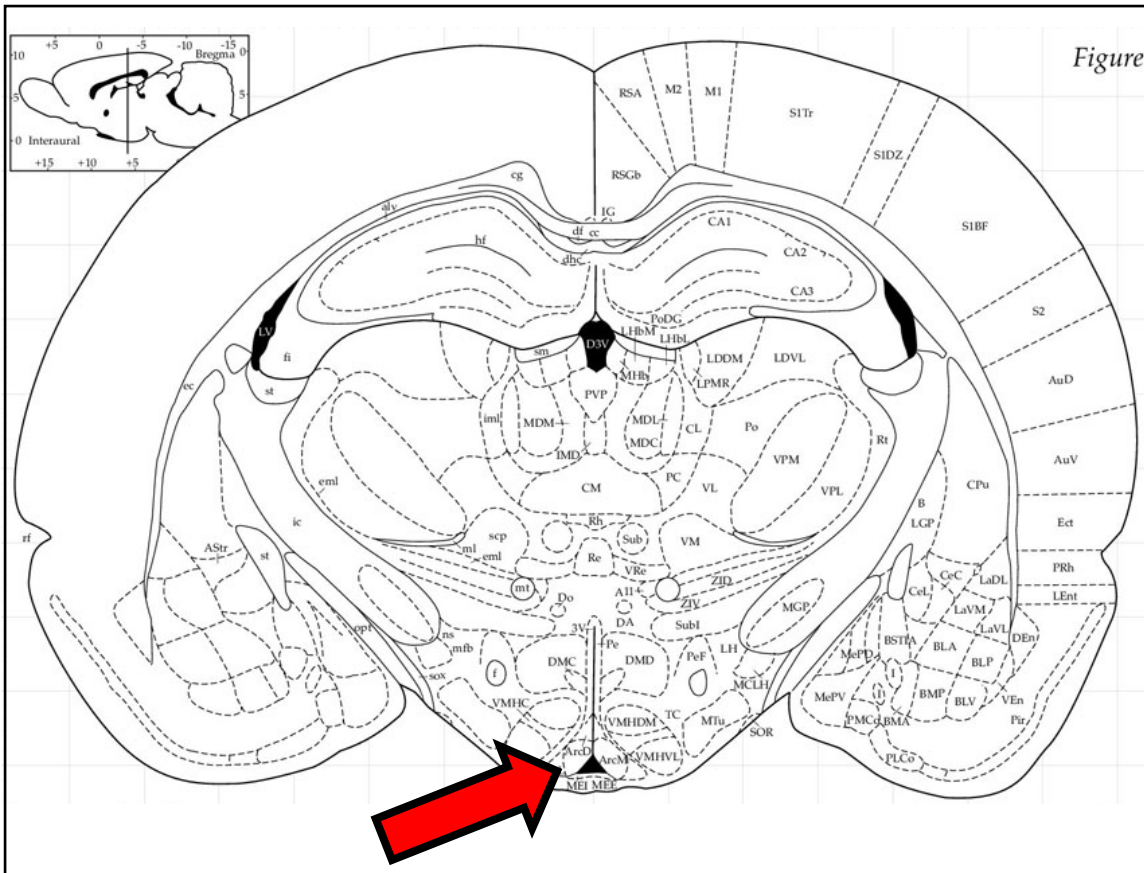

Figure 1.3.1 – Coronal plane diagram of the rat brain showing the anatomical location of the hypothalamic ARC. Red arrow indicates the location of the ARC region (ArcD/ArcM) of the MBH located next to the third ventricle and adjacent to the median eminence (MEI/MEE); ventromedial hypothalamus (VMH). Adapted from: Paxinos, G. & Watson, C. *The rat brain in stereotaxic coordinates.*

1.4 – Metabolic Effects of Central/Brain Glucocorticoid Action

Evidence clearly supports the MBH as a hormone-responsive glucoregulatory site, but less is known about how central/brain GC action modulates metabolism. Studies have demonstrated that chronically infusing synthetic GCs through the ICV route has metabolic consequences. In fact, it has previously been shown in rodent studies that a chronic 2-3 day ICV GC infusion increases body weight gain as a consequence of increased food intake, decreases energy expenditure, increases adipose tissue lipogenic enzyme expression, increases plasma triglyceride concentrations and increases circulating levels of insulin and leptin. In these studies, the metabolic outcomes following central GC-action occurs in parallel with an increase in the potent orexigenic peptide, NPY, in the ARC of the hypothalamus[163,164]. The effect of chronic GC central infusion on food intake, body weight and plasma insulin levels is proposed to be mediated through the parasympathetic nervous system as these GC-mediated actions are no longer observed in vagotomised animals[165]. Additionally, central GC action has shown to increase 11β-HSD1 activity in WAT and this mechanism may be of importance in the development of obesity[163].

In regards to glucose homeostasis, previous studies have revealed that a chronic 2-3 day ICV GC infusion promotes muscle insulin resistance during euglycemic-hyperinsulinemic clamp experimentation[165]. In addition, a study investigated the effect of short-term GC infusion delivered directly into the ARC by retrodialysis on hepatic GP and insulin sensitivity[166]. Acute GC signalling in the ARC of the hypothalamus was shown to have greater endogenous GP in response to a rise in systemic insulin as compared to controls, therefore indicating that local GC action in the ARC leads to hepatic insulin resistance. These effects were shown to be negated when a NPY inhibitor was

simultaneously infused through the ICV route as well as when hepatic sympathetic denervation was performed, suggesting that localized GR activation in the ARC stimulates sympathetic pre-autonomic output from the hypothalamus to liver as a result from GC-stimulated release of NPY[166].

The existence of neural regulatory circuits linking the brain to the periphery to regulate metabolism have been recurrently reported. In fact, it has been demonstrated that several nutrients or hormones sensed in the MBH engage a forebrain/hindbrain neuronal axis in order to control energy balance. It has been commonly reported that information from the MBH is projected to neurons located within regions of the brainstem, which can then communicate to the liver through either efferent sympathetic or parasympathetic projections and modulate metabolism[167–169]. Although the studies discussed above demonstrate that hypothalamic GC action clearly induces metabolic disturbances, intracellular mechanisms underlying the effects of brain GC signalling to elicit changes in glucose metabolism in healthy and pre-obese/obese states still remain largely unknown.

Chapter 2: OBJECTIVES, HYPOTHESIS & METHODS

2.1 – Objectives

This project is aimed towards elucidating GC action in the MBH brain region in relation to glucose tolerance, hepatic GP, insulin resistance, and obesity. In light of recent evidence supporting a role of hypothalamic GCs and data substantiating the MBH as a hormone-responsive glucoregulatory site[154,158,170,171], we hypothesize that GC action in the brain alters glucose metabolism. More specifically, we hypothesize that GCs will act on GRs in the MBH to modulate glucose homeostasis via increased hepatic GP (figure 2.1.1). The *in vivo* experiments performed will allow to delineate molecular and physiological mechanisms of GC action in the brain that modulate glucose homeostasis in normal and pre-obese/obese rodents. In addition, analysis of protein and gene expression of various enzymes in liver tissue will allow to understand how MBH GC action may subsequently affect the liver to modulate hepatic GP.

2.1.1 – Objective 1: To examine whether acute MBH GC action activates MBH GR to regulate glucose homeostasis in regular-chow (RC)-fed rats

These studies will assess for the first time the effects of acute GC infusion into the MBH on hepatic glucose production during basal insulin-euglycemic conditions, as well as test the requirement of MBH GRs in mediating the glucoregulatory effects of MBH GC action on hepatic insulin sensitivity in RC-fed rats. It is anticipated that acute MBH GC infusion using dexamethasone (DEX), a widely used GC to study GR-mediated signalling[172,173], will increase hepatic GP and induce hepatic insulin resistance.

Chemical and genetic loss-of-function approaches targeting GRs will be used to evaluate whether these intracellular, ligand-driven transcription factors are required for

MBH GC glucoregulatory action. Mifepristone (MIF), a known pharmacological antagonist to GR[174], will be co-administered with and without DEX into the MBH to test the requirement of MBH GRs to mediate the glucoregulatory effects of GCs. MBH GRs will be genetically inhibited in separate groups via MBH injection of a lentivirus (LV) that expresses GR shRNA (LV-GR shRNA), or a mismatch sequence (MM) as a control, and treated with and without DEX in the MBH, to alternatively examine the necessity of GRs to mediate glucoregulatory action of MBH GC.

Subsequently, to further determine whether GRs are indeed implicated in mediating the glucoregulatory effects of MBH GC action in normal rats, the next set of experiments will aim to investigate the role of cytoplasmic GR activation. Since the GR depends on Hsp90 for *in vivo* function[48], the effects of chemical inhibition of Hsp90 in the MBH with 17-AAG, a potent Hsp90 inhibitor[175–177], or genetic knockdown of MBH Hsp90 with LV-Hsp90 shRNA, will be investigated in order to determine whether the glucoregulatory effects of MBH GC action can also be negated through MBH Hsp90 inhibition.

After assessing the requirement of MBH GRs in mediating the glucoregulatory effects of MBH GC action in RC-fed rats, western blotting and qRT-PCR will be done in MBH wedges and the livers of rats from different MBH treatment groups in order to analyze protein levels and gene expression of different glucoregulatory enzymes. This will allow for the initial reveal of the underlying biochemical and molecular mechanisms that are responsible for some of the glucoregulatory effects of MBH GCs. There will be a focus on determining how MBH GC action successively affects the liver to modulate hepatic GP. In hypothalami, it will be investigated whether expression of MBH GR or Hsp90 differs in

MBH DEX compared to MBH saline RC-fed animals. In liver, enzymes involved in hepatic gluconeogenesis and glycolysis, as well as hepatic glycogen content will be investigated.

2.1.2 – Objective 2: To test whether MBH GR inhibition improves glucose homeostasis and reverses GC-induced changes in glucoregulation in 3-day high-fat diet (HFD)-fed rats

Acute 3-day HFD feeding has been previously shown to elicit changes in the metabolic profile of rats characterized by hyperinsulinemia and mild hyperglycemia[158,168]. Longer term HFD feeding (12 weeks) is associated with HPA hyperactivity and increased basal plasma GC levels[60]. Thus it is anticipated that our 3-day HFD feeding model will induce hypercorticosteronemia. As a result, the increased levels of circulating GCs will then increase MBH GC signalling and disrupt glucoregulation in these animals. In fact, elevated GC levels, signalling, and/or activity is commonly observed in diabetes and obesity and is associated with disrupted glucose homeostasis. These studies will allow to assess whether inhibition of MBH GRs or its related intracellular regulators such as Hsp90 would help improve metabolic profiles in diet-induced pre-obesity.

It will be assessed whether chemical or genetic MBH GR inhibition with either MBH MIF or MBH LV-GR shRNA attenuates GP to improve glucose homeostasis in pre-obese rodents. Once MBH GRs are determined to be implicated in mediating the glucoregulatory effects of 3-day HFD feeding, the effects of chemical inhibition of Hsp90 in the MBH with 17-AAG or genetic knockdown of MBH Hsp90 with LV-Hsp90 shRNA on glucose metabolism will be investigated.

After assessing the requirement of MBH GRs in mediating the glucoregulatory effects in pre-obese rats, western blotting and qRT-PCR will be done on the livers and MBH wedges of rats from different MBH treatment groups and compared to RC-fed rats or HFD MBH MIF rats in order to analyze changes in protein levels and gene expression. This will allow for an initial assessment into the underlying biochemical and molecular mechanisms that are responsible for some of the glucoregulatory effects of MBH GCs in 3-day HFD feeding. It will be investigated whether HFD feeding alters the expression of MBH GR or Hsp90 and if it is changed by acutely inhibiting MBH action with MBH MIF. In addition, enzymes involved in hepatic gluconeogenesis and glycolysis, as well as hepatic glycogen content will be investigated. These analyses will help link a role of brain GC action in contributing to aberrant glucose regulation in obesity and diabetes.

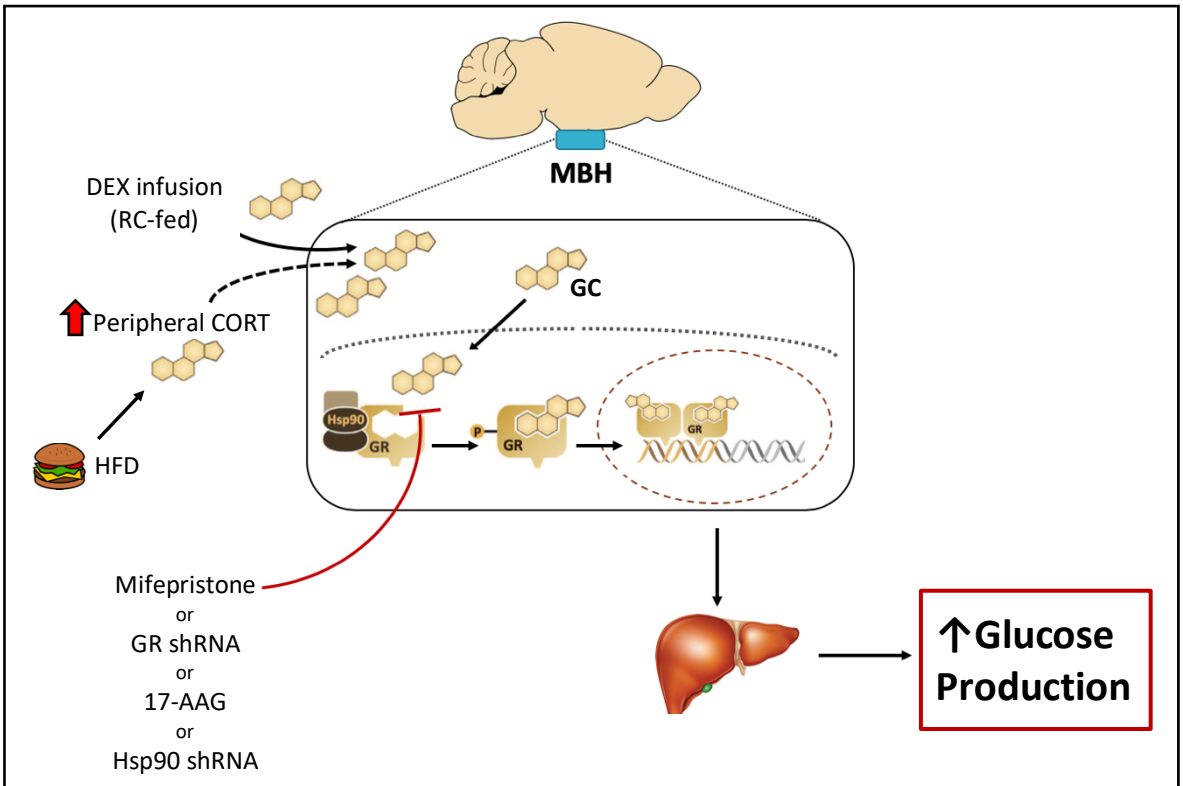

Figure 2.1.1 – Schematic representation of overall working hypothesis. GCs in the MBH act on classical GRs to modulate glucose homeostasis via increased glucose production. Inhibition of MBH GRs or MBH Hsp90 negates the effect of acute MBH GC infusion in healthy rats. 3-day HFD feeding increases circulating GCs and increases MBH GC signalling. Glucose homeostasis in HFD feeding can be restored through MBH GR or MBH Hsp90 inhibition.

2.2 – Hypothesis

It is hypothesized that both acute and chronic antagonism of GR will negate the effect of the glucoregulatory action of MBH GC infusion in RC-fed rats. In fact, our laboratory has previously generated preliminary data suggesting that MBH DEX impairs glucose tolerance as shown by an exaggerated plasma glucose response to an intravenous glucose challenge, and these effects are blunted with MBH GR antagonism with MIF. Chemical or genetic inhibition of Hsp90 in the MBH with 17-AAG or LV-Hsp90 shRNA is also hypothesized to prevent GC-GR action when co-infused with DEX, and therefore negate the glucoregulatory effects of MBH GC infusion.

We also hypothesize that inhibition of MBH GRs or its related intracellular regulators such as Hsp90 will improve the metabolic profile of diet-induced pre-obesity. At a molecular level, it is hypothesized that increased MBH GC-mediated signalling subsequent to a MBH DEX infusion or from 3-day HFD feeding will stimulate hepatic GP through an upregulation of gluconeogenic enzymes PEPCK and G6Pase in the liver.

2.3 – Methods

* All of the protocols for animal care and experiments were approved by the University of Alberta Animal Care and Use Committee (protocol Nº 1604) and in accordance with regulations set forth by the Canadian Council for Animal Care.

2.3.1 – Animal Care and Maintenance

Eight-week-old male Sprague Dawley (SD) rats (initially weighing 190-200g; Charles River Laboratories, Montreal, QC) were used for the *in vivo* experimentation in this study. Rats were individually housed in individual conventional cages on a standard 12-12h light-dark cycle and given ad libitum access to water and standard rat chow (RC) (LabDiet PicoLab® Laboratory Rodent Diet, 5L0D; 60% cal. from carbohydrate, 28% cal. from protein and 12% cal. from fat; 3.0 kcal/g of total metabolizable energy). Male SD rats were used because when fed with a 10% lard-oil enriched diet (HFD is comprised of 90% RC combined with 10% lard) (TestDiet Modified LabDiet® Laboratory Rodent Diet, 5001; 44% cal. from carbohydrate, 22% cal. from protein and 34% cal. from fat; 3.9 kcal/g of total metabolizable energy) for as little as 3 days (model of diet-induced pre-obesity), they acquire brain hormone sensing defects that dysregulate glucose metabolism[158], develop mild hyperglycemia and hyperinsulinemia[168,169], and develop hepatic insulin resistance[178,179].

2.3.2 – Stereotaxic Surgery

Following a one-week acclimatization period, the rats were subjected to bilateral stereotaxic cannulation while being anaesthetised (intraperitoneal administration of 60mg/kg ketamine (Ketalean, Bimeda-MTC), 8mg/kg xylazine (Rompun, Bayer)). 26-

gauge, stainless steel bilateral guide cannula (C235G, Plastics One Inc.) were stereotaxically implanted into the MBH following the coordinates 3.1mm posterior to bregma, 0.4mm lateral to midline, 9.6mm below the cranial surface[158,169]. This bilateral cannulation enabled direct MBH infusion of various brain treatments on experimentation day such as dexamethasone (DEX) (Sigma, D1756; 100ng/µl), mifepristone (MIF) (Tocris #1479; 25nM) and 17-AAG (Tocris #1515; 0.606nmol/µl). Immediately following stereotaxic surgery, a separate group of rats received through each cannula a 3µl injection of a lentivirus (LV) that expresses GR shRNA (Santa Cruz Biotechnology, sc-35506-V), Hsp90 shRNA (Santa Cruz Biotechnology, sc-156099-V), or a control mismatch (LV-MM) sequence (Santa Cruz Biotechnology, sc-108080). To verify that the MBH cannulation was correctly positioned and to confirm that brain infusions were localized to the MBH, 3µl of bromophenol blue dye was injected into the bilateral cannulae at the end of *in vivo* experimentation.

2.3.3 – Vascular Catheterization

Post-brain cannula implantation, rats recovered for 7-8 days before undergoing vascular catherization. The left carotid artery and right jugular vein were catheterized while the rats were anaesthetised (intraperitoneal administration of 90mg/kg ketamine, 10mg/kg xylazine) using catheters consisting of polyethylene (PE-50) (ID: 0.58mm, OD: 0.965mm; Becton, Dickinson and Company) and silastic tubing (*Jugular:* ID: 0.64mm, OD: 1.19mm; *Carotid*: ID: 0.51mm, OD: 0.94mm; Dow Corning Corporation)[158,169]. Postoperatively, the catheters were filled with 10% heparinized saline to maintain patency and sealed with a metal pin, and rats were treated with analgesic (2mg/kg Metacam) for 2 days after surgery. Vascular catherization allowed for intravenous (iv) infusions and repeated arterial blood

sampling to be performed in conscious, unrestrained rats. Recovery following surgeries was assessed daily by body weight and food intake measurements. Only rats that attained a minimum of 90% of their pre-vascular surgery body weight were used for the *in vivo* studies.

2.3.4 – Intravenous Glucose Tolerance Test

The intravenous glucose tolerance test (ivGTT) is an experimental tool that allows us to measure the ability to tolerate glucose and to eliminate glucose from the blood[180]. Four to five days following vascular catheterization, rats were subjected to an overnight fast (16-18h fast) and subsequently randomly assigned to brain treatment groups to undergo ivGTT experimentation (figure 2.3.1). On experiment day and for the entire duration of the experiment, conscious and unrestrained rats received a short-term continuous MBH infusion of their respective brain treatment (saline, DEX, MIF, or MIF+DEX) at an infusion rate of 0.33µl/h (CMA 400 syringe pump, CMA Microdialysis) (e.g. at t=-120 min). One hundred twenty minutes following the start of the MBH infusion (e.g. at t=0 min), blood samples were taken and baseline plasma glucose concentrations were measured by the glucose oxidase method (Glucose Analyzer GM9, Analox Instruments). With this method, glucose oxidase present in the reagent solution of the apparatus catalyzes the oxidation of glucose in the plasma sample to gluconic acid and hydrogen peroxide, and the rate of oxygen consumption is directly related to glucose concentration. The ivGTT was then initiated with a 20% glucose solution (0.25g/kg) injection administered into the jugular vein catheter and flushed with 0.8ml of a 0.2% heparinized isotonic saline over a 30-second injection period. Blood was sampled from the carotid catheter at several time points (2, 5, 10, 15, 20, 25, 30, 60, 90, 120min) for a duration of 120 minutes after the glucose injection.

These samples were immediately analyzed for glucose concentration measurement, and heparinized or protease inhibitor (Roche, #11836170001) treated plasma was stored at -20ºC for future hormone analysis. At the end of the experiment rats were anesthetized with a 50µl iv injection of ketamine and decapitated. MBH tissue wedges, dorsal vagal complex (DVC), pituitary, liver, adrenals, and WAT were immediately collected, flash frozen in liquid nitrogen and stored at −80°C for later analysis.

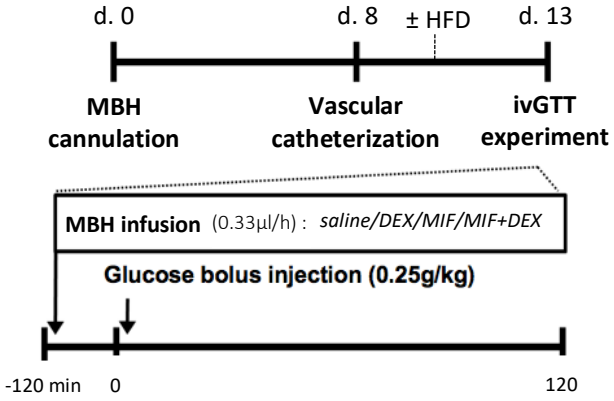

Figure 2.3.1 – ivGTT experimental Protocol. Schematic representation of experimental design: MBH stereotaxic surgery (d.0) was performed on male SD rats. After one week on recovery, vascular catheterization (d.8) was performed. After 4-5 days of surgical recovery, rats underwent ivGTT experimentation (d.13), with concurrent MBH infusion of either saline, DEX, MIF or MIF+DEX was given.

2.3.5 – Pancreatic (Basal Insulin & Mildly Hyperinsulinemic) Euglycemic Clamps

Pancreatic (basal insulin and mildly hyperinsulinemic) euglycemic clamps with tracer dilution methodology combined with MBH GC infusion ± GR inhibition (figure 2.3.2) enables measurement of glucose production (GP) and utilization rates (GU) during steady-state while assessing MBH GC binding with its MBH receptors independent of changes in plasma insulin and glucagon levels. In these experiments, a separate set of rats (eg. not used for ivGTT) fasted for ~5h prior to experiments received short-term continuous MBH infusions (saline, DEX, MIF, MIF+DEX, 17-AAG, or 17-AAG+DEX) in a similar manner as during our ivGTT experiments previously described. Blood is sampled at 10-minute intervals during the basal and clamp periods to closely monitor plasma glucose levels and heparinized or protease inhibitor treated plasma was stored at -20ºC for future hormone analysis. At t=0min, tritiated glucose ([3-^{3}H]-glucose, PerkinElmer) is infused (bolus followed by constant infusion rate of 40µl/min) for the duration of the clamp experiment to allow for adequate distribution of the radiolabeled tracer within the animal. During the steady-state basal period (t=60–90min), the total rate of appearance (R_a) corresponds to the rate of endogenous GP and is equivalent to the rate of glucose disappearance (R_d) or GU. In our experiments, the pancreatic euglycemic clamp is initiated at t=90min with a primed continuous infusion of a solution containing insulin (Sigma, I-5523; 0.8mU/kg/min-basal insulin, 1.2mU/kg/min-mildly hyperinsulinemic) and somatostatin (BACHEM, H-1490.0025; 3µg/kg/min), in addition to a variable infusion of 25% glucose solution to maintain glycemia at concentrations similar to those of the basal state until t=240min[158]. All solutions are infused simultaneously by infusion pumps (Harvard Apparatus PHD 2000 infusion pumps) into the jugular catheter using a multi-channeled PE-50 infusion line. During the clamp setting (defined as the steady-state period

during the final half hour of the experiment, e.g. t=210-240min), the rate of endogenous GP is calculated from the difference between R_d and the exogenous glucose infusion rate (GIR). At the end of the experiment rats were anesthetized with a 50µl iv injection of ketamine and decapitated. MBH tissue wedges, DVC, pituitary, liver, adrenals, and WAT were immediately collected, flash frozen in liquid nitrogen and stored at −80°C for later analysis.

Glucose turnover (R_a of glucose determined with [3-^{3}H]-glucose) is calculated using the following steady-state formula where R_a is equal to [3-^{3}H]-GIR divided by the specific activity of plasma [3-^{3}H]-glucose:

$$R_a = R_d = \frac{Constant\ tracer\ infusion\ rate\ \frac{\mu Ci}{min}}{Specific\ activity\ \frac{\mu Ci}{mg}}$$

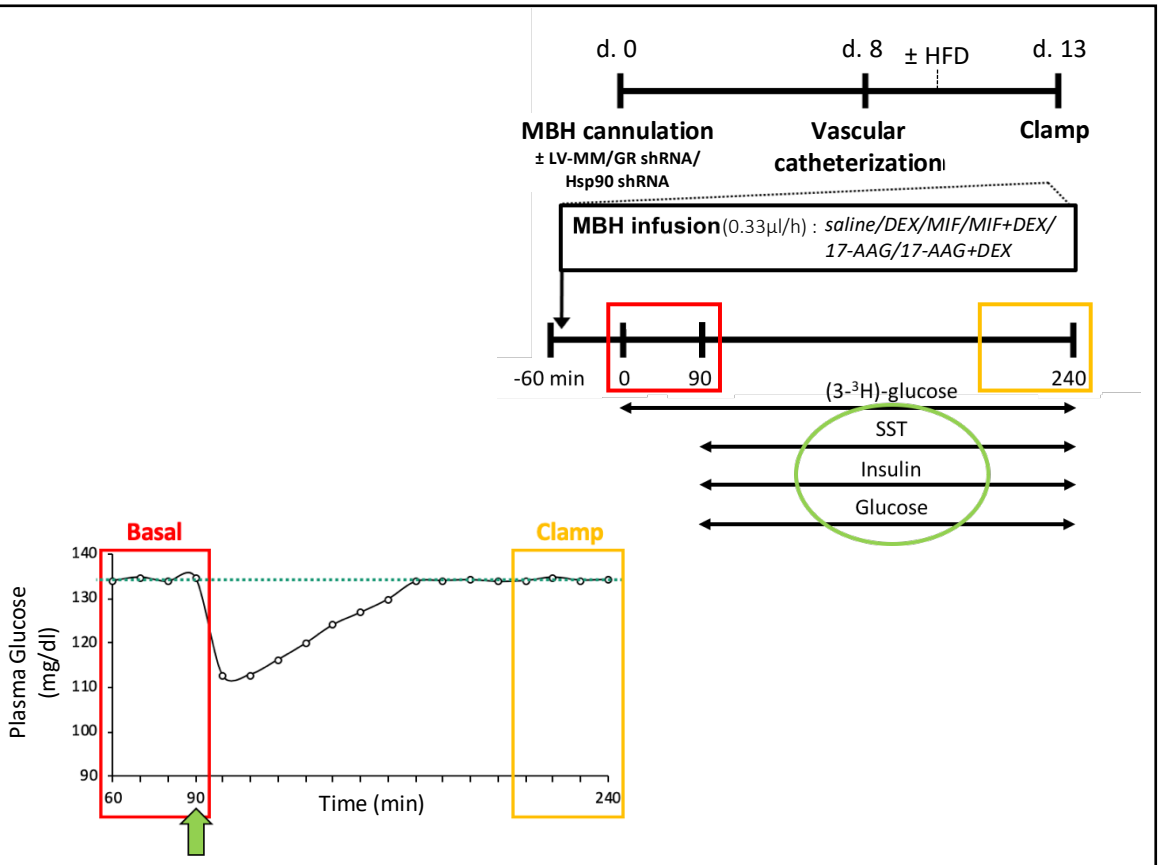

Figure 2.3.2 – Pancreatic (basal insulin and mildly hyperinsulinemic) euglycemic experimental protocol and visual representation of BG over time during pancreatic basal insulin euglycemic clamp experiments. Schematic representation of experimental design: MBH stereotaxic surgery (d.0) was performed on male SD rats with or without a LV injection. After one week on recovery, vascular catheterization (d.8) was performed. 4-5 days later, rats underwent clamp experimentation (d.13), upon which an MBH infusion of either saline, DEX, MIF, MIF+DEX, 17-AAG or 17-AAG+DEX was given. The basal period (t=60-90min) is represented by the red box and the clamped state (t=210-240) is represented by the yellow box. The green arrow at t=90min indicates the start of the SST, insulin, and glucose infusions.

2.3.6 – Plasma Glucose Tracer Assay

The radioactivity of [3-^{3}H]-glucose at various time points during clamp experimentation was determined by adding 100µl of barium hydroxide $Ba(OH)_2$ (Sigma, B4059; 0.3N) and 100µl of zinc sulphate $ZnSO_4$ (Sigma, Z2876; 0.3N) to 50µl aliquots of plasma following the end of experiment. $Ba(OH)_2$ and $ZnSO_4$ allows for the deproteinization of plasma. The plasma was vortexed and then centrifuged (10000rpm for 5min at 4°C) to separate the precipitate from the supernatant. 75µl of supernatant of each sample supernatant was pipetted into the bottom of a 20ml white PE plastic scintillation vial (Fischer Scientific, 03-337-23) and left for evaporation in the fume hood over night to remove any tritiated water in the sample. This ensures that liquid scintillation counting of the supernatant solely represents radioactivity from [3-^{3}H]-glucose in the plasma as tritium on the C-3 position of glucose is lost to water during glycolysis. The next day once the supernatant was fully evaporated, 150µl of distilled H_2O and 7ml of scintillation fluid (EcoLite(+)™, MP Biomedicals; 882475) was added to each vial. Samples were then counted individually for 5min in a beta scintillation counter (Beckman, LS 6500) to quantify radioactivity and subsequent measurement of glucose turnover.

2.3.7 – Plasma Insulin

Plasma insulin levels were measured by radioimmunoassay (RIA) using a 2-day commercial rat insulin RIA kit with 100% specificity (EMD Millipore Corporation, RI-13K). A RIA is a very sensitive assay technique that measures antigen (e.g.: insulin) concentrations by determination of the extent it to which it binds with its antibody. This principle of antigen-antibody binding occurs when a fixed concentration of labeled tracer antigen (e.g.: ^{125}I-labeled insulin) is incubated with a known amount of antibody. As a

result, the two specifically bind to one another. When unlabeled antigen from the plasma sample is added to this system, there is competition between the labeled and unlabeled antigen to bind to the limited amount of antibody binding sites. As the concentration of unlabeled antigen (originally from the plasma sample) is increased, a greater amount of it binds to the antibody and displaces the labeled tracer antigen, decreasing the amount of antibody-bound radiolabeled antigen and increasing free/unbound radiolabeled antigen. The bound antigens are then separated from the unbound ones by precipitation and centrifugation. The supernatant containing the free labeled tracer antigen is removed by decantation or aspiration and the radioactivity of the precipitate containing antibody-bound labeled tracer antigen is measured using a gamma counter[181]. A standard curve is generated with increasing known concentrations of standard unlabeled antigen and the unknown amount in the plasma samples can be calculated by interpolation of the reference curve.

The 2-day protocol provided with the assay kit was used as follows, and samples were assayed in duplicate. Borosilicate 12x75mm glass tubes (Fisher Scientific, 14-961-26) were used for this assay. On the first day, the insulin standard curve (0.156, 0.313, 0.625, 1.25, 2.5, 5.0, 10.0ng/ml) was prepared using the 10ng/ml standard provided. The assay was then set up by adding assay buffer to the Non-Specific Binding (NSB=blank) tubes (100µl) and Reference (B_0=100% binding) tubes (50µl). The standards, quality controls and each experimental plasma sample treated with protease inhibitor were then pipetted (50µl) into their respective tubes. ^{125}I-labeled insulin (50µl) was added to all tubes followed by the addition of insulin antibody (50µl) (guinea pig anti-rat insulin serum), which was not added to Total Count (TC) and NSB tubes. Each tube was vortexed, covered with parafilm and incubated overnight (20-24h) at 4°C. On the next day following the incubation, cold

precipitating reagent (500µl) was added to all tubes except TC tubes followed by vortexing and a 20-minute incubation at 4°C. All tubes except TCs were then centrifuged (2000xg for 20min at 4°C) to form an insulin-bound pellet. The supernatant in each tube was carefully removed by aspiration to ensure that the pellet was free from any excess liquid. The radioactivity of the pellet was then counted for 5 minutes by a gamma counter (Packard, Cobra II Series). The counts (B) for the samples and standards were expressed as a percentage of the mean counts of the total binding B_0 tubes:

$$\%\, Total\ binding\ = \%\frac{B}{B_0} = \frac{Sample\ or\ standard}{B_0}\ x\ 100$$

The percentage of total binding (%B/B_0) for each standard and experimental plasma sample was plotted against the reference curve from the known standards (0.156-10.0ng/ml) and insulin concentrations were determined by interpolation.

2.3.8 – Plasma Glucagon

Plasma glucagon levels were measured by RIA using a 3-day commercial rat glucagon RIA kit with 100% specificity (EMD Millipore Corporation, GL-32K). The principle of the assay was similar to that of the RIA for insulin described above. The protocol provided with the assay kit was used as follows, and samples were assayed in duplicate. Borosilicate 12x75mm glass tubes were used for this assay. On the first day, the glucagon standard curve (12.5, 25, 50, 100, 200pg/ml) was prepared using the 400pg/ml standard provided. The assay was then set up by adding assay buffer to the NSB tubes (300µl), B_0 tubes (200µl), standards and quality controls (100µl) and each sample tube

(150µl). The standards, quality controls (100µl) and each experimental plasma sample (50µl) treated with protease inhibitor were then pipetted into their respective tubes. Glucagon antibody (guinea pig anti-rat glucagon serum) (100µl) was added to all tubes except to TC and NSB tubes and each tube was vortexed, covered with parafilm and incubated overnight (20-24h) at 4°C. On the next day following the incubation, ^{125}I-labeled glucagon (100µl) was added to all tubes, followed by vortexing and covered with parafilm to be incubated overnight (22-24h) at 4°C. On the last day, cold precipitating reagent (1.0ml) was added to all tubes except TC tubes followed by vortexing and a 20-minute incubation at 4°C. All tubes except TCs were then centrifuged (2000xg for 20min at 4°C) to form a glucagon-bound pellet. The supernatant in each tube was carefully removed by aspiration to ensure that the pellet was free from any excess liquid. The radioactivity of the pellet was then counted for 5 minutes by a gamma counter. The counts for the samples and standards were expressed as a percentage of the mean counts of the total binding B_0 tubes and plotted against the reference curve from the known standards (12.5-200pg/ml) and glucagon concentrations were determined by interpolation and corrected for dilution factors..

2.3.9 – Plasma Corticosterone

Plasma corticosterone (CORT) levels were measured by RIA using a 1-day commercial rat/mouse CORT RIA kit with 100% specificity (MP Biomedicals, 07-120103) and no cross reactivity with DEX. The principle of the assay was similar to that of the RIA for insulin described above. The protocol provided with the assay kit was used as follows, and samples were assayed in duplicate. Borosilicate 12x75mm glass tubes were used for this assay. Experimental plasma samples were initially diluted to a ratio of 1:200 with

steroid diluent (5µl plasma, 1.0ml diluent). Steroid diluent was added to NSB tubes (300µl) and B_0 (100µl) tubes. The pre-made CORT standards (25, 50, 100, 250, 500, 1000ng/ml), quality controls and each diluted plasma sample were then pipetted (100µl) into their respective tubes. ^{125}I-labeled CORT (200µl) was added to all tubes followed by the addition of CORT antibody (rabbit anti-CORT serum) (200µl) ,which was not added to TC and NSB tubes. Each tube was vortexed, covered with parafilm and incubated for 2h at room temperature (22-25°C). Succeeding the incubation, precipitating reagent (500µl) was added to all tubes except TC tubes, vortexed and centrifuged (2000xg for 20min at 4°C) to form a CORT-bound pellet. The supernatant in each tube was carefully removed by aspiration to ensure that the pellet was free from any excess liquid. The radioactivity of the pellet was then counted for 5 minutes by a gamma counter. The counts for the samples and standards were expressed as a percentage of the mean counts of the total binding B_0 tubes and plotted against the reference curve from the known standards (25-1000ng/ml) and CORT concentrations were determined by interpolation.

2.3.10 – Liver Glycogen Content

Liver glycogen concentrations were measured by colorimetric analysis using a commercial glycogen assay kit (Abcam, ab65620). The principle behind this assay is based on the hydrolysis of glycogen to glucose by the digestive enzyme glucoamylase. The hydrolysis of glycogen to glucose is then specifically oxidized to generate a product that reacts with the OxiRed probe and generates a color that can then be measured on a microplate spectrophotometer at optimal density.

The protocol provided with the assay kit was used as follows in duplicates. Non-treated polystyrene 96 well assay plates (Corning, 9017) were used for this assay. Liver samples for the assay were prepared by harvesting 10mg of tissue followed by a wash with cold 1xPBS (200µl). Tissue was resuspended in ddH_2O (200µl) and homogenized with a Dounce homogenizer sitting on ice. The liver homogenates were then boiled (10min at 95°C) and centrifuged (18000xg for 10min at 4°C). The supernatant was collected and transferred into a new tube on ice to be later used for the glycogen assay as the sample. A glycogen standard curve (0, 0.4, 0.8, 1.2, 1.6, 2.0µg/well) was prepared using the 2mg/ml standard provided. The assay was then set up by adding standards (50µl), samples and sample background controls (3µg) to the wells, and hydrolysis buffer (47µl) was added to both sample and sample background control wells to adjust the total volume to 50µl. Hydrolysis enzyme mix (2µl) was then added to each standard and sample wells, but not to background controls. The plate was then incubate at room temperature for 30 minutes, followed by the addition of reaction mix (50µl) to each well, which contains development buffer, development enzyme mix and OxiRed probe. The plate incubated at room temperature for another 30 minutes but protected from light, followed by the measurement of output on a microplate reader (Epoch, BioTek) at OD 570nm. The sample background controls were subtracted from the sample reading and the absorbance values for these corrected samples were plotted against the reference curve from the known standards (0-2.0µg/well) to determine the amount of glycogen per well (µg/well). The concentration of glycogen in the experimental samples (µg/µl) was then calculated by the following formula:

$$Glycogen\ concentration\ \frac{\mu g}{\mu l} = \frac{Sample\ concentration\ \frac{\mu g}{well}}{Sample\ volume\ \frac{\mu l}{well}}\ x\ Sample\ dilution\ factor$$

Since the exact weight of harvest liver tissue may vary, samples were subjected to a BCA protein assay (Pierce™ BCA Protein Assay, Thermo Scientific; #23225) in order to determine sample protein concentration. Samples were diluted to a ratio of 1:10 with ddH_2O and the protocol provided with the protein assay kit was used. Once sample protein concentration (μg/μl) was determined, the final concentration of glycogen in the experimental samples were expressed in the units of glycogen(μg)/protein(μg).

2.3.11 – Western Blotting

Liver (≈20mg) and MBH tissue wedges (≈10mg) were homogenized with a Dounce homogenizer at a dilution factor of 1:10 in 1% NP-40 lysis buffer containing 20mM Tris-HCl (pH 7.4), 5mM EDTA, 1% (w/v) Non-idet P40, 2mM sodium orthovanadate, 5mM sodium pyrophosphate tetrabasic, 100mM sodium fluoride, phosphatase and protease inhibitor. The homogenates sat on ice for 30 minutes and were then centrifuged (1200xg for 30min at 4°C). The supernatant was collected and transferred into a new tube on ice to be later used as the lysate. Protein concentration of the lysate and amount of sample to be used for loading for western blotting was determined using the Pierce™ BCA Protein Assay. Samples were diluted to a ratio of 1:20 for liver and 1:10 for MBH with ddH_2O and the protocol provided with the protein assay kit was used.

Liver and MBH lysates were subjected to electrophoresis (Mini-PROTEAN® Tetra Vertical Electrophoresis Cell, Bio-Rad) using 10% polyacrylamide gels and transferred (90V for 2h30min at 4°C) to nitrocellulose membranes (0.45μm, Bio-Rad, #1620115). Membranes were then stained, destained and erased (MemCode™ Reversible Protein Stain

Kit, Thermo Scientific; #24580) to confirm the efficiency of protein transfer. Membranes were then incubated with blocking buffer (5% milk in Tris-buffered saline containing 0.2% Tween-20 (TBST)) for 1h at room temperature and rinsed with 1xTBST to rinse off the milk. Membranes were incubated overnight at 4°C in primary antibody solutions diluted as shown in table 2.3.1 for liver samples (pPDH-E1α, PDH-E1α, PDK1, PDPc, HXK II, PEPCK) and table 2.3.2 for MBH tissue (GR, Hsp90α/β, Hsp70). Tubulin (Tub) was used as a loading control for all primary antibodies investigated. Following incubation in primary antibody solution, membranes were washed with 1xTBST and incubated for 1h at room temperature in horseradish peroxidase (HRP)-linked secondary antibody (table 2.3.3) solution diluted 1:1000 in blocking buffer. Membranes were then washed with 1xTBST and protein expression was enhanced using a chemoluminescence reagent (Western Lighting® Plus-ECL, PerkinElmer; NEL105001EA). Immunoblots were detected using chemiluminescent imaging system (Bio-Rad ChemiDoc) and quantified by densitometry with ImageJ image analysis software and normalized for the total protein (Tub).

2.3.12 – qRT-PCR

Liver gluconeogenic enzymes PEPCK (*Pck1*) and G6Pase (*G6pc*) mRNA expression was analyzed using two-step quantitative realtime polymerase chain reaction (qRT-PCR). Total RNA was extracted from liver using Trizol and quantified using a Nanodrop spectrophotometer (260/280nm). After first DNAse treatment, first-strand complementary DNA was synthesized using SuperScript II™ IV VILO Master Mix kit (Invitrogen, #11756050). Total RNA was first aliquoted by adding 1µg of total RNA in a 9µl final volume using RNAse free H_2O. Samples were then primed by adding 2µl of

1μg/μl of Random Hexamer Primers (Invitrogen, #48190011) to each sample and ran through a PCR program to be denatured (70°C for 10min). Master mix (9μl) was then added to each sample and ran through a PCR program (40°C for 1h) to yield cDNA at a concentration of 50ng/μl. cDNA samples were diluted to a ratio of 1:10 with RNAse free H_2O for Pck1 and G6pc gene analysis and 1:100 for cyclophilin which was used as a control. Quantitative RT-PCR was performed (StepOne™ Real-Time PCR System, Applied Biosystems™) in duplicates on a MicroAmp™ Fast Optical 48-Well Reaction Plate (Applied Biosystems™, #4375816) using TaqMan™ Gene Expression Assays (FAM) (table 2.3.4) and TaqMan™ Universal PCR Master Mix (Applied Biosystems™, #4304437) per the manufacturer's instructions. Expression values were normalized to the internal control gene, cyclophilin, for the efficiency of amplification and quantified by the $2^{-\Delta\Delta Ct}$ method[182]. Expression values of cyclophilin did not vary between experimental groups, deeming it a suitable control gene.

2.3.13 – Statistical Analysis

Statistical analyses were calculated with GraphPad Prism software. Unpaired Student's t-tests were performed in the statistical analysis of two groups. Where comparisons were made across more than two groups, analysis of variance (ANOVA) was performed, and if significant, was followed by Dunnett's or Tukey's post hoc tests when appropriate. The measurements that were taken repeatedly over time were compared using repeated-measures ANOVA. If the time and treatment interaction between groups was found to be significant, t-tests or Duncan's multiple range post-hoc test were used to

determine the statistical significance at specific time points between groups. The P value o0.05 was considered statistically significant.

Antibody & Molecular Weight	Company & Catalog Number	Dilution	Secondary Antibody
Anti-PDH-E1α (pSer^{293}) **(pPDH-E1α) – 43kDa**	MilliporeSigma - #AP1062	1:500	GAR
Anti-PDH-E1α (D-6) **(PDH-E1α) – 43kDa**	Santa Cruz - #sc377092	1:500	GAM
Anti-PDK1 (E-10) **(PDK1) – 49kDa**	Santa Cruz - #sc515944	1:500	GAM
Anti-PDPc (D-11) **(PDPc) – 53kDa**	Santa Cruz - #sc398117	1:500	GAM
Anti-HXK II (1A7) **(HXK II) – 100kDa**	Santa Cruz - #sc130358	1:500	GAM
Anti-PEPCK (F-2) **(PEPCK) – 62kDa**	Cell Signaling - #2144	1:500	GAR
Anti-α-Tubulin **(Tub) – 50kDa**	Cell Signaling - #2144	1:1000	GAM

Table 2.3.1 – Primary antibodies used for western blotting in liver tissue.

Antibody & Molecular Weight	Company & Catalog Number	Dilution	Secondary Antibody
Anti-Glucocorticoid Receptor (D8H2) **(GR) – 94kDa**	Cell Signaling - #3660	1:1000	GAR
Anti-Hsp90α/β (F-8) **(Hsp90α/β) – 90kDa**	Santa Cruz - #sc13119	1:1000	GAM
Anti-Hsp70 (3A3) **(Hsp70) – 70kDa**	Santa Cruz - #sc32239	1:1000	GAM
Anti-α-Tubulin **(Tub) – 50kDa**	Cell Signaling - #2144	1:1000	GAM

Table 2.3.2 – Primary antibodies used for western blotting in MBH tissue.

Secondary Antibody	Company & Catalog Number	Dilution
Anti-mouse IgG, HRP-linked Antibody **(GAM)**	Cell Signaling - #7076	1:1000
Anti-rabbit IgG, HRP-linked Antibody **(GAR)**	Cell Signaling - #7074	1:1000

Table 2.3.3 – Secondary antibodies used for western blotting in liver and MBH tissue.

Gene Name	Reference Number	Dilution
Glucose-6-phosphatase catalytic subunit **(G6pc)**	Mm00839363_m1	1:10
Phosphoenolpyruvate carboxykinase 1, cytosolic **(Pck1)**	Mm01247058_m1	1:10
Cyclophilin-A **(PPIA)**	Mm02342430_g1	1:100

Table 2.3.4 – TaqMan™ gene and probes used for gene expression analysis in liver tissue.

Chapter 3: RESULTS

ivGTT experiments in this section were performed by undergraduate students Aleesha Amjad Hafeez (AAH) (RC groups) and Hyejun Kim (HK)(HFD groups) as part of the undergraduate project courses PHYSL 467 (2015-2016) and CELL 398/498 (2017-2018) respectively. Western blotting was performed by EBB and Carrie-Lynn Soltys (CLS). qRT-PCR analysis was performed by CLS.

This chapter will first cover results obtained from in vivo experimentation in RC-fed rats (objective 1) and then will cover in vivo experimentation in 3-day HFD-fed rats (objective 2). The chapter will conclude with the results obtained following molecular analysis for both diets.

3.1 – MBH GCs act on MBH GRs to impair glucose tolerance in healthy RC-fed rats

To first evaluate the glucoregulatory impact of acute MBH GC infusion in an unclamped setting, undergraduate students in our laboratory, Aleesha Amjad Hafeez and Hyejun Kim, performed ivGTT experiments on a group of rats which allowed us to evaluate the rodents' ability to tolerate glucose and eliminate glucose from the blood. Saline, DEX, MIF or MIF+DEX was infused directly into the MBH of unrestrained, healthy rats, and plasma glucose levels were monitored over time. Compared to control animals receiving MBH saline, rats that received a MBH DEX infusion for 4h had impaired glucose tolerance, as shown by a greater excursion of plasma glucose levels in response to an iv glucose bolus. Whereas MBH infusion of GR antagonist MIF alone had no effect on glucose tolerance, co-infusing MIF with DEX prevented the higher peak and delayed glucose clearance in the bloodstream induced by DEX, suggesting GR involvement in mediating GC action on glucoregulation (figure 3.1.1).

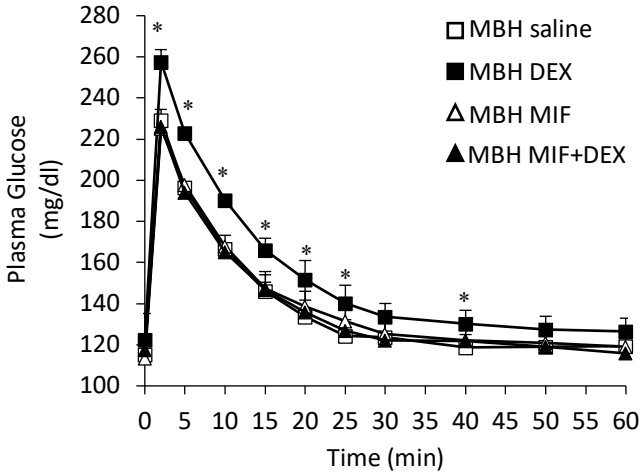

Figure 3.1.1 – MBH GC action impairs glucose tolerance during ivGTT experimentation in RC-fed rats. Plasma glucose levels with MBH infusion of saline (n=11, white squares), DEX (n=13, black squares), MIF (n=7, white triangles) and MIF+DEX (n=9, black triangles). $^{*}P<0.05$ for MBH saline versus MBH DEX. *Experiments performed by undergraduate student AAH (2015-2016)*.

3.2 – MBH GC action stimulates hepatic glucose production in healthy RC-fed rats

3.2.1 – Basal insulin-euglycemic clamp experiments

To begin delineating a role of MBH GC action in the modulation of glucoregulation in normal healthy rodents, we tested whether MBH DEX regulates glucose GP or GU in rats during pancreatic euglycemic clamps. In a first set of clamp experiments using a basal insulin dose of 0.8mU/min/kg, infusion of DEX directly into the MBH of conscious unrestrained rats decreased the requirement for exogenous glucose infusion to maintain euglycemia (figure 3.2.1a) and potently stimulated hepatic GP during clamp conditions (figure 3.2.1b) compared with MBH infusions of saline. Analysis of plasma samples collected during *in vivo* experimentation demonstrated that infusing MBH DEX increased plasma insulin levels during the basal period. During the clamp period, the glucostimulatory effects of MBH DEX occurred without any differences in peripheral CORT concentrations (table 3.2.1), and independently of any differences in body weight (0.329±0.010kg for MBH saline; 0.336±0.008kg for MBH DEX). MBH DEX therefore stimulated hepatic glucose production without affecting GU (figure 3.2.1c) and acted independently of changes in plasma glucose (figure 3.2.1d) and glucagon levels (table 3.2.1).

3.2.2 – Mildly hyperinsulinemic euglycemic clamp experiments

Mild hyperinsulinemic euglycemic clamps using an insulin dose of 1.2mU/min/kg were next performed to induce a greater suppression in hepatic GP while minimally affecting GU in peripheral tissues. High plasma insulin levels induced by intravenously infusing larger doses of insulin (e.g. 2.0-3.6mU/min/kg) increase insulin levels in the brain.

As such, mildly hyperinsulinemic clamp protocol was chosen to prevent a rise in hypothalamic insulin levels, which affects hepatic GP independent of insulin's direct effect on the liver[154,183]. Increasing the insulin dose had no effect on circulating CORT levels (table 3.2.1-3.2.2). In congruence with the data obtained from clamp experimentation using a basal insulin dose, MBH DEX infusion decreased the GIR (figure 3.2.2a) and significantly increased GP compared to MBH saline controls (figure 3.2.2b) during the clamp under mild hyperinsulinemic conditions without altering GU or glucose levels (figure 3.2.2c-d). Increasing the insulin dose by 1.5x compared to the dose used for basal insulin clamps doubled plasma insulin levels during the clamp (table 3.2.2). MBH infusion of MIF alone had no effect on glucose kinetics when compared to MBH saline controls (figure 3.2.2a-d). Similar to basal insulin clamp conditions, co-infusing MIF with DEX negated the ability of MBH GCs to increase hepatic GP (figure 3.2.2b) during the clamp and normalized GIRs to a rate comparable to MBH saline controls (figure 3.2.2a), further confirming that the glucostimulatory effect of MBH GCs is mediated via MBH GRs.

Furthermore, mild hyperinsulinemic euglycemic clamps where also performed on rats with chronically knocked-down MBH GRs using GR shRNA. This chronic loss of function approach allows to investigate with more specificity the involvement of MBH GRs by downregulating GR gene and protein expression. The cohort of rats involved in this set of experiments received a MBH bilateral LV injection that expresses either GR shRNA or a control mismatch (MM) sequence immediately following stereotaxic surgery occurring approximately two weeks prior to clamp experimentation. Western blots performed on MBH tissue wedges collected at the end of clamp experiments confirmed that GR shRNA

yielded a 56% reduction of 94-kDa GR expression in the MBH compared with the MM sequence (figure 3.2.3).

In MBH MM animals, as expected MBH DEX infusion decreased the GIR (figure 3.2.4a) and significantly increased GP compared to MM MBH saline controls (figure 3.2.4b) during the clamp under mild hyperinsulinemic conditions independent of changes to GU or plasma glucose levels (figure 3.2.4c-d). Animals with MBH GR shRNA receiving either MBH saline or DEX showed no differences in GIR or GP at clamp (figure 3.2.4a-b) when compared to the MBH MM saline control group. Therefore, chronic loss of function of MBH GRs through GR shRNA negates the glucoregulatory actions of MBH DEX similarly to acute MBH GR inhibition with MBH MIF, validating the hypothesis that the glucostimulatory effect of MBH GCs is mediated via MBH GRs.

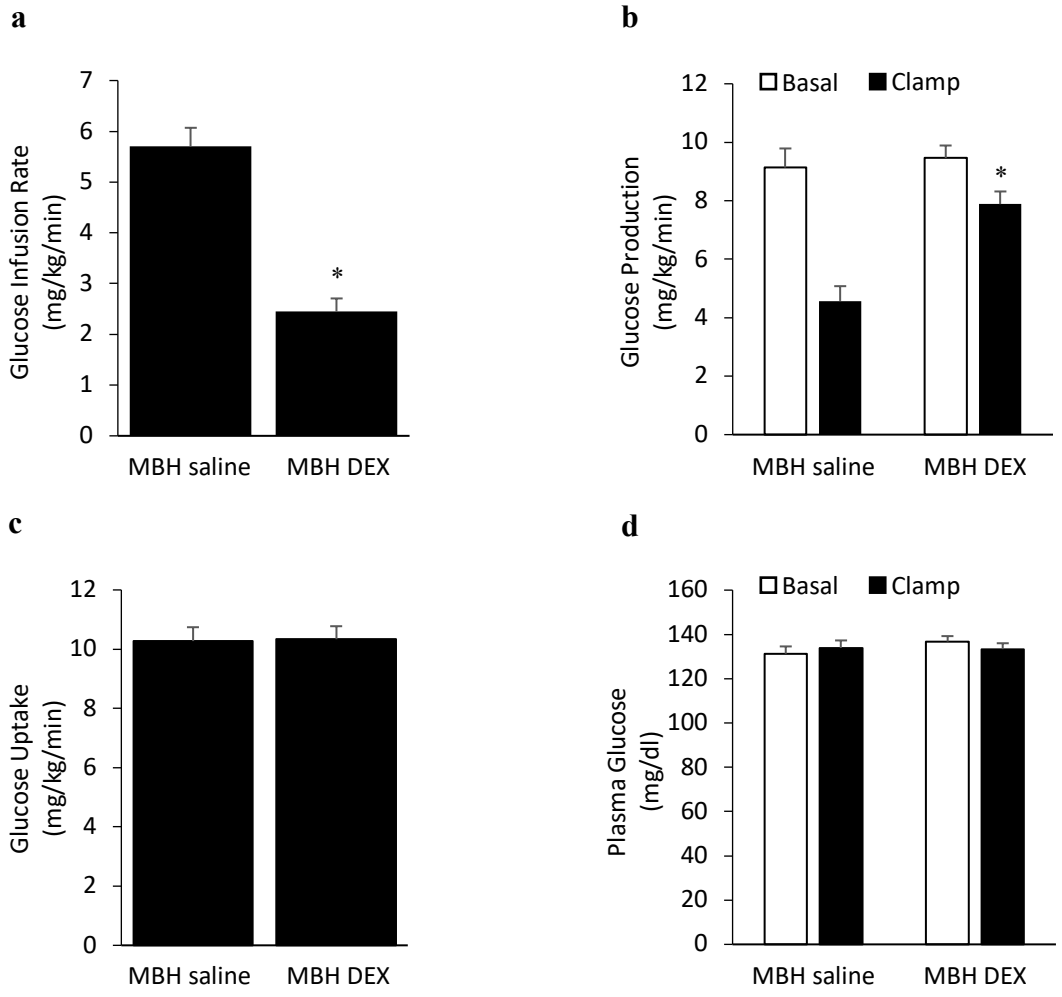

Figure 3.2.1 – MBH GC action stimulates hepatic glucose production during pancreatic basal insulin (0.8mU/min.kg) euglycemic clamp experimentation in RC-fed rats. a) Glucose infusion rates, b) glucose production, c) glucose uptake and d) blood glucose levels. MBH infusion of saline (n=12) and DEX (n=14). $^{*}P<0.05$ for MBH DEX versus MBH saline.

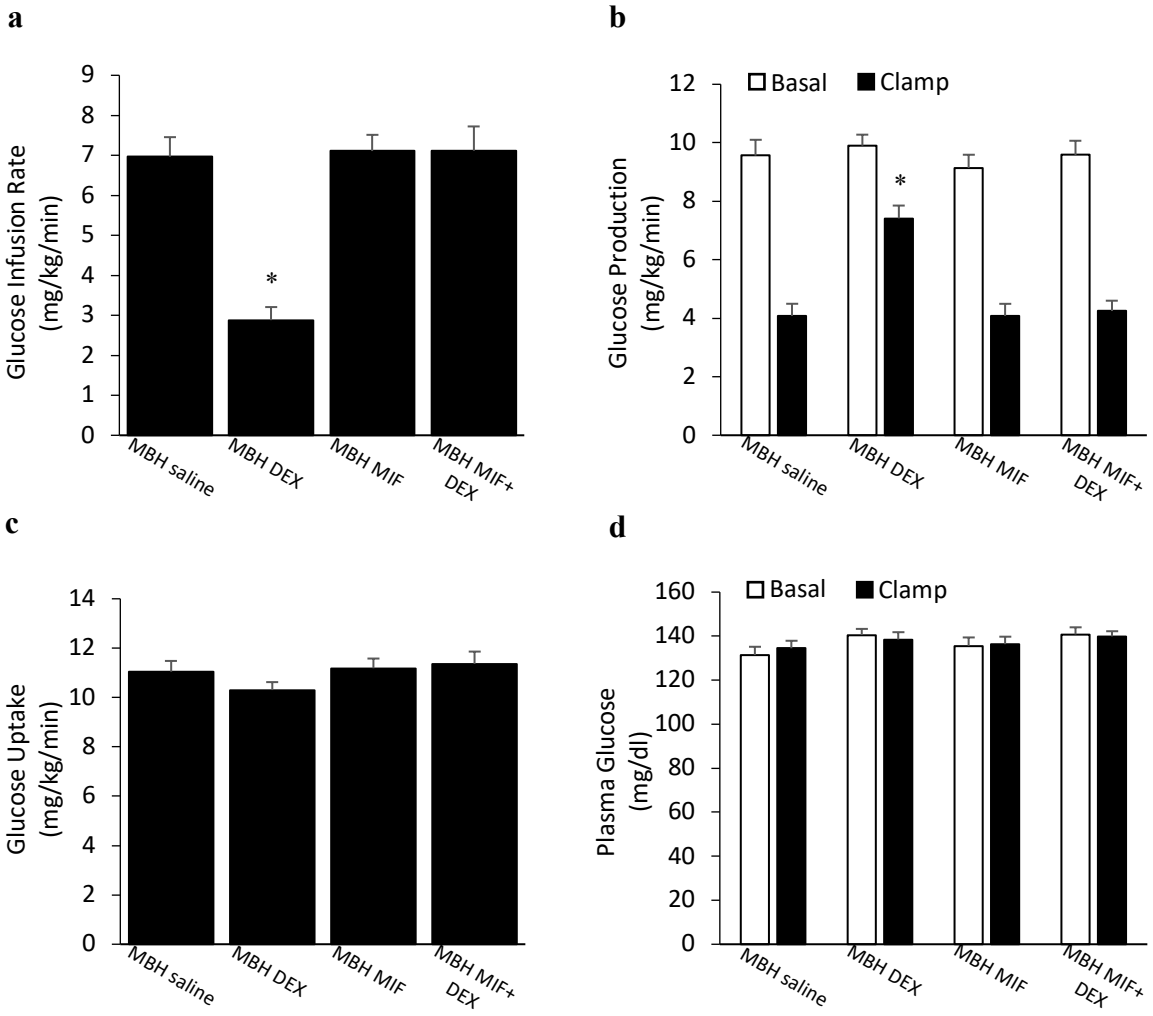

Figure 3.2.2 – Chemical inhibition of MBH GRs negates the glucoregulatory effects of MBH DEX during pancreatic mild hyperinsulinemic (1.2mU/min/kg) euglycemic clamp experimentation in RC-fed rats. a) Glucose infusion rates, b) glucose production, c) glucose uptake and d) plasma glucose levels. MBH infusion of saline (n=13), DEX (n=14), MIF (n= 8) and MIF+DEX (n=9). $^{*}P<0.05$ for MBH DEX versus MBH saline, MBH MIF and MBH MIF+DEX.

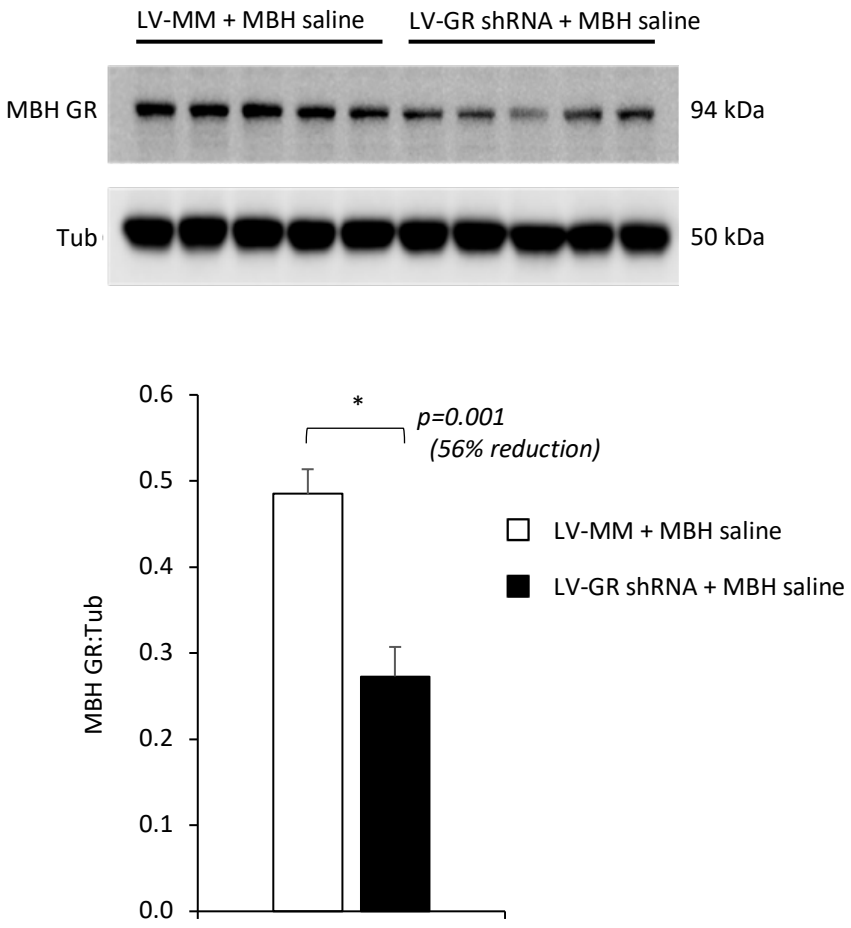

Figure 3.2.3 – Representative western blots and protein levels of MBH GR normalized to tubulin (Tub) in RC-fed rats. MBH wedges of rats 13-day post MBH lentiviral (LV) injection of GR shRNA (n=5, black bar) or a mismatch sequence (MM; n=5, white bar) as a control**.** *P=0.001.

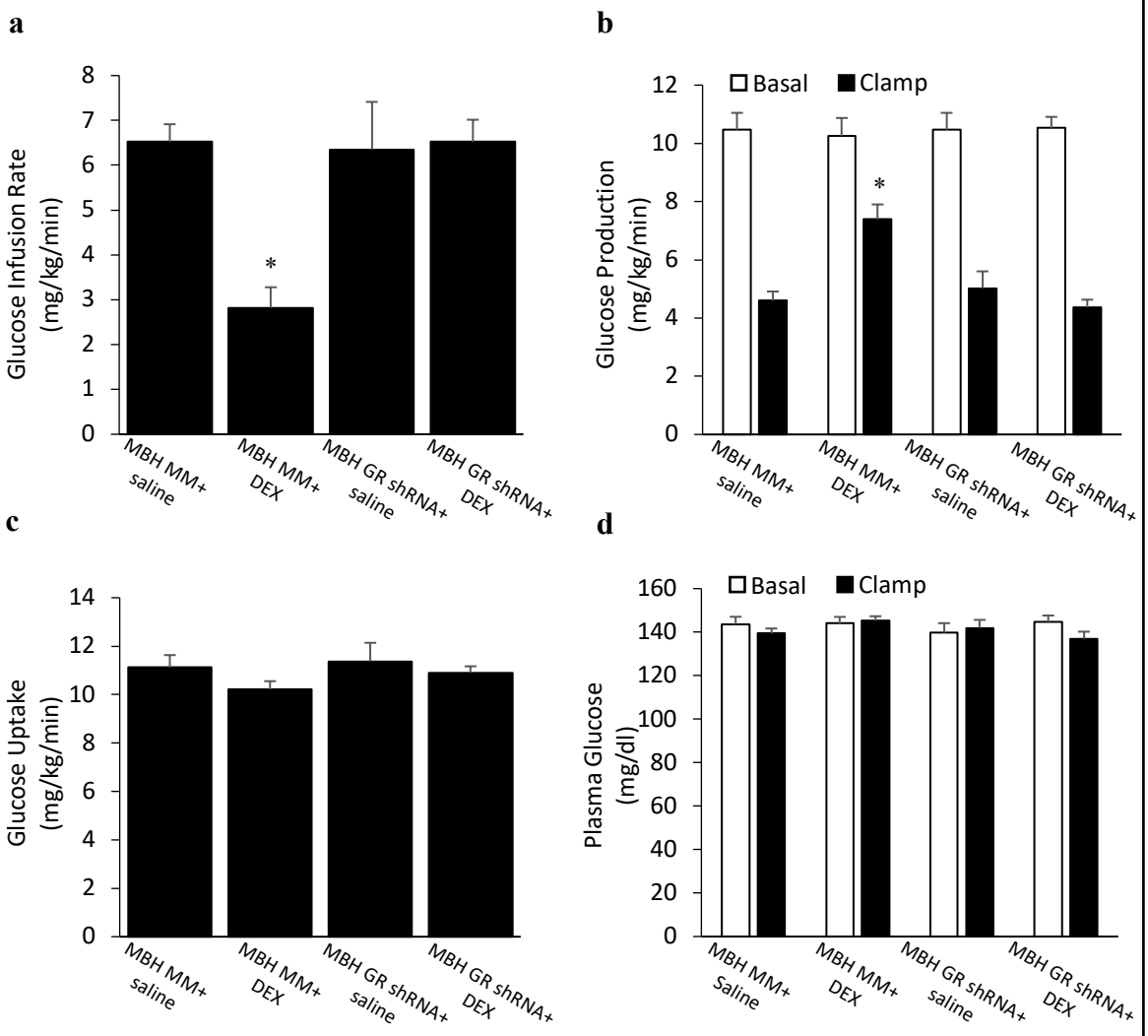

Figure 3.2.4 – Molecular knockdown of MBH GRs negates the glucoregulatory effects of MBH DEX during pancreatic mild hyperinsulinemic (1.2mU/min/kg) euglycemic clamp experimentation in RC-fed rats. a) Glucose infusion rates, b) glucose production, c) glucose uptake and d) plasma glucose levels. MBH infusion of LV-MM+saline (n=12), LV-MM+DEX (n=9), LV-GR shRNA+saline (n=7) and LV-GR shRNA+DEX (n=7). $^{*}P<0.05$ for LV-MM+DEX versus LV-MM+saline, LV-GR shRNA+saline and LV-GR shRNA+DEX.

3.3 – MBH Hsp90 is required to mediate the glucoregulatory actions of MBH GCs in RC-fed rats

Given that the glucostimulatory effect of MBH GCs is mediated via MBH GRs, the role of Hsp90 on MBH GC-mediated signalling was next investigated. Since Hsp90 is required for cytosolic ligand binding to occur and for the GR to become active, inhibition of MBH Hsp90 should consequently prevent MBH GC-mediated stimulation of hepatic glucose production. In healthy RC-fed rats, infusing the pharmacological Hsp90 inhibitor 17-AAG alone into the MBH had no effect on hepatic GP, GIR, GU and plasma glucose levels when compared to MBH saline controls (figure 3.3.1a-d). Meanwhile, co-infusing MBH 17-AAG with MBH DEX negated the ability of MBH DEX to increase hepatic GP (figure 3.3.1b) during the clamp and normalized GIRs to a rate comparable to MBH saline controls (figure 3.3.1a), implying the requirement of MBH Hsp90 to mediate MBH GC actions on hepatic GP.

The involvement of MBH Hsp90 in MBH GC-mediated signalling was further supported with data obtained from mild hyperinsulinemic euglycemic clamp experimentation performed on rats with chronically knocked-down MBH Hsp90 using Hsp90 shRNA. When DEX was infused into the MBH of animals with MBH Hsp90 shRNA, the glucoregulatory effects of MBH DEX were negated and GP during the clamp was equally supressed to values comparable to MM MBH saline controls (figure 3.3.2a-b), independent of changes in GU and plasma glucose levels (figure 3.3.2c-d). Since both acute inhibition as well as chronic loss of function of MBH Hsp90 negates the glucoregulatory actions of MBH DEX, MBH Hsp90 is involved in the mechanism of MBH GC-mediated signalling that modulates glucose metabolism in healthy rats.

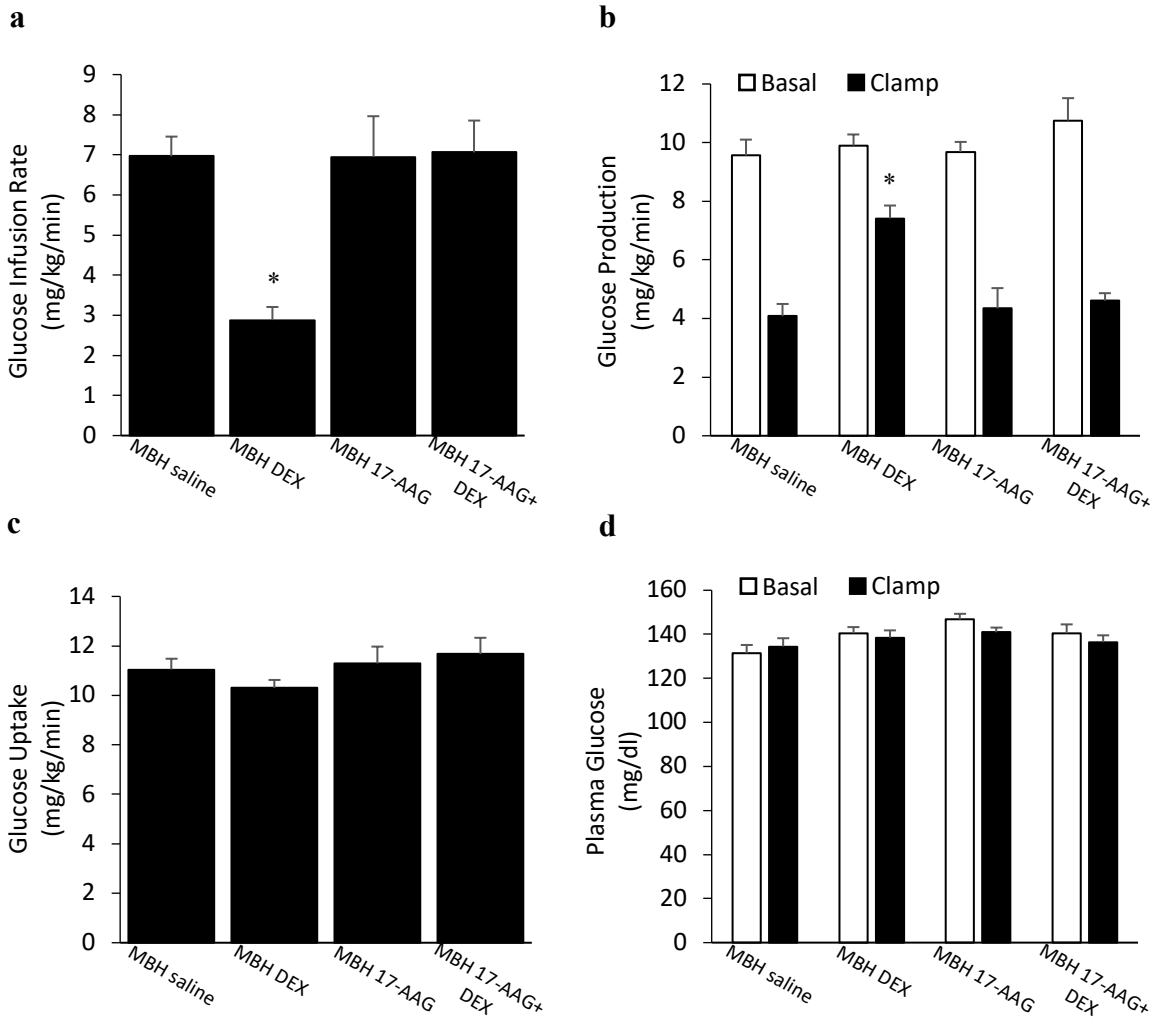

Figure 3.3.1 – Chemical inhibition of MBH Hsp90 negates the glucoregulatory effects of MBH DEX during pancreatic mild hyperinsulinemic (1.2mU/min/kg) euglycemic clamp experimentation in RC-fed rats. a) Glucose infusion rates, b) glucose production, c) glucose uptake and d) plasma glucose levels. MBH infusion of saline (n=13), DEX (n=14), 17-AAG (n= 7) and 17-AAG+DEX (n=7). $^{*}P<0.05$ for MBH DEX versus MBH saline, MBH 17-AAG and MBH 17-AAG+DEX.

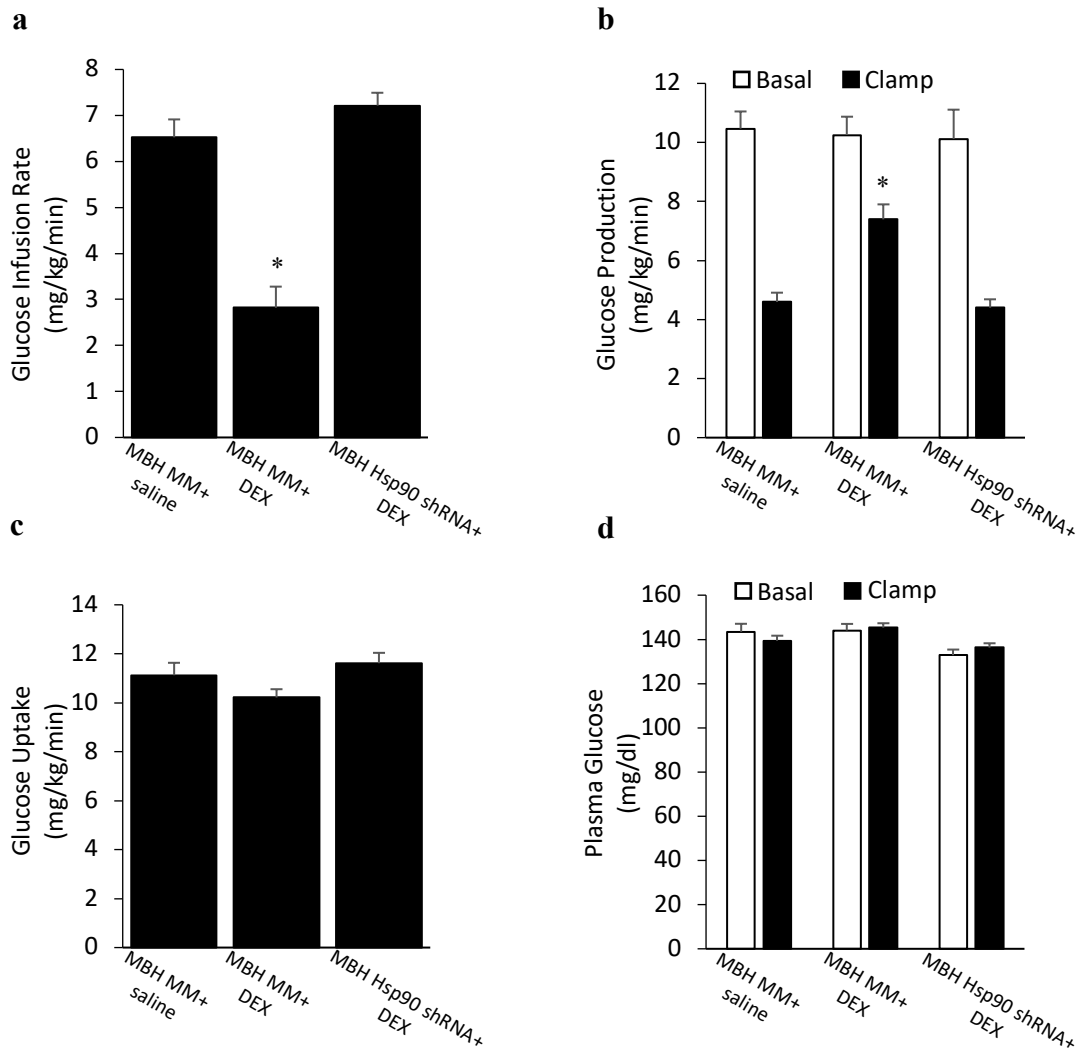

Figure 3.3.2 – Molecular knockdown of MBH Hsp90 negates the glucoregulatory effects of MBH DEX during pancreatic mild hyperinsulinemic (1.2mU/min/kg) euglycemic clamp experimentation in RC-fed rats. a) Glucose infusion rates, b) glucose production, c) glucose uptake and d) plasma glucose levels. MBH infusion of LV-MM+saline (n=12), LV-MM+DEX (n=9) and LV-Hsp90 shRNA+DEX (n=6). *P<0.05 for LV-MM+DEX versus LV-MM+saline and LV-Hsp90 shRNA+DEX.

3.4 – 3-day HFD feeding induces metabolic disturbances independent of changes in body weight

In order to assess a therapeutic relevance for MBH GR inhibition on improving glucose homeostasis, we investigated the effects of our acute model of HFD feeding on glucoregulation. We first confirmed that a separate group of rats fed with a 10% HFD for 3 days had elevated plasma CORT levels that were measured in the morning (e.g. at the circadian trough) and were mildly hyperglycemic and hyperinsulinemic when compared to the rats fed on a RC-diet (figure 3.4.1a-c) independent of changes in body weight (figure 3.4.1d). Therefore, our model of acute HFD feeding for 3 days induced metabolic disturbances before the onset of obesity, in line with what has been previously documented with this model[168,169,178,179].

In addition, 3-day HFD feeding impaired glucose tolerance. When compared to RC-fed rats, HFD increased basal and peak plasma glucose levels and slowed glucose clearance rate in MBH saline control animals subjected to a glucose bolus during ivGTT experimentation (figure 3.4.2a). Interestingly, insulin levels were also generally increased throughout the experiment in the HFD-fed group (figure 3.4.2b) in line with elevated plasma glucose levels. Future AUC analyses for plasma glucose and insulin responses could shed light into the extent glucose intolerance.

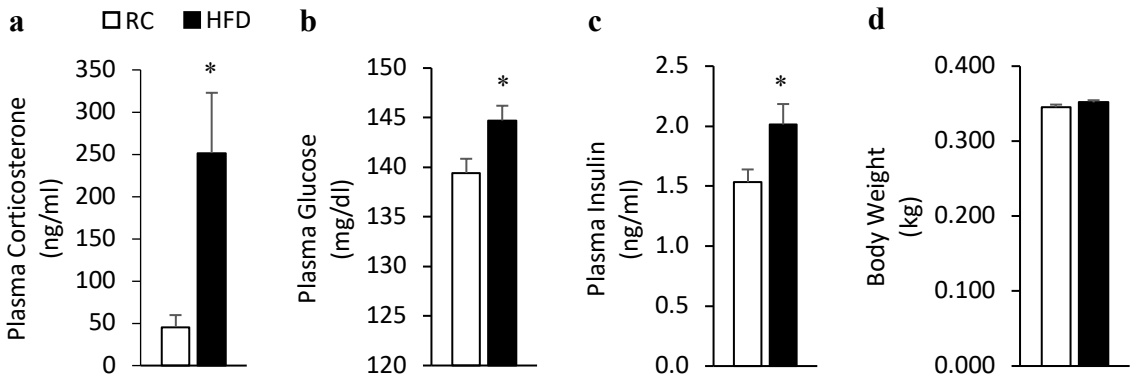

Figure 3.4.1 – Basal levels of corticosterone, blood glucose, insulin, and body weights of 3-day HFD-fed rats compared to RC controls (5h fast). Data corresponds to plasma collected and body weights morning of clamp experimentation. a) Plasma corticosterone in RC group (n=9, white bars) and HFD (n=10, black bars). b) Plasma glucose in RC group (n=56) and HFD (n=37). c) Plasma insulin in RC group (n=26) and HFD (n=19). d) Body weight in RC group (n=56) and HFD (n=38). $^{*}P<0.05$. *Pooled data at start of experiments prior to dividing animals into experimental groups.*

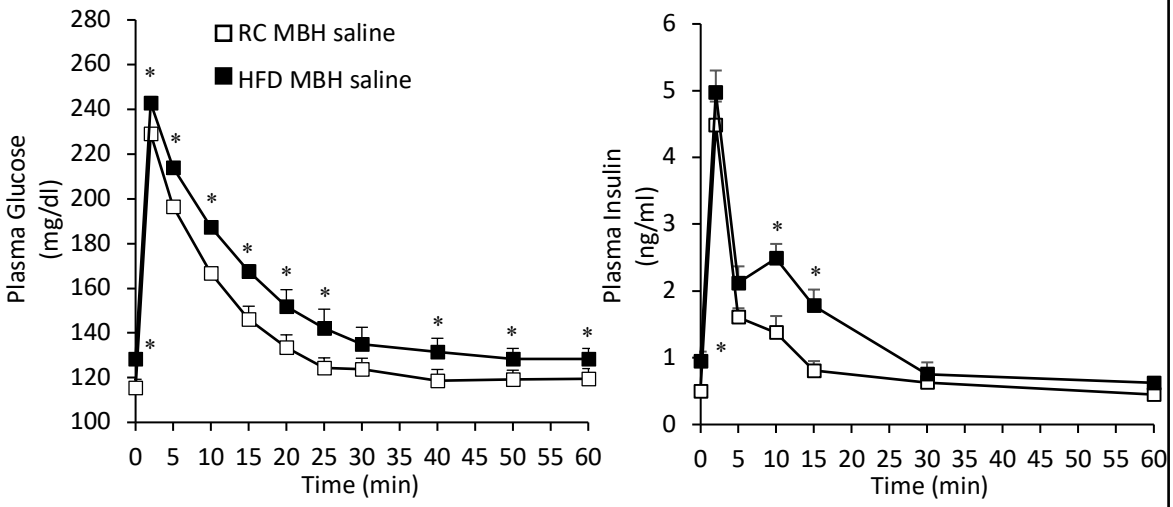

Figure 3.4.2 – 3-day HFD feeding impairs glucose tolerance during ivGTT experimentation compared to RC MBH saline controls. a) Plasma glucose in RC group (n=9, white squares) and HFD (n=9, black squares). b) Plasma insulin in RC group (n=9) and HFD (n=10). *P<0.05. *Experiments performed by undergraduate student HK (2017-2018)*.

3.5 – 3-day HFD feeding induces hepatic insulin resistance

Given that rats fed a 3-day HFD had altered glucose homeostasis, basal insulin (0.8mU/min.kg) euglycemic clamps were next performed to investigate more closely what glucose kinetic mechanisms were involved in this disruption. When compared to RC MBH saline controls, HFD animals had significantly decreased GIRs in order to maintain euglycemia (figure 3.5.1a) despite their elevated plasma glucose levels (figure 3.5.1d). In addition, HFD stimulated an increase in hepatic GP during the clamp and insulin induced suppression of GP was of only 23% compared to 51% in RC MBH saline controls (figure 3.5.1b) independent of changes in GU (figure 3.5.1c) and glucagon levels (table 3.2.1). Analysis of plasma samples following clamp experimentation demonstrated that HFD MBH saline control animals maintain elevated levels of plasma insulin until the end of the clamp, but peripheral CORT concentrations are not different later in the afternoon at the diurnal peak when the clamp period occurs (table 3.2.1). In other words, HFD for as little as 3 days led to hepatic insulin resistance in rats but did not induce peripheral insulin resistance[179].

We next wondered what would be the effect on glucose kinetics in HFD-fed MBH saline control animals if the dose of insulin would be increased to be mildly hyperinsulinemic (1.2mU/min/kg). When compared to basal insulin doses, mild hyperinsulinemic clamp experimentation performed on HFD-fed rats showed similar suppression of hepatic GP from basal (23% vs 29%, 0.8 vs 1.2mU/min/kg insulin dose; figure 3.5.2b) and similar GIR needed to maintain euglycemia (2.1±0.6 vs 3.7±0.8mg/kg/min, 0.8 vs 1.2mU/min/kg insulin dose; figure 3.5.2a) without affecting GU in peripheral tissues (figure 3.5.2c). Most importantly, increasing the insulin dose by 1.5x

still resulted in HFD-fed rats needing a considerably lower amount of exogenous glucose to maintain euglycemia compared to RC MBH saline controls (figure 3.5.3a). Furthermore, HFD-mediated stimulation of hepatic GP was maintained during the clamp under mild hyperinsulinemic conditions (figure 3.5.3b).

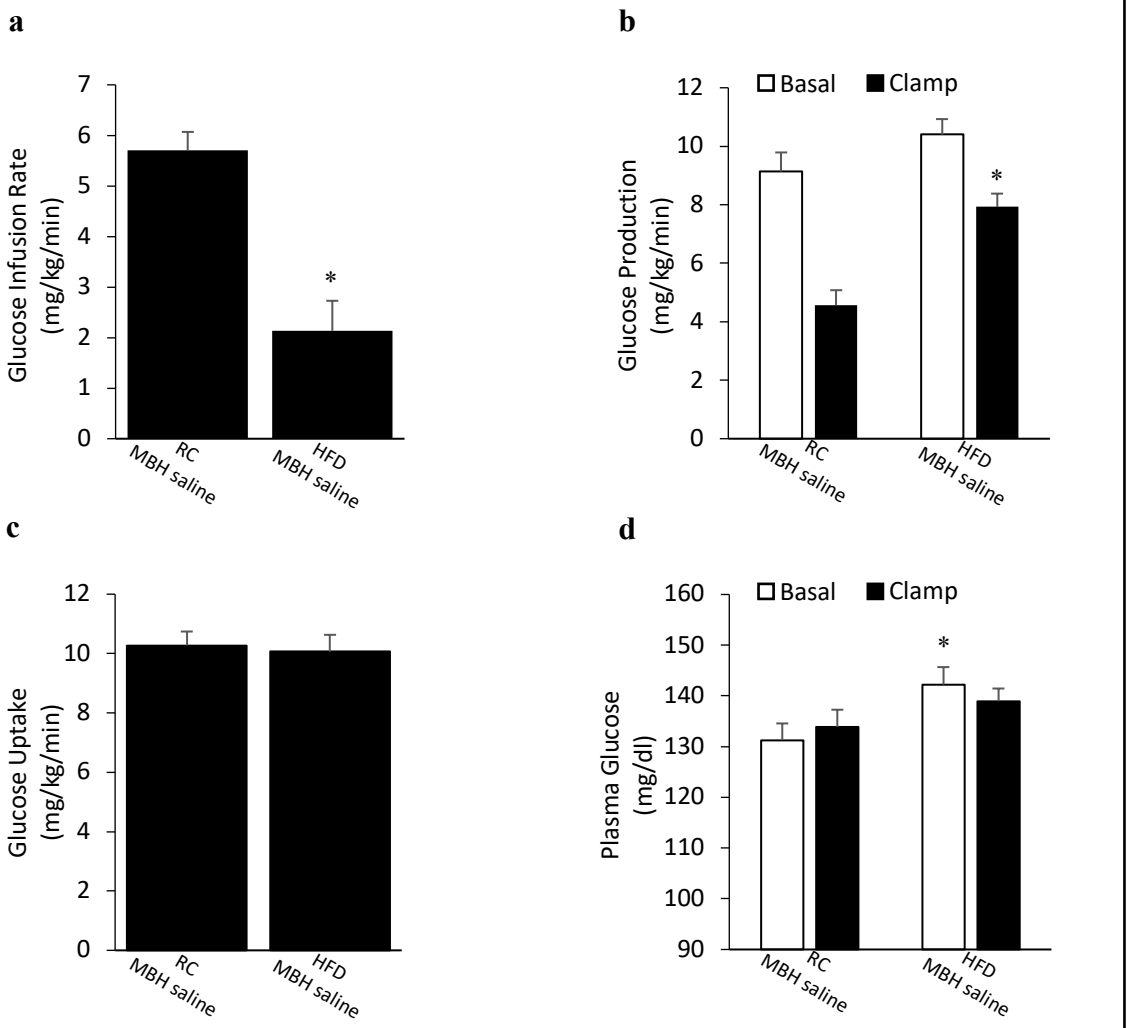

Figure 3.5.1 – 3-day HFD feeding stimulates hepatic glucose production during pancreatic basal insulin (0.8mU/min/kg) euglycemic clamp experimentation compared to RC-fed rats. a) Glucose infusion rates, b) glucose production, c) glucose uptake and d) plasma glucose levels. RC group (n=12) and HFD (n=10). $^{*}P<0.05$ for HFD versus RC.

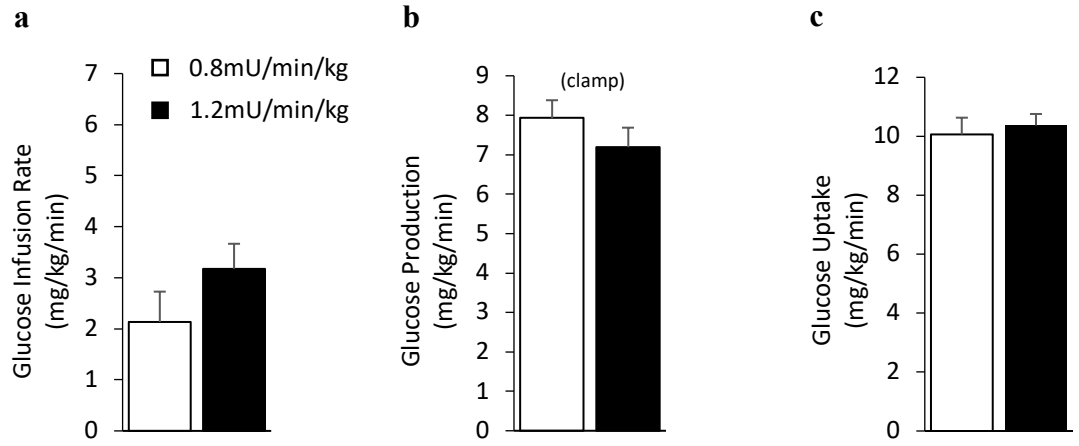

Figure 3.5.2 – Glucose infusion rates, glucose production and glucose uptake during pancreatic basal insulin (0.8mU/min/kg) compared to mild hyperinsulinemic (1.2mU/min/kg) euglycemic clamp experimentation in 3-day HFD-fed controls. HFD MBH saline+0.8mU/min.kg group (n=10, white bars) and HFD MBH saline+1.2mU/min.kg group (n=10, black bars).

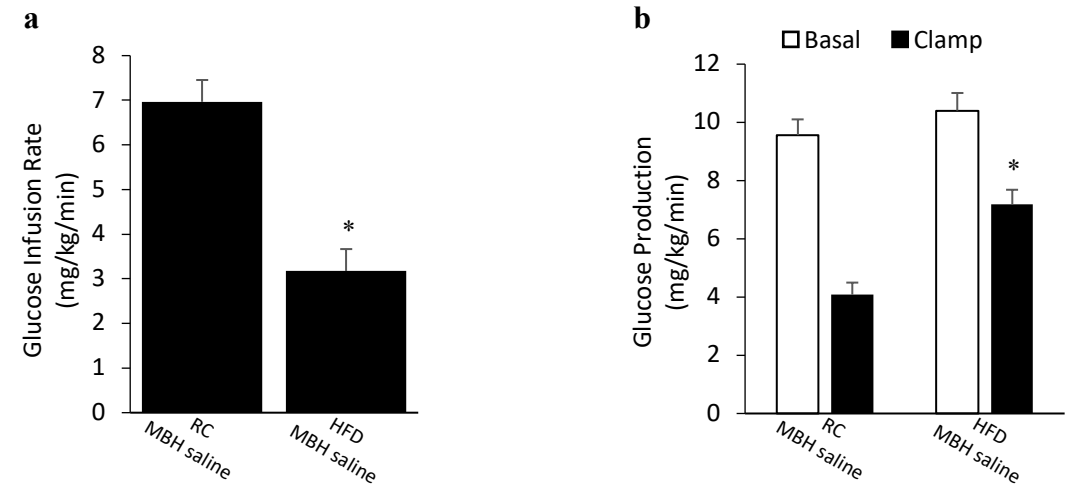

Figure 3.5.3 – 3-day HFD feeding stimulates hepatic glucose production during pancreatic mild hyperinsulinemic (1.2mU/min/kg) euglycemic clamp experimentation compared to RC-fed rats. a) Glucose infusion rates and b) glucose production. RC group (n=13) and HFD (n=10). *P<0.05 for HFD versus RC.

3.6 – Stimulation of hepatic glucose production following 3-day HFD feeding is mediated through MBH GRs

Given that 3-day HFD feeding elevated plasma CORT levels and impaired glucose homeostasis compared to regular RC-fed rats, we postulated that elevated circulating CORT, which crosses the blood-brain-barrier, would activate MBH GRs similar to MBH DEX infusions in RC-fed rats. In other words, we postulated that this increase in MBH GC action in HFD-fed rats contributes to dysregulated glucose metabolism. Thus, we next investigated whether blocking excessive MBH GC action would attenuate GP to improve glucose homeostasis in our model of pre-obesity. In 3-day HFD-fed rats, an MBH infusion of the GR antagonist MIF during mild hyperinsulinemic clamp experimentation drastically increased the need for exogenous glucose (figure 3.6.1a) and significantly suppressed GP at clamp (51%) compared to HFD MBH saline controls (29%) (figure 3.6.1b). These changes occurred independently of any differences in body weight (0.354±0.004kg for MBH saline; 0.346±0.003kg for MBH MIF). MBH MIF in HFD successfully restored hepatic GP at clamp (4.8±0.2mg/kg/min) to glucose production rates comparable to RC MBH saline controls (4.1±0.4mg/kg/min; figure 3.5.3b) independent of changes in GU or plasma glucose levels (figure 3.6.1c-d). This data suggests that elevated levels of circulating CORT induced by HFD feeding is sensed by MBH GRs and that subsequent MBH GC action impairs hepatic insulin sensitivity. In addition, further stimulating MBH GRs in HFD with a MBH DEX infusion does not further impair glucose kinetics (figure 3.6.1).

In addition to acute MBH GR inhibition with MBH MIF, we also investigated whether chronically knocking down MBH GRs using GR shRNA would also improve glucose homeostasis in HFD-fed rats. As expected, HFD MBH LV injection did not affect

HFD-induced impairments in metabolism (figure 3.6.2). Likewise to an acute MBH MIF infusion, MBH GR shRNA negated the glucostimulatory effects of HFD feeding on glucose homeostasis. MBH GR shRNA increased the need for exogenous glucose to maintain euglycemia (figure 3.6.2a) and suppressed hepatic GP at clamp when compared to HFD MBH MM saline controls (figure 3.6.2b). The improvement in hepatic insulin sensitivity in HFD feeding following chronic inhibition of MBH GRs occurred without any changes in basal and clamp plasma glucose levels (figure 3.6.2d) and independently of changes in GU (figure 3.6.2c). Therefore, blocking excessive MBH GC action with either acute or chronic MBH GR inhibition attenuates HFD-stimulated hepatic GP and leads to an improvement in glucose homeostasis.

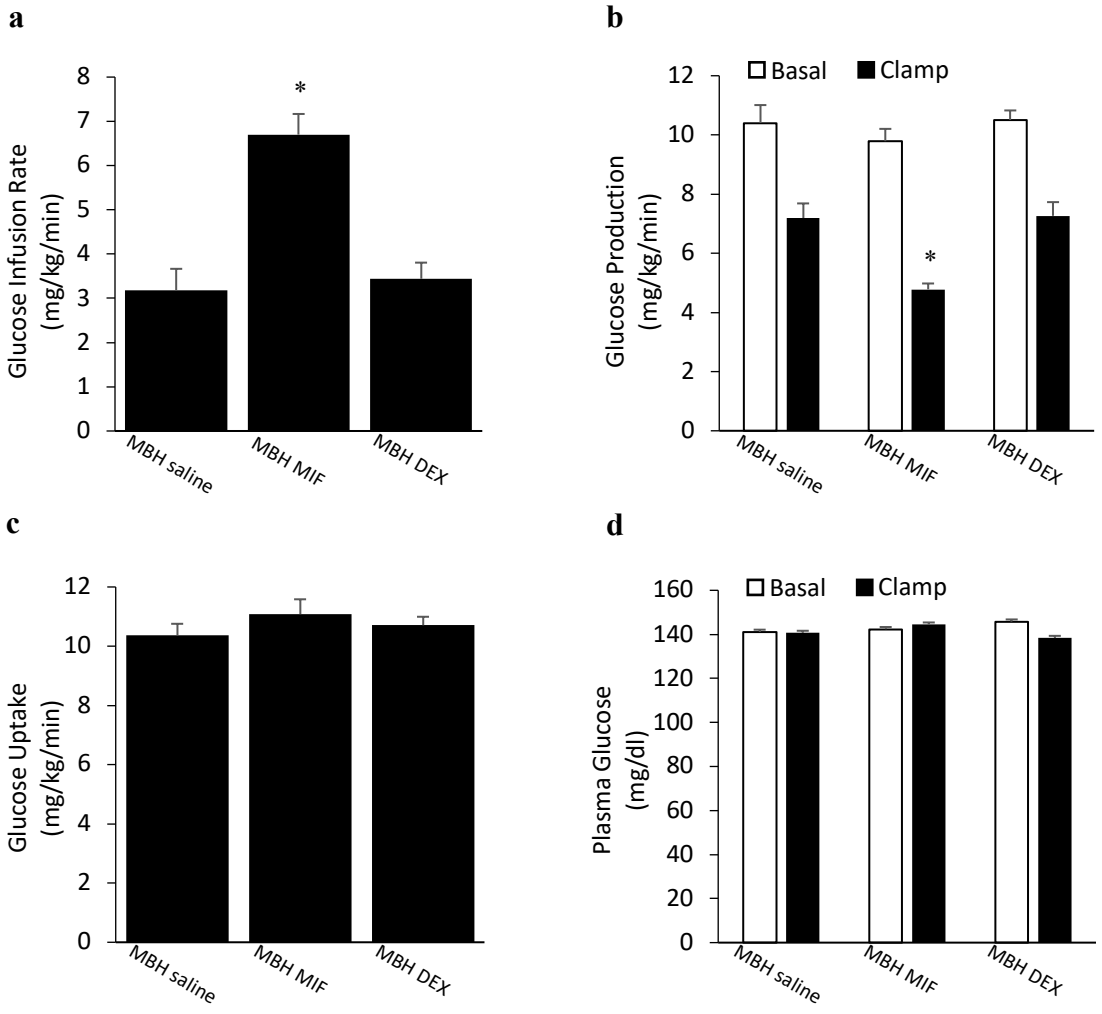

Figure 3.6.1 – Chemical inhibition of MBH GRs negates the glucoregulatory effects of 3-day HFD during pancreatic mild hyperinsulinemic (1.2mU/min/kg) euglycemic clamp experimentation. a) Glucose infusion rates, b) glucose production, c) glucose uptake and d) plasma glucose levels. MBH infusion of saline (n=10), MIF (n=11) and DEX (n=7). $^{*}P<0.05$ for MBH MIF versus MBH saline and MBH DEX.

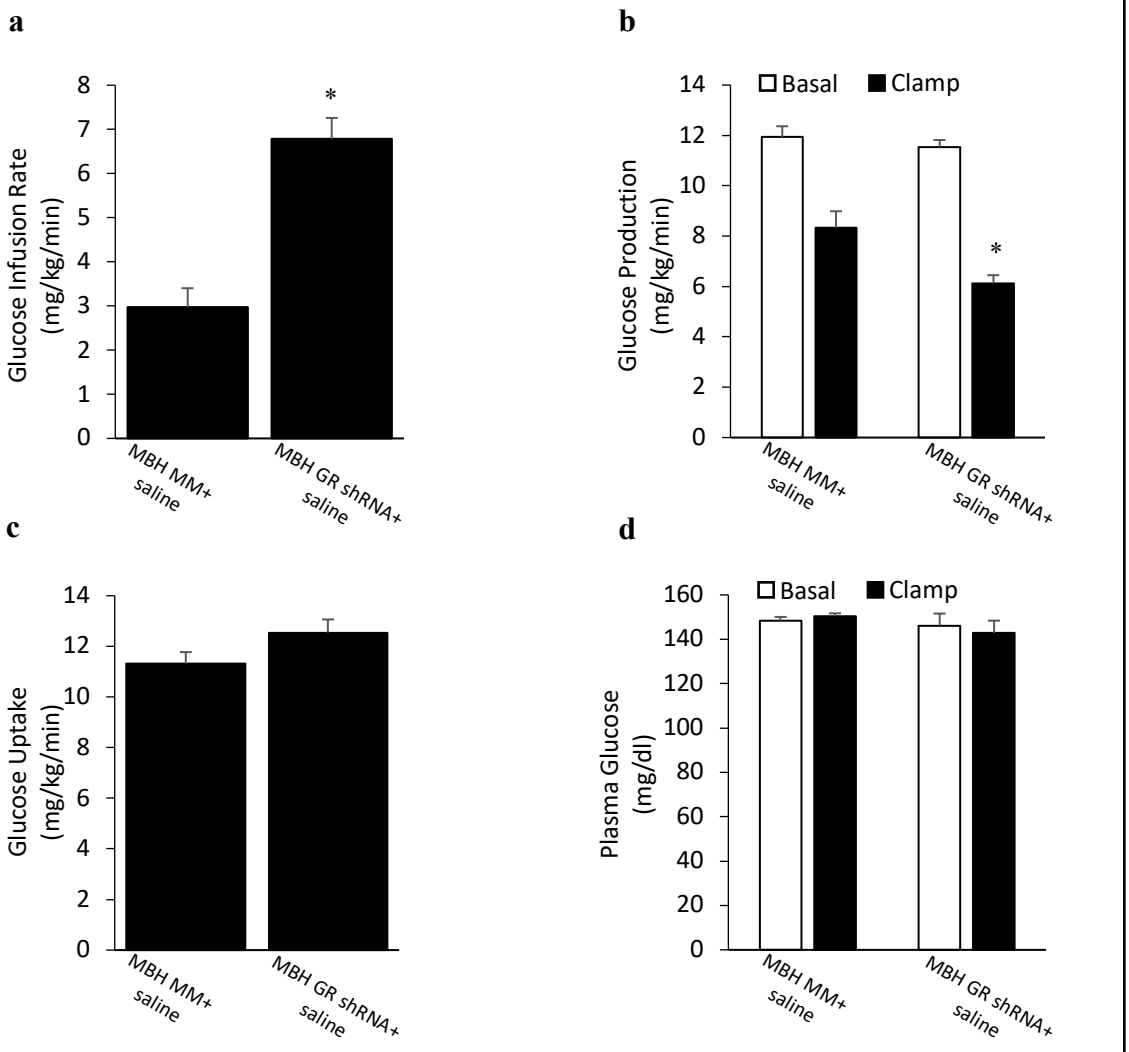

Figure 3.6.2 – Molecular knockdown of MBH GRs negates the glucoregulatory effects of 3-day HFD during pancreatic mild hyperinsulinemic (1.2mU/min/kg) euglycemic clamp experimentation. a) Glucose infusion rates, b) glucose production, c) glucose uptake and d) plasma glucose levels. MBH infusion of LV-MM+saline (n=9) and LV-GR shRNA+saline (n=8). *P<0.05 for LV-GR shRNA+saline versus LV-MM+saline.

3.7 – Inhibition of MBH Hsp90 does not improve glucose homeostasis in 3-day HFD feeding

Given that MBH GRs are involved in HFD-mediated stimulation of hepatic GP and that blocking excessive MBH GC action improves glucose homeostasis, and that we had demonstrated that inhibition of MBH Hsp90 prevents MBH DEX induced stimulation of GP in RC-fed rats, it was hypothesised that MBH Hsp90 inhibition would yield a similar improvement and restore glucose metabolism in pre-obese rats. Unexpectedly, acutely infusing the pharmacological Hsp90 inhibitor 17-AAG into the MBH of 3-day HFD-fed rats had no effect on the GIR, GP, GU or plasma glucose levels when compared to HFD MBH saline controls (figure 3.7.1) during mild hyperinsulinemic euglycemic clamp experimentation.

The involvement of MBH Hsp90 in MBH GC-mediated signalling in HFD-fed rodents was further investigated in rats with chronically knocked-down MBH Hsp90 in order to assess whether longer term MBH Hsp90 inhibition could help improve glucose homeostasis. In RC-fed rats, in congruence with acute MBH Hsp90 inhibition with 17-AAG, chronic inhibition with MBH Hsp90 shRNA did not affect the GIR, GP, GU or plasma glucose levels when compared to HFD MM MBH saline controls (figure 3.7.2) during mild hyperinsulinemic euglycemic clamp experimentation. According to this data, it would seem like MBH GC-mediated signalling in HFD-fed differs from healthy RC-fed rats and is mediated through a non-classical nuclear signalling pathway occurring independently of MBH Hsp90.

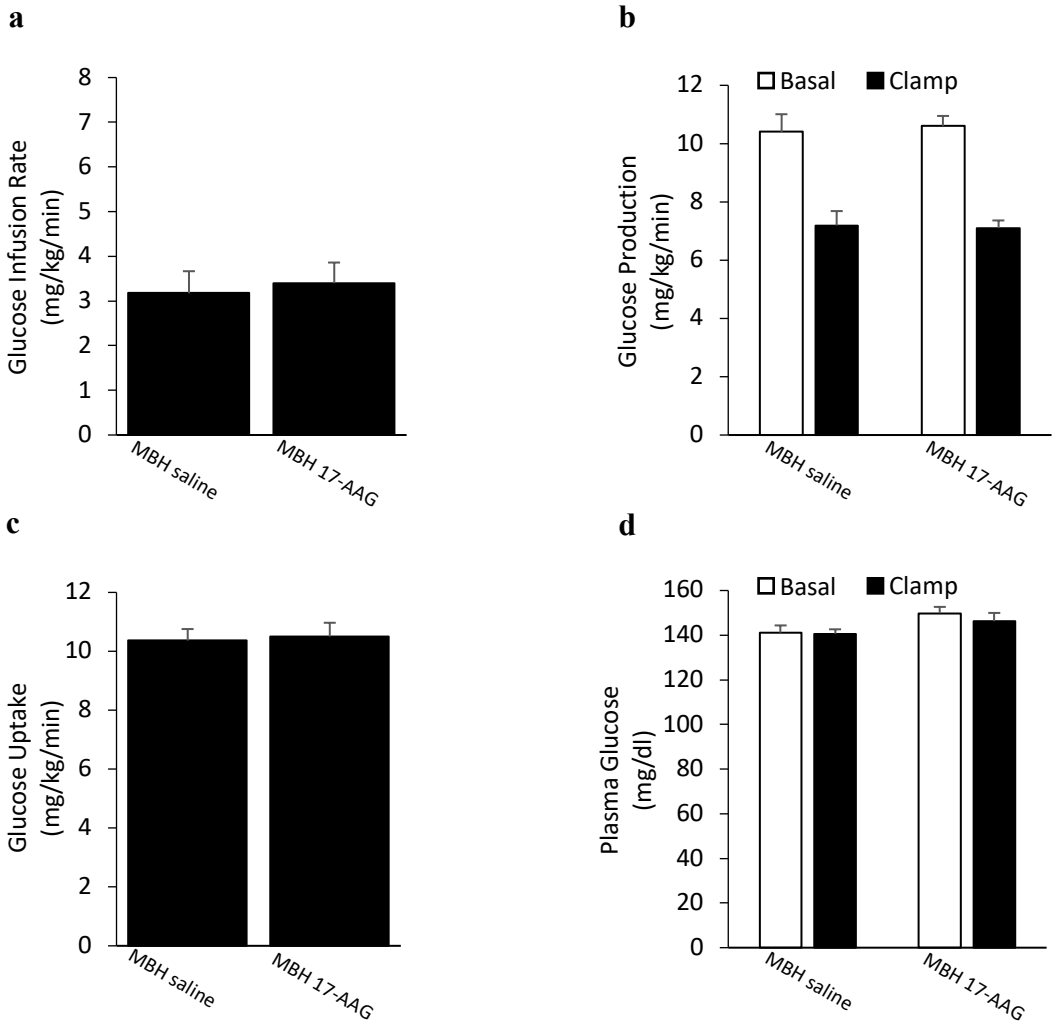

Figure 3.7.1 – Chemical inhibition of MBH Hsp90 does not negate the glucoregulatory effects of 3-day HFD during pancreatic mild hyperinsulinemic (1.2mU/min/kg) euglycemic clamp experimentation. a) Glucose infusion rates, b) glucose production, c) glucose uptake and d) plasma glucose levels. MBH infusion of saline (n=10) and 17-AAG (n=11).

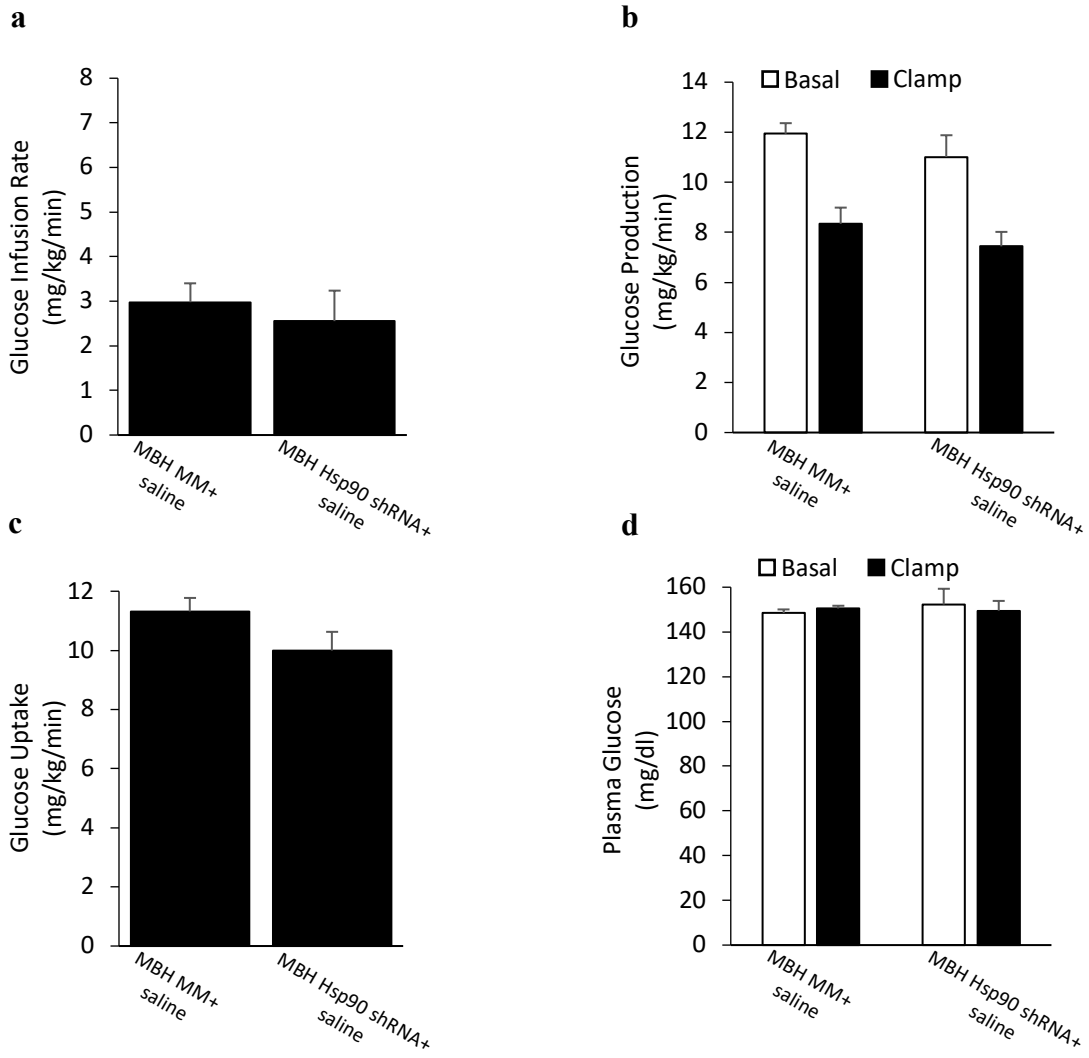

Figure 3.7.2 – Molecular knockdown of MBH Hsp90 does not negate the glucoregulatory effects of 3-day HFD during pancreatic mild hyperinsulinemic (1.2mU/min/kg) euglycemic clamp experimentation. a) Glucose infusion rates, b) glucose production, c) glucose uptake and d) plasma glucose levels. MBH infusion LV-MM+saline (n=9) and LV-Hsp90 shRNA+saline (n=8).

	MBH saline RC	MBH DEX RC	MBH saline HFD
Basal			
Insulin (ng/ml)	0.8 ± 0.1	1.3 ± 0.1*	1.9 ± 0.2*
Glucagon (pg/ml)	40.8 ± 2.4	46.1 ± 3.6	43.2 ± 3.1
Corticosterone (ng/ml)	81.5 ± 36.0	23.6 ± 1.6	348.1 ± 48.1*
Clamp			
Insulin (ng/ml)	0.9 ± 0.1	1.1 ± 0.1*	1.6 ± 0.2*
Glucagon (pg/ml)	34.4 ± 5.3	41.3 ± 2.1	40.3 ± 2.2
Corticosterone (ng/ml)	301.9 ± 59.0	343.6 ± 82.3	417.7 ± 62.5

Table 3.2.1 – Plasma insulin, glucagon and corticosterone concentrations during basal and clamp periods of basal insulin (0.8mU/min/kg) euglycemic clamp experimentation. Basal: t=60-90min, Clamp: t=210-240min. Error bars represent S.E.M. *P<0.05 for RC MBH DEX and HFD MBH saline versus RC MBH saline.

	MBH saline RC	MBH DEX RC	MBH saline HFD	MBH MIF HFD
Basal				
Insulin (ng/ml)	0.8 ± 0.1	1.7 ± 0.3*	1.8 ± 0.2*	1.4 ± 0.2*
Clamp				
Insulin (ng/ml)	2.1 ± 0.2^{T}	2.3 ± 0.2^{T}	1.8 ± 0.2	1.6 ± 0.1
Corticosterone (ng/ml)	448.7 ± 63.2	363.0 ± 138.3	512.4 ± 43.8	390.2 ± 88.6

Table 3.2.2 – Plasma insulin and corticosterone concentrations during basal and clamp periods of mildly hyperinsulinemic (1.2mU/min/kg) euglycemic clamp experimentation. Basal: t=60-90min, Clamp: t=210-240min. Error bars represent S.E.M. *P<0.05 for RC MBH DEX, HFD MBH saline and HFD MBH MIF versus RC MBH saline. ^{T}P<0.05 for value during mildly-hyperinsulinemic clamp versus basal-insulin clamp (table 3.2.1).

3.8 – MBH-specific biochemical and molecular mechanisms involved in MBH GC-mediated regulation of hepatic glucose production

In order to begin revealing the underlying biochemical and molecular mechanisms that are responsible for some of the glucoregulatory effects of MBH GC in healthy and pre-obese states, western blotting was done on MBH wedges from different MBH treatment groups. In RC-fed animals, it was investigated whether acute MBH GC action following an infusion of MBH DEX during euglycemic clamp experimentation locally altered MBH GR, Hsp90 and Hsp70 protein levels. As aforementioned, in the cytosol GCs bind to a GR complex which includes chaperon proteins such as Hsp90 and Hsp70. While Hsp90 is required for GR activation and migration to the nucleus, Hsp70 is known to inactivate the GR through partial unfolding[48]. Quantification by densitometry of western blots demonstrated that following acute MBH DEX infusion, changes in MBH GR ($P=0.24$) and Hsp90 ($P=0.44$) protein levels are not significant while MBH Hsp70 protein abundance is modestly upregulated (figure 3.8.1). In HFD-fed animals, MBH GR protein levels were upregulated compared to healthy RC-fed rats but MBH Hsp90 ($P=0.29$) and MBH Hsp70 ($P=0.73$) protein levels were unaffected by 3-day HFD feeding (figure 3.8.2).

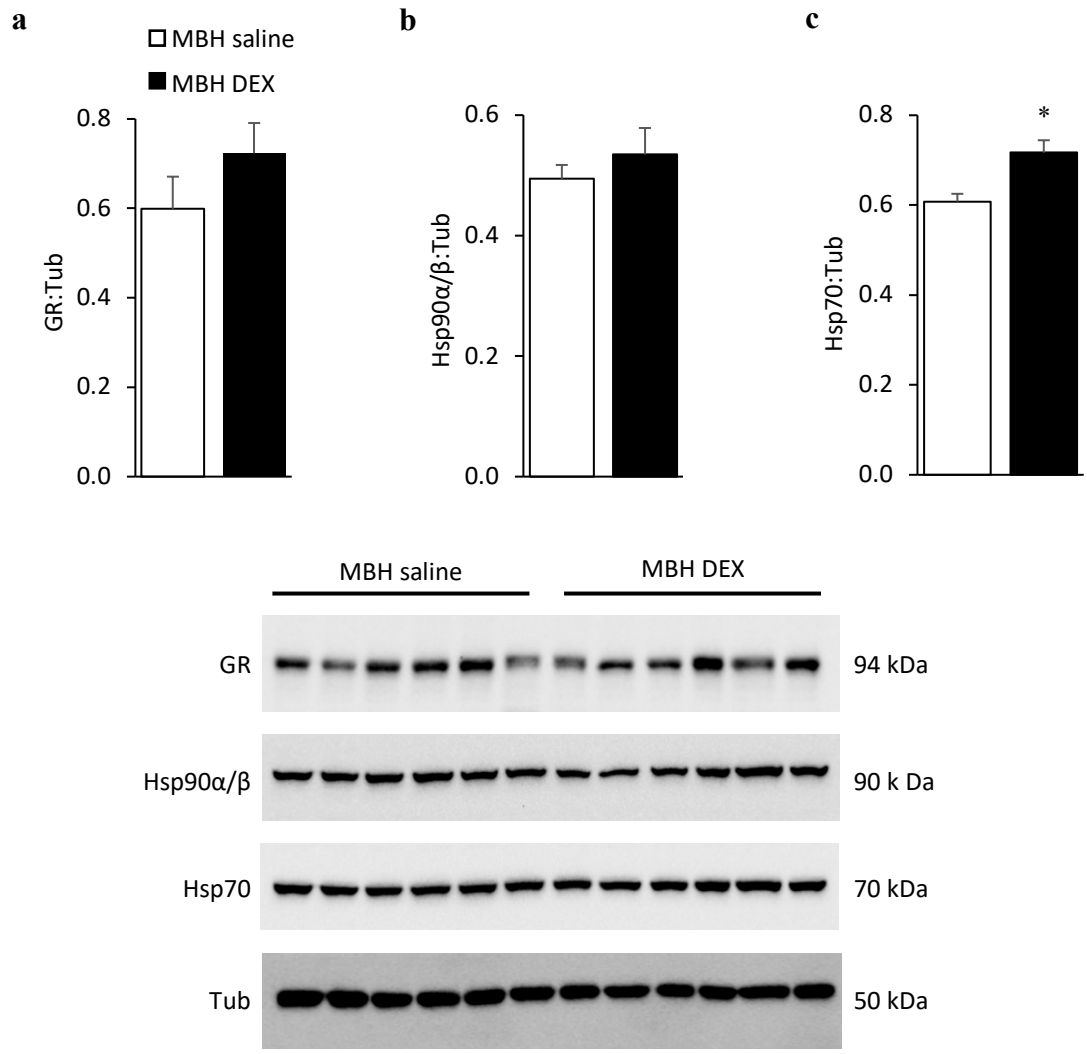

Figure 3.8.1 – Representative western blots and protein levels in MBH wedges normalized to tubulin (Tub) in RC-fed rats. a) GR, b) Hsp90α/β and c) Hsp70. MBH infusion saline (n=6, white bars) and DEX (n=6, black bars). $^{*}P<0.05$.

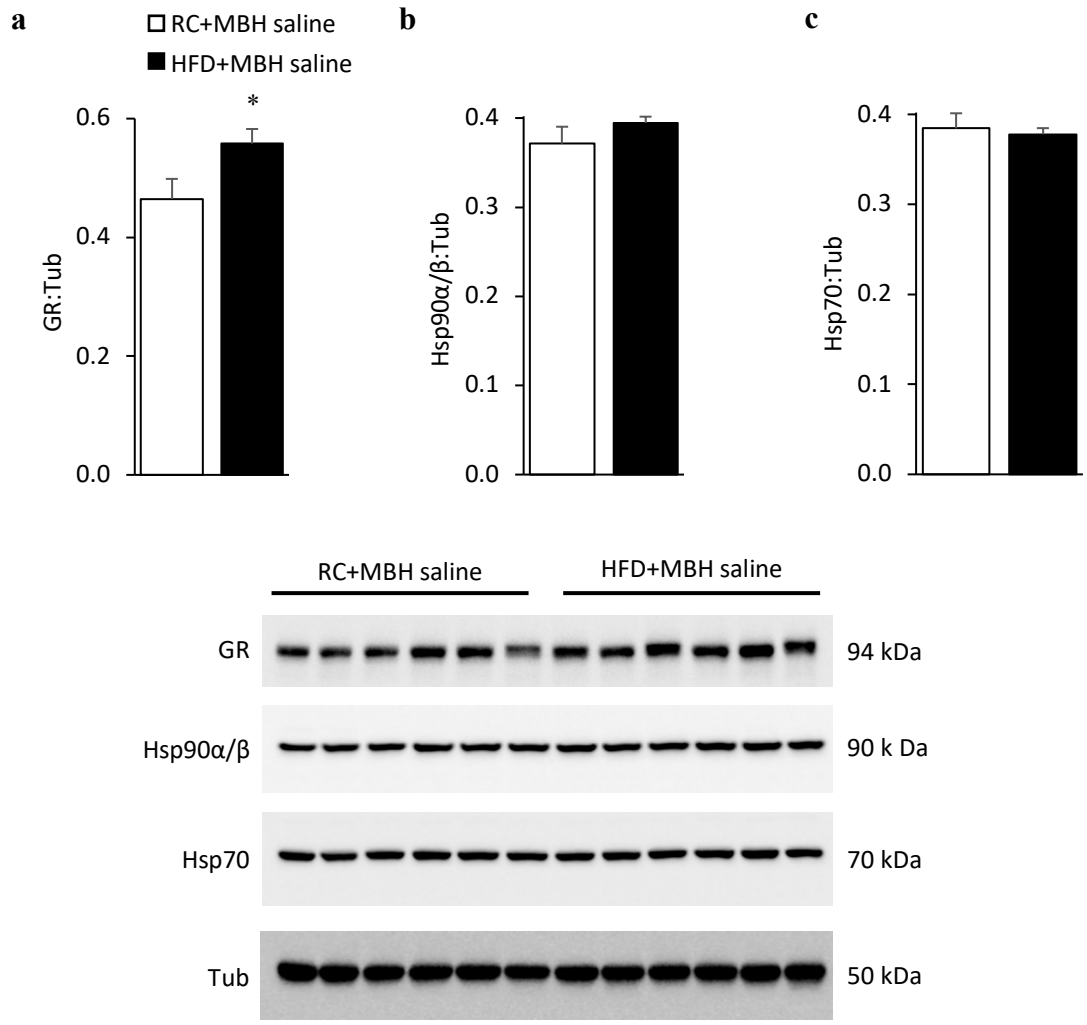

Figure 3.8.2 – Representative western blots and protein levels in MBH wedges normalized to tubulin (Tub) in 3-day HFD-fed compared to RC-fed rats. a) GR, b) Hsp90α/β and c) Hsp70. RC group (n=6, white bars) and HFD (n=6, black bars). *P<0.05.

3.9 – Liver-specific biochemical and molecular mechanisms involved in MBH GC-mediated regulation of hepatic glucose production

Western blotting and qRT-PCR were done on liver tissue from rats that underwent different MBH treatment groups and diets in order to start to understand the mechanisms underlying how brain GC signalling regulates peripheral tissues to elicit changes in glucose metabolism in healthy and pre-obese conditions. We first investigated whether MBH GC action following an acute infusion of MBH DEX or from 3-day HFD feeding induced any changes in protein levels of hepatic glucoregulatory enzymes (pPDH-E1α, PDH-E1α, PDK1, PDPc, HXK II, PEPCK) given that MBH DEX and HFD stimulates hepatic GP during euglycemic clamp experimentation. Whereas PEPCK is an enzyme involved in the gluconeogenesis pathway, HXK and PDH are involved in glycolysis. PDK inhibits PDH through phosphorylation (pPDH) and PDP reverses the effects of PDK on PDH by dephosphorylating pPDH (see figure 1.2.3 schematic of enzyme activities of glucose metabolism pathway).

Quantification by densitometry of western blots demonstrated that neither acute MBH DEX infusion, nor MBH MIF and MBH MIF+DEX infusions affected the protein levels of any of the glucoregulatory enzymes examined in the liver compared to MBH saline controls after being normalized to tubulin (figure 3.9.1 and 3.9.2). In HFD-fed animals, the same series of hepatic glucoregulatory enzymes were investigated. Although an acute infusion of MBH MIF improved glucose homeostasis in 3-day HFD-fed rats, this improvement in glucoregulation occurred independently of any significant changes in protein levels of the hepatic glucoregulatory enzymes examined (figure 3.9.3).

Gluconeogenic enzyme gene expression was next investigated as hypothalamic signalling following nutrient and hormone sensing has shown to regulate peripheral glucose through the modulation of hepatic expression of G6Pase and PEPCK. After being normalized to cyclophilin, qRT-PCR analysis demonstrated that in RC-fed rats acute MBH DEX infusion upregulated G6pc mRNA compared to MBH saline controls and this effect was blunted with a co-infusion of MBH MIF+DEX (figure 3.9.4a). In contrast, Pck1 expression was unaffected by any of the MBH treatments (figure 3.9.4b). In addition, MBH MIF had no effect on either G6pc or Pck1 gene expression in 3-day HFD-fed rats compared to MBH saline controls (figure 3.9.5).

Hepatic glycogen content was also measured in livers that were immediately feezed-clamped following euglycemic clamp experimentation. Acute MBH DEX infusion had no effect on glycogen content in the liver when compared to RC MBH saline controls (figure 3.9.6a). However, it should be noted that following a 5h fast plus 5h food deprivation during clamp experimentation glycogen content in rat livers would be expected to be low. In addition, MBH MIF did not significantly affect hepatic glycogen levels in 3-day HFD-fed rats compared to MBH saline controls (figure 3.9.6b), but it is important to note that sample sizes for this assay were small. Because glycogen breakdown contributes to hepatic GP and MBH MIF decreased GP compared to MBH saline, it could be expected that hepatic glycogen content would be greater in MBH MIF HFD-fed rats.

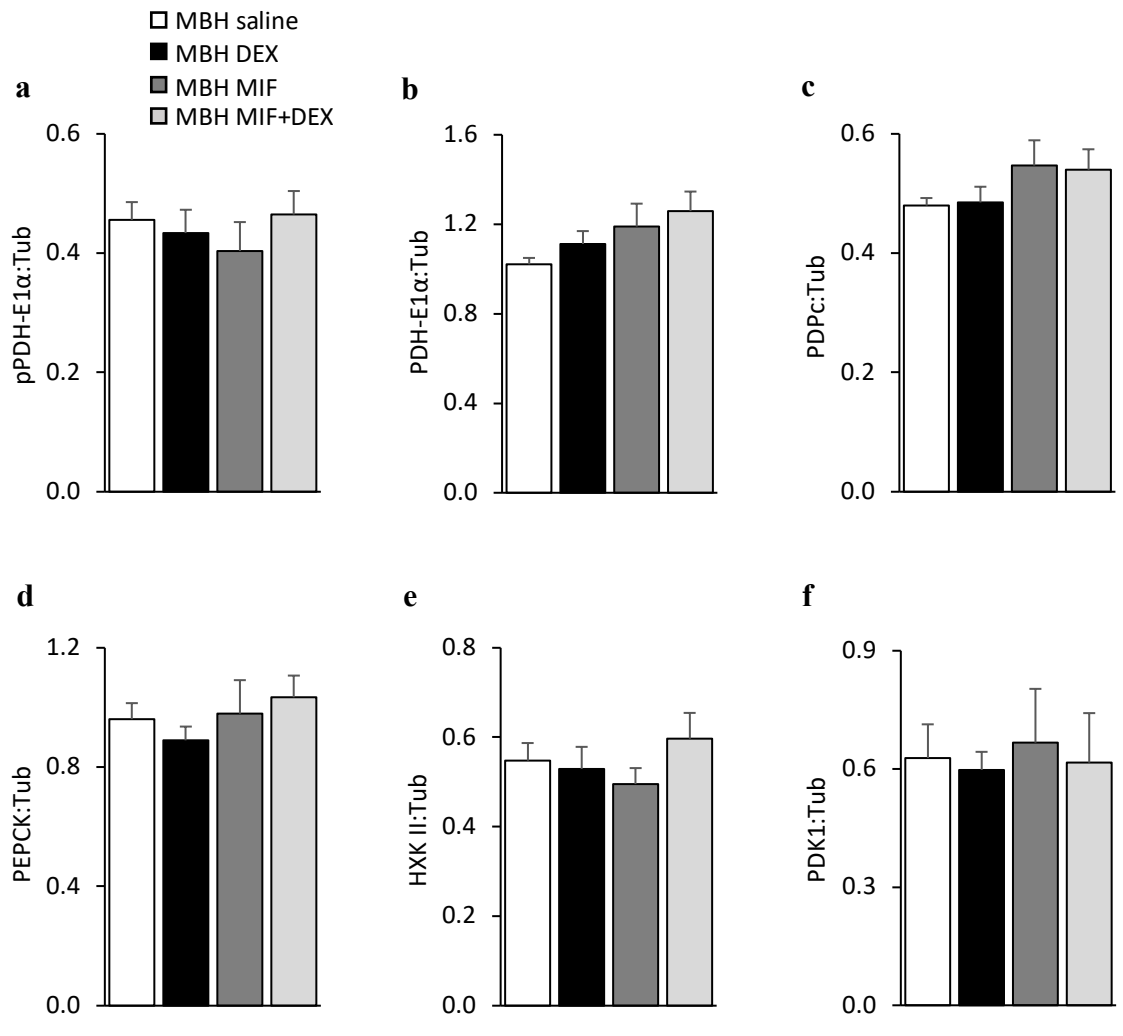

Figure 3.9.1 – Protein levels of glucoregulatory enzymes in liver tissue normalized to tubulin (Tub) in RC-fed rats. a) pPHD-E1α, b) PHD-E1α, c) PDPc, d) PEPCK, e) HXK II and f) PDK1. MBH infusion of saline (n=8), DEX (n=8), MIF (n=4) and MIF+DEX (n=5). Associated western blots are represented in figure 3.9.2.

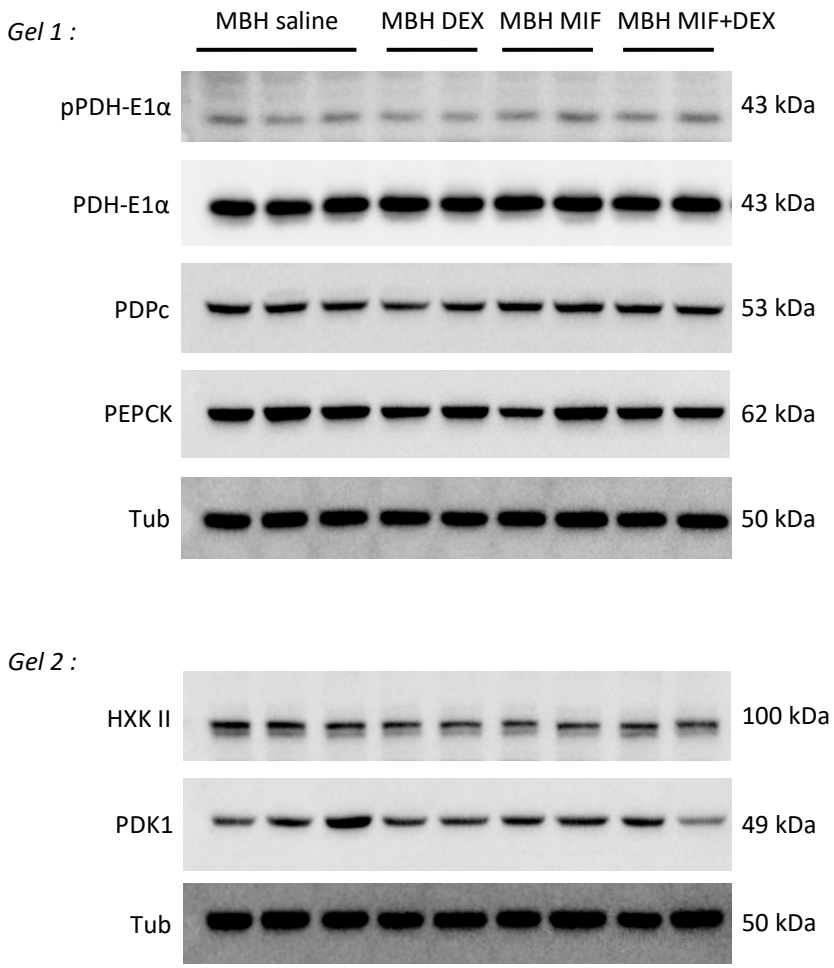

Figure 3.9.2 – Representative western blots for glucoregulatory enzymes in liver tissue normalized to tubulin (Tub) in RC-fed rats. Gel 1: pPHD-E1α, PHD-E1α, PDPc and PEPCK. Gel 2: HXK II and PDK1. MBH infusion of saline (n=8), DEX (n=8), MIF (n=4) and MIF+DEX (n=5). Associated with figure 3.9.1.

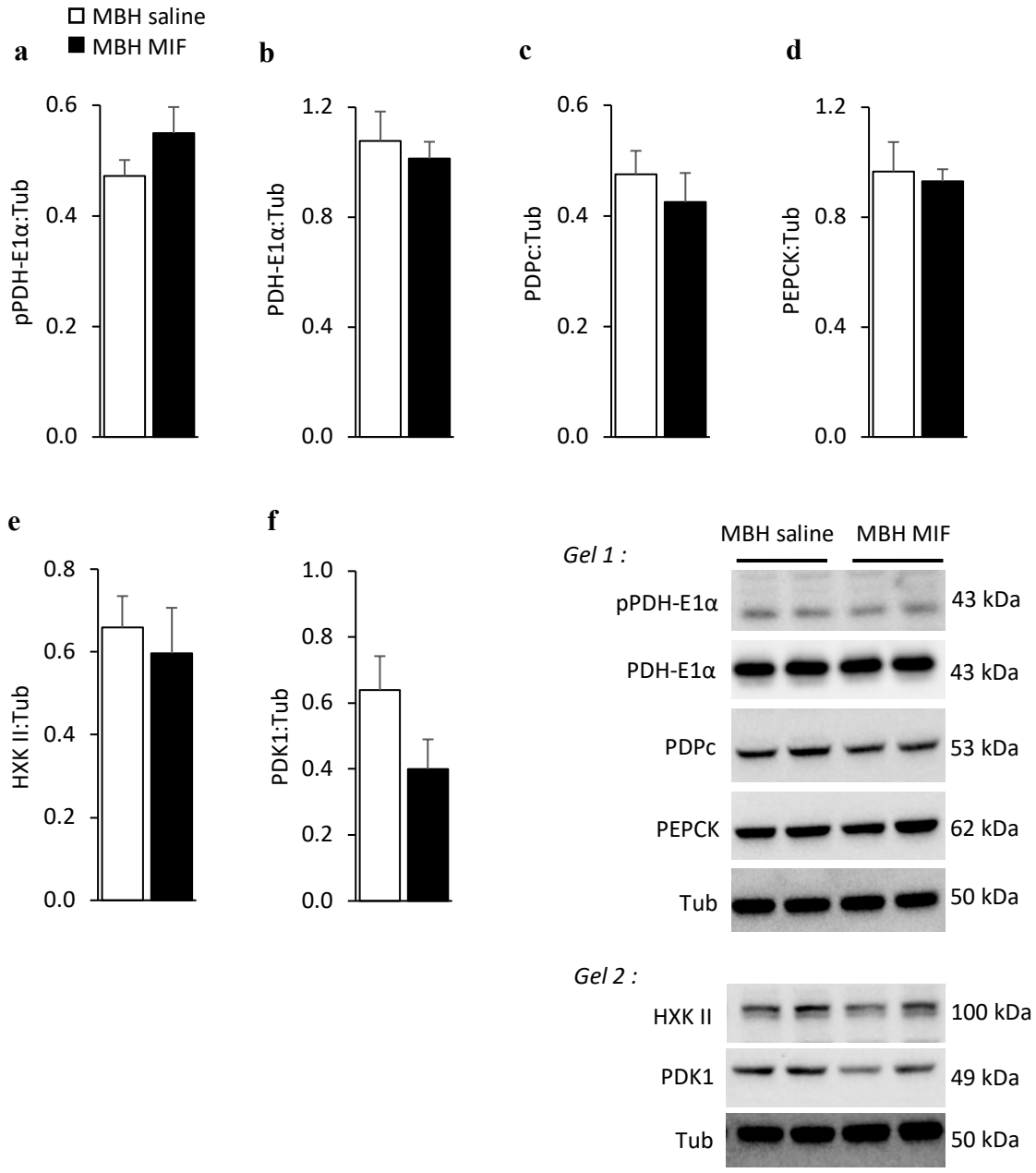

Figure 3.9.3 – Representative western blots and protein levels of glucoregulatory enzymes in liver tissue normalized to tubulin (Tub) in 3-day HFD-fed rats. Gel 1: a) pPHD-E1α, b) PHD-E1α, c) PDPc and d) PEPCK. Gel 2: e) HXK II and f) PDK1. MBH infusion of saline (n=5) and MIF (n=5).

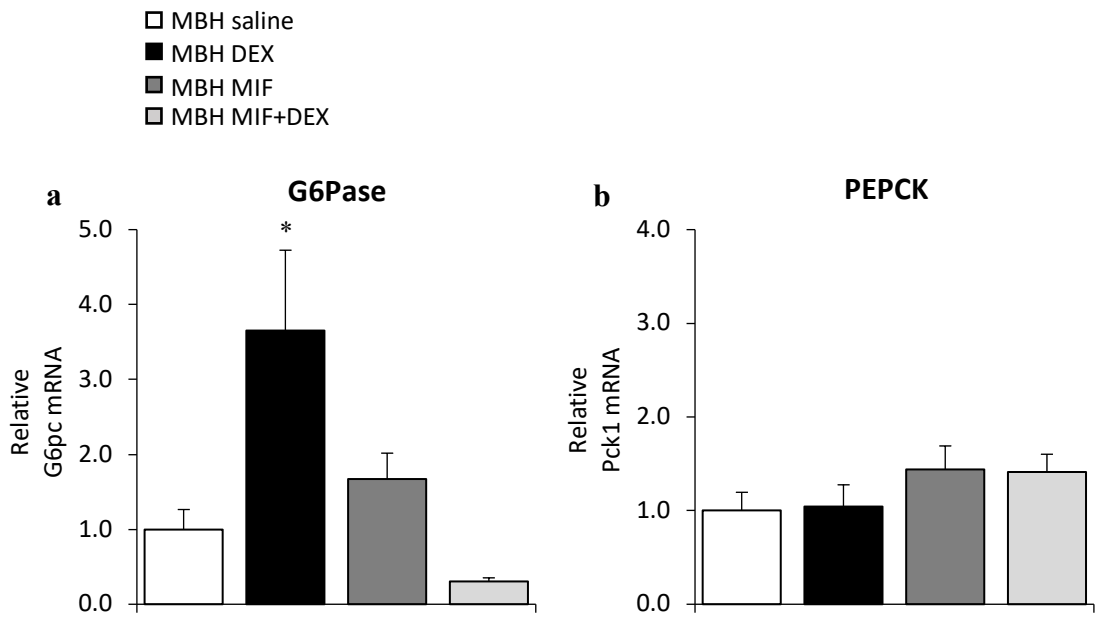

Figure 3.9.4 – Relative gene expression of gluconeogenic enzymes in liver tissue in RC-fed rats. a) G6pc gene (G6Pase), b) Pck1 gene (PEPCK). MBH infusion of saline (n=7/n=8), DEX (n=7/n=8), MIF (n=3/n=6) and MIF+DEX (n=5/n=8) [G6pc/Pck1]. MBH saline control normalized to 1.0. $^{*}P<0.05$ for MBH DEX versus MBH saline and MBH MIF+DEX.

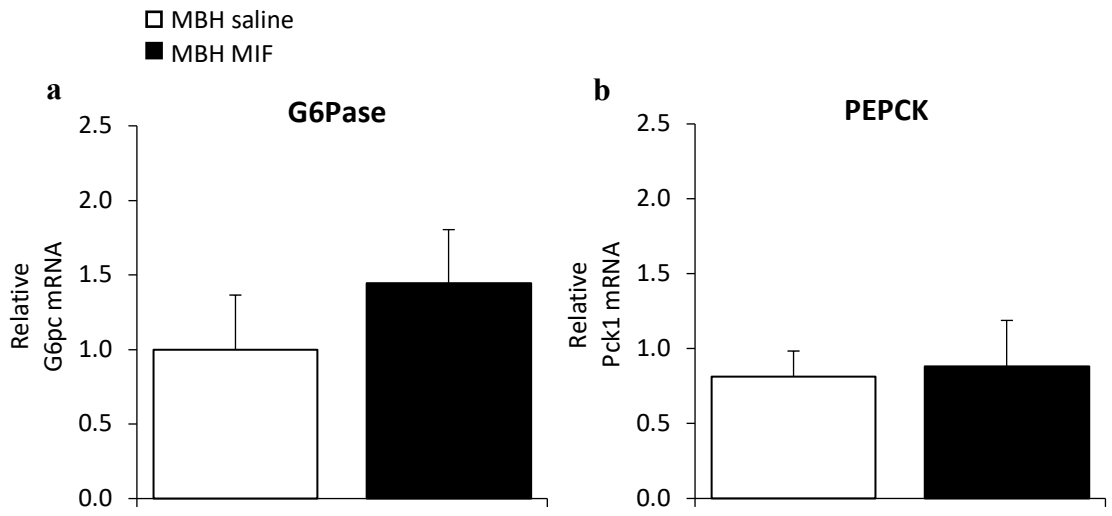

Figure 3.9.5 – Relative gene expression of gluconeogenic enzymes in liver tissue in 3-day HFD-fed rats. a) G6pc gene (G6Pase), b) Pck1 gene (PEPCK). MBH infusion of saline (n=5) and MIF (n=5). MBH saline control normalized to 1.0.

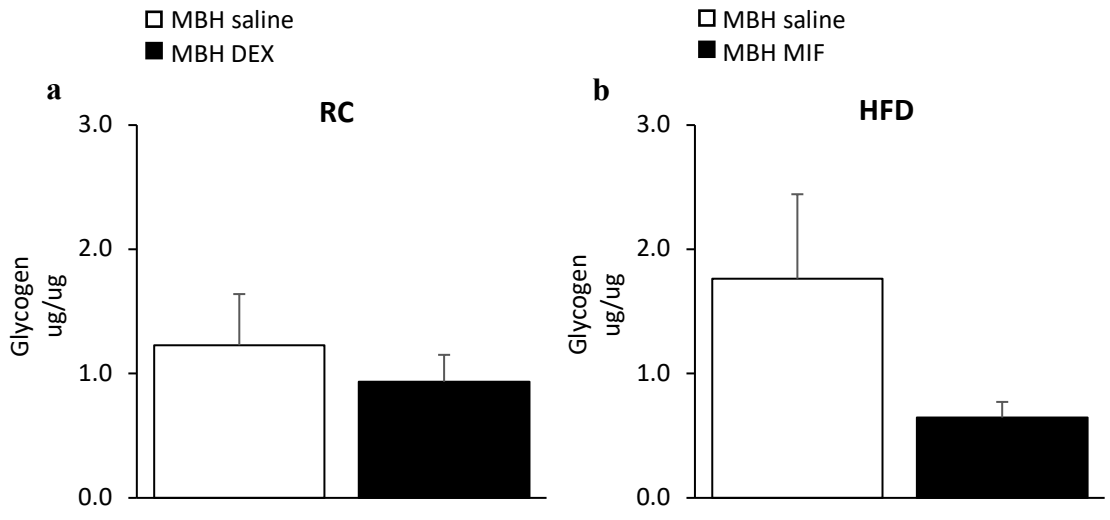

Figure 3.9.6 – Hepatic glycogen content in liver tissue in RC and 3-day HFD-fed rats. a) RC; MBH infusion of saline (n=5) and DEX (n=6)**,** b) HFD; MBH infusion of saline (n=4) and MIF (n=5). Glycogen is expressed in μg/μg of protein.

Chapter 4: DISCUSSION, LIMITATIONS & CONCLUSION

4.1 – Overview of Significance

As discussed in the introduction of this thesis, hypothalamic regions of the brain can sense fluctuations in hormones and nutrients such as glucose[139–141], amino acids[142], fatty acids[143,145], insulin[146–148,151–154] and glucagon[157,158] to control metabolic homeostasis[137]. This list is not exhaustive, and in fact, the brain can sense other hormones such as leptin[184], GLP-1[185] and resistin[186] to regulate glucose metabolism, and impairments in hypothalamic sensing has been demonstrated to disrupt metabolic homeostasis by promoting aberrant glucose regulation and the development of obesity[160,161]. Although fluctuations in extracellular glucose can be sensed by hypothalamic neurons, changes in brain interstitial fluid glucose levels are delayed compared to changes occurring in the systemic circulation[187]. Given that the brain cannot solely rely on local concentrations of glucose for adequate glucoregulation, the integration of numerous efferent signals plays an important part in the brain's ability to effectively regulate whole-body glucose homeostasis[187].

Data presented in this thesis contributes to the knowledge of how the hypothalamus senses GCs to contribute to CNS-mediated whole-body glucoregulation. Elevated GC levels, signalling, and/or activity is commonly observed in diabetes and obesity and is associated with disrupted glucose homeostasis. Hypothalamic GC action has been previously shown to induce metabolic disturbances such as alter insulin sensitivity in peripheral tissues responsible for regulating glucose uptake as well as dampen the suppressive effect of insulin to inhibit endogenous GP during clamp experimentation[165,166]. Despite clear evidence linking MBH GC action to aberrant glucose regulation, intracellular mechanisms underlying the effects of brain GC signalling to elicit changes in glucose metabolism in healthy and pre-obese/obese states still remain largely unknown.

4.2 – Discussion of Results

	MBH treatment group	Hepatic glucose production	Hepatic insulin sensitivity
RC	MBH DEX	↑	↓
	MBH MIF+DEX	n.p.	↔ (blocked DEX)
	MBH GR shRNA+DEX	n.p.	↔ (blocked DEX)
	MBH 17-AAG+DEX	n.p.	↔ (blocked DEX)
	MBH Hsp90 shRNA+DEX	n.p.	↔ (blocked DEX)
HFD	MBH MIF	n.p.	↑
	MBH GR shRNA	n.p.	↑
	MBH 17-AAG	n.p.	↔ (no improvement)
	MBH Hsp90 shRNA	n.p.	↔ (no improvement)

Table 4.2.1 – Summary of experimental results. Arrows (↑,↓) represent changes or no change (↔) in hepatic glucose production and insulin sensitivity compared to MBH saline controls in the two diet groups**.** Hepatic glucose production and insulin sensitivity is based on clamp periods of basal insulin (0.8mU/min/kg) and mildly hyperinsulinemic (1.2mU/min/kg) euglycemic clamp experimentation respectively. *n.p.= data not presented.*

4.2.1 – MBH GR signalling in RC-fed rats

Results obtained from this study highlight the role of the MBH in modulating whole body glucose metabolism in response to GC action. In RC-fed rats, acute MBH infusion of the synthetic GC DEX impaired glucose tolerance and elicited an increase in hepatic GP under both basal and mild hyperinsulinemic euglycemic clamp conditions without affecting

peripheral GU. These results are in harmony with previous work that has demonstrated that acute GC infusion delivered directly into the ARC by retrodialysis induces hepatic insulin resistance but does not affect GU[166]. In contrast to our results, hypothalamic GC action has been reported to induce muscle insulin resistance[165]. This difference can be explained by the fact that these studies infused DEX more chronically (2 days) into the brain[165] and that the onset of hepatic insulin resistance occurs prior to impairments in peripheral insulin sensitivity[179].

With chemical and genetic loss-of-function approaches, we demonstrate that MBH GC glucoregulatory action requires MBH GRs and MBH Hsp90 as targeted inhibition of either of these structures negates the effects of MBH DEX. We observe an upregulation in MBH Hsp70 with MBH DEX, and this may be the result of a neuroprotective response because Hsp70 plays a role in the protection from oxidative stress[188,189]. In fact, DEX treatment on rat hippocampal slices and cortical neurons has been shown to induce neurotoxicity via GR activation[189,190]. In these experiments, DEX-mediated oxidative stress peaked after only 4 hours of initial exposure to DEX, and pre-treatment with MIF for 30 minutes prevented reactive oxygen species formation[190]. The implication of Hsp90 and Hsp70 in regulating different aspects of metabolism has more recently emerged. Targeting the manipulation of the expression of these chaperones in different tissues has been considered a therapeutic prospective in the treatment of obesity and T2D[191]. For example, upregulating whole body Hsp70 through heat shock treatment reduces the expression of inflammatory markers in the pancreas, liver and skeletal muscles as well as improves hepatic and skeletal muscle insulin sensitivity in mouse models of insulin resistance and T2D[192–195]. In contrast, Hsp70 knockout mice are phenotypically insulin resistant and gain

more body weight than controls[196]. Furthermore, diet-induced obesity has shown to upregulate Hsp90 in skeletal muscle of mice while Hsp90 inhibition improves glucose tolerance and insulin sensitivity in obese and diabetic mouse models[197,198]. Taken together, Hsp70 seems to play a beneficial role in the maintenance of metabolic homeostasis, at least in peripheral tissues, in contrast to Hsp90 which seems to be associated with adverse metabolic outcomes.

In these RC-fed animals, MBH DEX modulation of hepatic GP associates with a upregulation of hepatic G6pc mRNA expression, which is in line with previous metabolic studies that link hypothalamic hormone and nutrient sensing and subsequent increases in hepatic GP with increased gluconeogenesis[141,152,155,156]. This occurred independently of any changes in hepatic Pck1 mRNA, any changes in protein expression of hepatic glucoregulatory enzymes pPDH-E1α, PDH-E1α, PDK1, PDPc, HXK II and PEPCK, as well as hepatic glycogen content. G6Pase is a rate limiting gluconeogenic enzyme that hydrolyzes glucose-6-phosphate to free glucose. Following this final step in the gluconeogenesis pathway, glucose is exported out from the liver and released into systemic circulation. Given that local GC action in the liver directly upregulates gluconeogenesis and that T2D and obesity are characterized by increased hepatic GP and insulin resistance[11,12], we postulate that MBH GC action also contributes to the stimulation of hepatic GP through an upregulation of gluconeogenesis driven by CNS-liver neurocircuitry, which could involve innervation of the liver by the hepatic vagus nerve[165] or hepatic sympathetic nerve[166], which will be discussed in further detail below in section 4.3.3.

4.2.2 – MBH GR signalling in 3-day HFD feeding

Since MBH GR and MBH Hsp90 inhibition restored glucose homeostasis in MBH DEX-treated RC-fed animals that had stimulated hepatic glucose production, we postulated that blocking MBH GC action in a model of diet-induced pre-obesity, which has elevated GC levels, would have therapeutic relevance for improving glucoregulation. Evidence supports the notion that the hypothalamus is an important site to regulate glucose metabolism, and that changes to the hypothalamus induces aberrant glucose regulation in animal models of HFD feeding and obesity[160,161]. Upon 3-days of HFD feeding, the rats exhibited altered metabolic profiles compared to heathy RC-fed counterparts. Consistent with previous reports, rats fed with a 10% HFD for 3 days were hyperinsulinemic, mildly hyperglycemic and hepatic insulin resistant[158,168,179]. We now show that 3-day HFD feeding also led to hypercorticosteronemia and impaired glucose tolerance without affecting insulin sensitivity in metabolically active tissues.

Given that circulating levels of CORT is elevated in these animals, we proposed that elevated circulating GCs, which cross the blood-brain-barrier, contribute to increased MBH GC signalling to affect glucose metabolism in HFD-fed rats. Using both chemical and genetic loss-of-function approaches, we demonstrate that MBH GC glucoregulatory action in pre-obese rodents requires MBH GRs but surprisingly not MBH Hsp90 because inhibition of MBH GRs improves glucoregulatory control whereas blocking MBH Hsp90 has no effect. It should be acknowledged that we did not have a positive control to directly assess if MBH 17-AAG and Hsp90 shRNA worked during these experiments. Nonetheless, the same batch of 17-AAG and Hsp90 shRNA was used in concurrent experiments in RC-fed rats to show that it blocked the effects of MBH DEX. However, we cannot confirm if

the dose of 17-AAG, or extent of knockdown with Hsp90 shRNA, used for HFD experiments was sufficient to block the postulated higher level of GC action in the MBH of 3-day HFD-fed rats.

Although it was initially thought that acute HFD feeding would stimulate hepatic GP through an upregulation of gluconeogenic enzymes, amelioration of glucose homeostasis with MBH MIF occurred independently of any changes in hepatic G6pc and Pck1 mRNA, any changes in protein expression of hepatic glucoregulatory enzymes pPDH-E1α, PDH-E1α, PDK1, PDPc, HXK II and PEPCK, as well as glycogen content. Given this lack of change in hepatic enzymes following acute MBH GR inhibition, future analyses could investigate whether chronic MBH GR inhibition with GR shRNA yields the same enzymatic phenotype or whether more prolonged inhibition is needed to observe hepatic glucoregulatory enzyme modulation in our chronic 3-day HFD model.

4.2.3 – MBH GC-mediated signalling in pre-obesity differs from RC-fed rodents

Taken together, our results suggest that MBH GC-mediated signalling in HFD-fed rats differs from RC-fed rats and is possibly mediated through a non-classical GR signalling pathway occurring independently of MBH Hsp90. One such non-classical GR signalling pathway that does not require Hsp90 is that which is mediated via GRs that are found in the plasma membrane (mGRs). Importantly, evidence supports the existence of mGRs in neuronal membranes[131]. It should be noted that the GR loss-of-function techniques that we employed – pharmacologically with MIF and genetically with GR shRNA – inhibits both cytosolic and mGR in our experiments and as such, the type of GR that mediated the effects of GCs could not be confirmed. Furthermore, the physiological

presence of mGRs has been observed in immune cells, and it has been documented that their frequency is upregulated with immunostimulation[130]. In fact, patients with rheumatoid arthritis have an increased frequency of mGR positive monocytes, and this upregulation is positively correlated with disease severity[130]. Thus, mGRs mediate immune responses, and whether they do so in the brain also remains to be determined.

Interestingly, hypothalamic inflammation, which involves immune cells of the brain (e.g. microglia and macrophages[199]), rapidly occurs following the overconsumption of calorie dense food in humans and in rodents[200]. Significant increases in markers of hypothalamic inflammation can be detected within a few days of the commencement of HFD feeding in rodents prior to any weight gain[200]. Using MRI techniques, gliosis has been demonstrated to be upregulated in the MBH of obese humans which indicates the presence of hypothalamic inflammation and neuronal injury[200,201]. In addition, prolonging a fat-rich diet has shown to lead to the activation of cellular stress mechanisms in the MBH demonstrated by an upregulation in inflammatory cytokines such as TNFα and IL-1β and increased gliosis[137,188,202]. Other studies have also demonstrated that ICV administration of TNFα stimulates neuronal cell death through hypothalamic apoptotic signalling[203]. Most importantly, it has been demonstrated that inhibiting the NF-κB pathway in the hypothalamus restores hypothalamic control of metabolism in diet induced obesity[204].

Given the relationship between inflammation and mGRs[130], the fact that neural cells express mGRs[131], and that mGRs mediate GC signalling[128,129], investigating whether 3-day HFD feeding increases mGR abundance within the MBH may help explain the discrepancy between MBH GC-mediated signalling in HFD feeding and RC-fed rats. HFD for 3 days

increased total MBH GR protein abundance compared to RC-fed controls, and it is therefore possible that the observed increase results from an upregulation in mGR. Future analyses by our lab will quantify MBH GR protein levels in the cytoplasm versus plasma membrane in both RC- and HFD-fed rats to determine if HFD selectively upregulates mGRs. In addition, to determine a potential role of mGRs to mediate the glucostimulatory actions of MBH GCs, future experiments could investigate the involvement of MBH mGRs on hepatic GP following MBH DEX infusion and 3-day HFD feeding by specifically inhibiting mGR signalling or with the use of membrane-limited GCs such as DEX-BSA[205], although the infusion of BSA into the brain *in vivo* may warrant caution[206]. Findings from these experiments may help explain why MBH GR inhibition, but not MBH Hsp90 inhibition, improves hepatic insulin sensitivity in HFD-fed rats.

4.3 – Future Directions: *Further delineating the mechanisms underlying the effects of brain GC signalling on glucose metabolism*

4.3.1 – FFA contribution to hepatic GP

Another mechanism that may be contributing to the increase in hepatic GP following MBH GC action, especially with short-term HFD feeding, may be through an increase in circulating levels of FFAs. Hypercorticosteronemia promotes lipolysis in WAT and consequently leads to the release of FFAs into the systemic circulation[83]. It would therefore be important to investigate in the future if plasma FFA concentrations in our animals were modulated following MBH DEX infusion or 3-day HFD feeding given that FFAs can stimulate gluconeogenesis through an increased pyruvate flux[107]. Despite this possible mechanism involving the contribution of FFAs in increased hepatic GP, others have reported that 3-day HFD feeding does not elicit any changes in plasma FFA levels[169].

4.3.2 – Hypothalamic neural populations

In the brain, neural expression of GRs is ubiquitous and all glial cells express GRs as well[207]. However, biochemical and immunohistochemical studies have demonstrated that Hsp90 is present in almost all neurons of the brain, including the hypothalamus, but Hsp90 expression is undetected in glial cells[208,209]. In addition to neurons, glial cells have recently been given a role in being important modulators in CNS-mediated regulation of energy homeostasis[210]. Similarly to neurons, glia are equipped with hormone and nutrient sensing mechanisms. For example, hypothalamic astrocytes can sense extracellular glucose and insulin to help assist with CNS-mediated regulation of glucose metabolism[211,212]. Thus, the

relative contribution of neurons versus glia in sensing GCs to regulate glucose metabolism warrants future investigation.

Although the findings from this study clearly demonstrate that hypothalamic GR signalling stimulates the MBH to modulate glucose metabolism, the specific hypothalamic neuronal population(s) involved in mediating the glucoregulatory action of MBH GC-action remains unknown. GR loss-of-function with genetic approaches targeted to specific neural populations such as POMC and NPY/AgRP neurons would allow further delineation of molecular mechanisms of GC action in the brain that modulate glucose homeostasis in normal and pre-obese/obese rodents. Given that orexigenic AgRP neurons are necessary for the maintenance of whole body glucose homeostasis[152,153], it can be postulated that MBH DEX or HFD feeding disrupts glucose homeostasis through NPY release following MBH GC action on GRs colocalized in AgRP neurons. In fact, it has been previously demonstrated that hepatic insulin resistance following GR activation in the ARC results from GC-stimulated hypothalamic release of NPY[166]; however, whether HFD-induced increases in GC action in the MBH follows this signalling mechanism remains to be investigated. Downregulation of hypothalamic anorexigenic POMC neuron activity may also contribute to the mechanism involved in mediating the glucoregulatory action of MBH GC-action. In fact, POMC neuron activity has shown to be reduced in diet-induced obese mice fed a HFD[213]. Furthermore, it has been demonstrated that hypothalamic inflammation and apoptotic activity following HFD feeding selectively reduces hypothalamic POMC expression in comparison to NPY[214]. Given the differential roles of AgRP/NPY and POMC neuronal activity on glucose regulation, future studies directed at identifying a role for GCs to stimulate these neuronal populations are warranted.

4.3.3 – CNS-liver neurocircuitry

Following MBH GC action, it still remains unclear how the brain mechanistically stimulates hepatic GP. Neural signals from the MBH can be relayed to other neurons in integrative brain regions, including within nuclei in the brainstem, which can subsequently communicate to the liver through either efferent sympathetic or parasympathetic projections and modulate metabolism[167–169]. The literature presents conflicting evidence regarding whether the metabolic effects following MBH GC action are driven through sympathetic or parasympathetic signals to the liver[165,166]. Whereas one group of researchers demonstrated that the metabolic effects of ICV DEX infusion were inhibited in vagotomized rats[165], another group didn't find any evidence supporting the involvement of the hepatic vagus nerve[166]. In contrast, the latter group demonstrated that ARC DEX infusion affected metabolism through sympathetic nerves to the liver[166].

Hypercorticosteronemia may stimulate afferent vagal signals carried out from the liver to the brain which may in turn also play a role in contributing to hepatic insulin resistance[215]. For example, elevated levels of GCs have been demonstrated to activate PPARα signalling in the liver, which in turns drives an afferent signal to the brain via the hepatic vagus nerve. The brain then integrates the signal and subsequently stimulates hepatic GP[215]. Therefore, performing hepatic sympathetic and parasympathetic denervation surgeries on our animals undergoing euglycemic clamp experimentation would allow us to further understand the CNS-liver neurocircuitry that drives the stimulation of hepatic GP following MBH GC action.

4.4 – Limitations

4.4.1 – HFD feeding studies

The *in vivo* experiments performed in this study allowed delineation of molecular and physiological mechanisms of GC action in the brain that modulate glucose homeostasis in RC-fed and hypercorticosteronemic pre-obese rodents, but MBH GR signalling should also be investigated in animal models of obesity and diabetes, which are more chronic states of metabolic disease, to further emphasize physiological relevance. The same *in vivo* experiments that were initially performed in 3-day HFD-fed rats should be recapitulated in for example, rats with diet-induced obesity and in rats with low-dose streptozotocin-nicotinamide-induced T2D (nicotinamide helps protect β-cells against total STZ-induced destruction[168]), and examine whether MBH GR antagonism can also improve glucose homeostasis in a more established diseased state[168,216].

4.4.2 – Pharmaceuticals used for MBH treatments

Although the results following *in vivo* experimentation clearly demonstrate that MBH GCs act on MBH GRs to elicit changes in glucose metabolism, some limitations exist regarding the pharmaceuticals used to study the intracellular mechanisms underlying the effects of brain GC signalling. Although DEX is a widely used synthetic GC, its structure and affinity to GRs differs from biologically occurring CORT. Synthetic DEX is removed from the circulation at a slower rate and has a higher receptor binding affinity to GR and higher potency than endogenous CORT[217,218]. The structure of DEX differs from CORT at three positions where DEX has 1) an extra double bond between carbons C1-C2, 2) a C-16-α-methylation and 3) a C-9-α-halogenation (figure 4.4.1)[218]. The C1-C2 double bond of

DEX allows for all the hydrophilic groups to form an extensive hydrogen bond network with the GR and thereby increase its binding affinity[218,219]. Although the use of DEX has its advantages over CORT for studying MBH GC signalling as DEX almost exclusively binds to GRs and has minimal effects on MR activity[220], it would be important to also verify the effects of MBH CORT infusion on glucose metabolism as well as MBH MR inhibition.

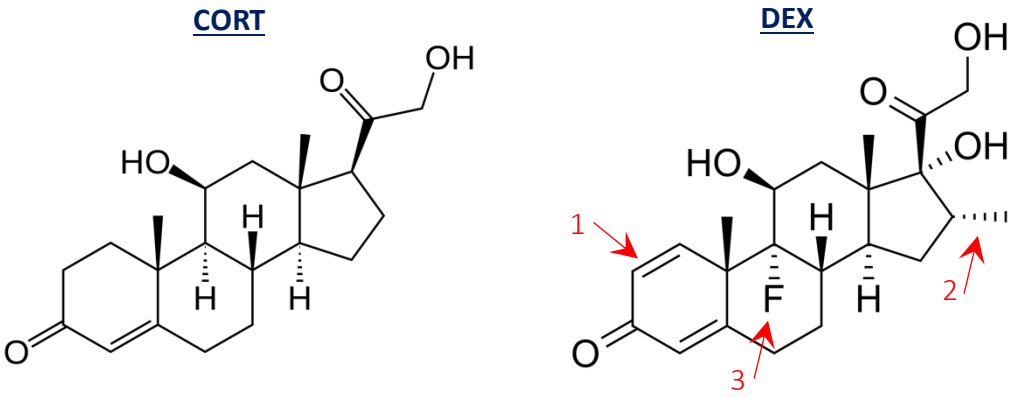

Figure 4.4.1 – Chemical structures of corticosterone (CORT) and dexamethasone (DEX). The structure of DEX (right) differs from CORT (left) at three positions indicated by red arrows: 1) an extra double bond between carbons C1-C2, 2) a C-16-α-methylation and 3) a C-9-α-halogenation.

The use of MIF as a GR antagonist is also a limitation in this study. The competitive receptor antagonist MIF is historically known as an abortion drug that acts through the

inhibition of progesterone receptors (PR)[221]. In addition to inhibiting PRs, MIF also antagonizes GRs and androgen receptors (IC_{50}: PR<GR<AR)[222,223], but has no effect on MRs or estrogen receptors[224]. In addition, PRs are found in hypothalamic regions of the brain such as the ARC and VMH[225,226] and GCs have been reported to non-selectively bind to GRs by binding to PRs[227]. Since MIF and GCs have the ability to bind to various steroid receptors and less is known about how MBH PRs regulate peripheral glucose metabolism in male rats, future studies are warranted to rule out PR involvement in mediating GC signalling to elicit changes in glucose metabolism. However, we can demonstrate in our study MBH MIF acted on MBH GRs to inhibit the glucoregulatory actions of MBH GC as complementary genetic loss-of-function approaches with GR shRNA also negated the effects of MBH DEX on glucose metabolism, recapitulating the same results as MBH MIF.

4.4.3 – Measurement of brain physiological concentrations of CORT

Although GCs cross the blood-brain barrier and act on GRs in the brain, less is known about the extracellular levels of CORT within the MBH of rats *in vivo*. Microdialysis assessment in RC-fed and 3-day HFD-fed rats would allow us to quantify the local physiological increase in GCs in the MBH following HFD-induced systemic hypercortisolemia.

4.4.4 – Euglycemic clamp experimentation

Although pancreatic euglycemic clamp experimentation with tracer dilution methodology is the gold standard technique for studying glucose turnover, the pancreas cannot respond physiologically in this setting. During clamp conditions, insulin is infused into the animal at a pre-determined continuous dose matched to the animal's body weight

and subsequently allows measurement of hepatic GP and insulin sensitivity. Insulin replacement values are then assessed by measuring plasma insulin levels during basal and clamp periods. In a glucose clamp setting, somatostatin is infused to "clamp" the pancreas such that hepatic GP can be quantified independent of changes to circulating insulin and glucagon levels. Despite this limiting factor, *in vivo* experimentation was complimented with ivGTT experiments and demonstrated that under physiological conditions MBH GC signalling decreases glucose tolerance.

4.5 – Conclusion

In summary, we reveal novel insight on intracellular mechanisms underlying the effects of brain GC signalling to elicit changes in glucose metabolism in both healthy and pre-obese hypercorticosteronemic animal models (figure 4.5.1). In humans, excessive levels and/or action of GCs is associated with T2D, obesity, insulin resistance, and hyperglycemia[24,25]. Clear evidence linking MBH GC action to aberrant glucose regulation has been previously reported and results from this study newly demonstrates that MBH GC-mediated signalling is mediated via MBH GRs in both RC-fed and 3-day HFD-fed rats. Blocking excessive MBH GC action with either acute or chronic MBH GR inhibition attenuates MBH DEX and HFD-stimulated hepatic GP leading to an improvement in glucose homeostasis. Furthermore, we demonstrate that MBH Hsp90 is also involved in MBH GC-mediated signalling in RC-fed rats, but not in 3-day HFD feeding. In our model of pre-obesity, MBH GC-mediated signalling is most likely mediated through a non-classical GR signalling pathway occurring independently of MBH Hsp90 such as mGRs given the relationship between HFD feeding and inflammation, and the latter with mGRs[130,137,188,200,202].

The CNS has emerged as a potential target for clinical intervention and elucidating MBH GC action and signalling that modulates glucose metabolism in disease states could help identify prospective therapies that would restore metabolic balance in obesity-related metabolic diseases such as diabetes. In fact, a growing body of evidence in animal studies supports that brain pathways also play an imperative role in glucose homeostasis in humans[228–230]. Pharmaceuticals have already been implicated in ameliorating metabolism in humans by triggering brain pathways. For example, lorcaserin was FDA approved in 2012

as an anti-obesity drug and acts to reduce food intake by activating 5-HT_{2C} serotonin receptors in the hypothalamus[231]. In addition, the anti-diabetic drug liraglutide which acts to reduce blood glucose levels through glucagon-like-peptide 1 receptor agonism in the pancreas also induces anorectic effects and decreases body weight by stimulating POMC neuron activity in the ARC[232–234]. Not only is brain GC action research beneficial for restoring disturbances in nutrient and energy homeostasis in obesity and T2D, but may offer additional health applications. Given that hypercortisolemia is also implicated in depression, neurodegeneration, and age-related disorders, the development of therapies targeting MBH GC-mediated signalling could have a wide spread of clinical applications[29,235,236].

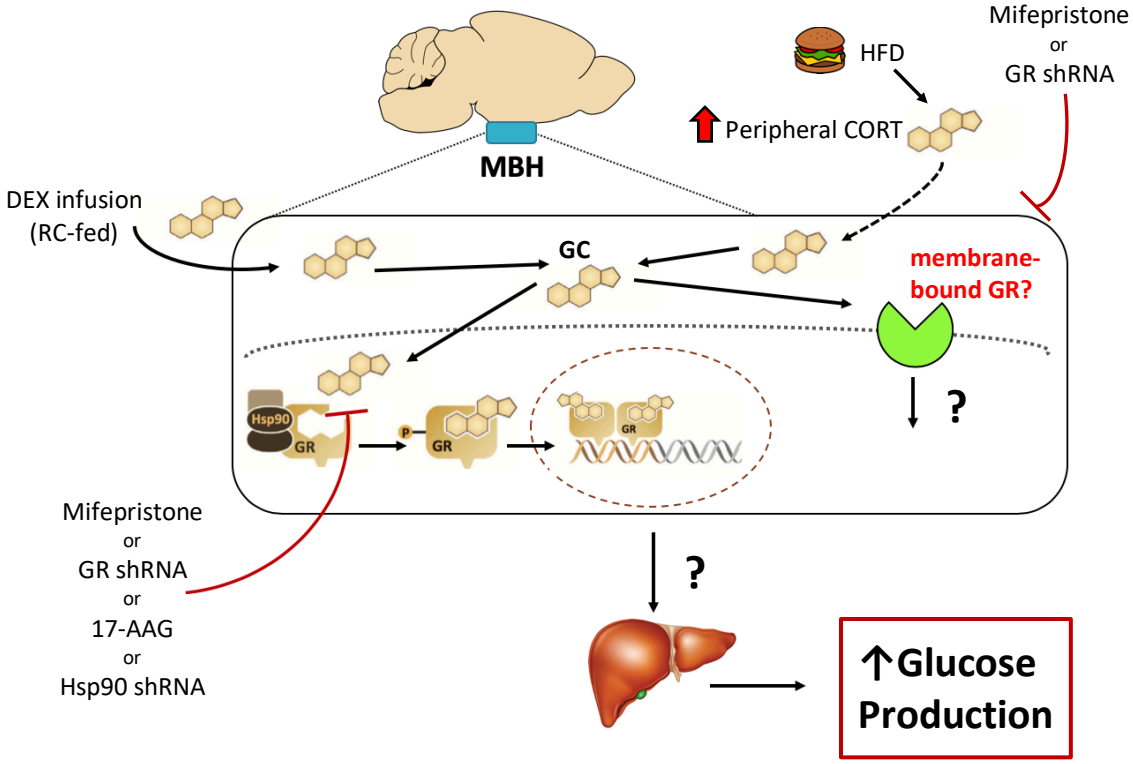

Figure 4.5.1 – Summary of thesis results and proposed intracellular mechanisms underlying the effects of brain GC signalling to elicit changes in glucose metabolisms in both healthy and pre-obese hypercorticosteronemic animal models. Inhibition of MBH GRs or MBH Hsp90 negates the effect of acute MBH GC infusion in healthy RC-fed rats. 3-day HFD feeding increases circulating GCs and increases MBH GC signalling. Glucose homeostasis in HFD feeding can be restored through MBH GR but not MBH Hsp90 inhibition.

REFERENCES

1. Diabetes Canada. Type 2 diabetes. Available at: https://www.diabetes.ca/recently-diagnosed/type-2-toolkit. (Accessed: 5th July 2019)

2. World Health Organization. Diabetes. (2018). Available at: https://www.who.int/news-room/fact-sheets/detail/diabetes. (Accessed: 3rd July 2019)

3. Rhodes, E. T., Prosser, L. A., Hoerger, T. J., Lieu, T., Ludwig, D. S. & Laffel, L. M. Estimated morbidity and mortality in adolescents and young adults diagnosed with Type 2 diabetes mellitus. *Diabet. Med.* **29**, 453–463 (2012).

4. World Health Organization. Obesity. (2014). Available at: https://www.who.int/topics/obesity/en/. (Accessed: 5th July 2019)

5. Obesity Canada. Obesity in Canada. Available at: https://obesitycanada.ca/obesity-in-canada/. (Accessed: 3rd July 2019)

6. Statistics Canada. Overweight and obese adults, 2018. (2019). Available at: https://www150.statcan.gc.ca/n1/pub/82-625-x/2019001/article/00005-eng.htm. (Accessed: 3rd July 2019)

7. World Health Organization. Obesity and overweight. (2018). Available at: https://www.who.int/news-room/fact-sheets/detail/obesity-and-overweight. (Accessed: 3rd July 2019)

8. Bloomgarden, Z. T. Prevention of obesity and diabetes. *Diabetes Care* **26**, 3172–3178 (2003).

9. Centers for Disease Control and Prevention. *National Diabetes Statistics Report, 2017 Estimates of Diabetes and Its Burden in the United States Background*. (2017).

10. Wadden, T. A., Berkowitz, R. I., Womble, L. G., Sarwer, D. B., Phelan, S., Cato, R. K., Hesson, L. A., Osei, S. Y., Kaplan, R. & Stunkard, A. J. Randomized Trial of Lifestyle Modification and Pharmacotherapy for Obesity. *N. Engl. J. Med.* **353**, 2111–2120 (2005).

11. Reaven, G. M. & Greenfield, M. S. Diabetic hypertriglyceridemia: evidence for three clinical syndromes. *Diabetes* **30**, 66–75 (1981).

12. Reaven, G. M., Chen, Y. D. I., Jeppesen, J., Maheux, P. & Krauss, R. M. Insulin resistance and hyperinsulinemia in individuals with small, dense, low density lipoprotein particles. *J. Clin. Invest.* **92**, 141–146 (1993).

13. Monteiro, R. & Azevedo, I. Chronic Inflammation in Obesity and the Metabolic

Syndrome. *Mediators Inflamm.* **2010**, (2010).

14. Ye, J. Mechanisms of insulin resistance in obesity. *Front. Med.* **7**, 14–24 (2013).

15. van Harmelen, V., Dicker, A., Ryden, M., Hauner, H., Lonnqvist, F., Naslund, E. & Arner, P. Increased Lipolysis and Decreased Leptin Production by Human Omental as Compared With Subcutaneous Preadipocytes. *Diabetes* **51**, 2029–2036 (2002).

16. You, T., Nicklas, B. J., Ding, J., Penninx, B. W. J. H., Goodpaster, B. H., Bauer, D. C., Tylavsky, F. A., Harris, T. B. & Kritchevsky, S. B. The Metabolic Syndrome Is Associated With Circulating Adipokines in Older Adults Across a Wide Range of Adiposity. *Journals Gerontol. Ser. A Biol. Sci. Med. Sci.* **63**, 414–419 (2008).

17. Bertin, E., Nguyen, P., Guenounou, M., Durlach, V., Potron, G. & Leutenegger, M. Plasma levels of tumor necrosis factor-alpha (TNF-alpha) are essentially dependent on visceral fat amount in type 2 diabetic patients. *Diabetes Metab.* **26**, 178–182 (2000).

18. DeFronzo, R. A. & Tripathy, D. Skeletal muscle insulin resistance is the primary defect in type 2 diabetes. *Diabetes Care* **32 Suppl 2**, S157-163 (2009).

19. Rui, L. Energy metabolism in the liver. *Compr. Physiol.* **4**, 177–197 (2014).

20. Geer, E. B., Islam, J. & Buettner, C. Mechanisms of glucocorticoid-induced insulin resistance: Focus on adipose tissue function and lipid metabolism. *Endocrinol. Metab. Clin. North Am.* **43**, 75–102 (2014).

21. Robertson, R. P. Beta-cell deterioration during diabetes: what's in the gun? *Trends Endocrinol. Metab.* **20**, 388–393 (2009).

22. Perley, M. & Kipnis, D. M. Plasma Insulin Responses to Glucose and Tolbutamide of Normal Weight and Obese Diabetic and Nondiabetic Subjects. *Diabetes* **15**, 867–874 (1966).

23. Kahn, S. E., Hull, R. L. & Utzschneider, K. M. Mechanisms linking obesity to insulin resistance and type 2 diabetes. *Nature* **444**, 840–846 (2006).

24. Björntorp, P. & Rosmond, R. Hypothalamic origin of the Metabolic Syndrome X. *Ann. N. Y. Acad. Sci.* **892**, 297–307 (1999).

25. Beaudry, J. L., D'souza, A. M., Teich, T., Tsushima, R. & Riddell, M. C. Exogenous glucocorticoids and a high-fat diet cause severe hyperglycemia and hyperinsulinemia and limit islet glucose responsiveness in young male Sprague-Dawley rats. *Endocrinology* **154**, 3197–3208 (2013).

26. Pasquali, R., Cantobelli, S., Casimirri, F., Capelli, M., Bortoluzzi, L., Flamia, R., Labate, A. M. & Barbara, L. The hypothalamic-pituitary-adrenal axis in obese women with different patterns of body fat distribution. *J. Clin. Endocrinol. Metab.*

77, 341–346 (1993).

27. Engeli, S., Böhnke, J., Feldpausch, M., Gorzelniak, K., Heintze, U., Janke, J., Luft, F. C. & Sharma, A. M. Regulation of 11β-HSD Genes in Human Adipose Tissue: Influence of Central Obesity and Weight Loss. *Obes. Res.* **12**, 9–17 (2004).

28. Lu, N. Z. & Cidlowski, J. A. Glucocorticoid receptor isoforms generate transcription specificity. *Trends Cell Biol.* **16**, 301–307 (2006).

29. De Kloet, E. R., Joëls, M. & Holsboer, F. Stress and the brain: From adaptation to disease. *Nat. Rev. Neurosci.* **6**, 463–475 (2005).

30. Ulrich-Lai, Y. M. & Herman, J. P. Neural regulation of endocrine and autonomic stress responses. *Nat. Rev. Neurosci.* **10**, 397–409 (2009).

31. Miller, W. L. & Auchus, R. J. The Molecular Biology, Biochemistry, and Physiology of Human Steroidogenesis and Its Disorders. *Endocr. Rev.* **32**, 81–151 (2011).

32. Stocco, D. M. Clinical disorders associated with abnormal cholesterol transport: mutations in the steroidogenic acute regulatory protein. *Mol. Cell. Endocrinol.* **191**, 19–25 (2002).

33. Miller, W. L. Steroidogenesis: Unanswered Questions. *Trends Endocrinol. Metab.* **28**, 771–793 (2017).

34. Hanukoglu, I. Steroidogenic enzymes: Structure, function, and role in regulation of steroid hormone biosynthesis. *J. Steroid Biochem. Mol. Biol.* **43**, 779–804 (1992).

35. Bremer, A. A. & Miller, W. L. Regulation of Steroidogenesis. in *Cellular Endocrinology in Health and Disease* 207–227 (2014). doi:10.1016/B978-0-12-408134-5.00013-5

36. Chapman, K., Holmes, M. & Seckl, J. 11β-hydroxysteroid dehydrogenases: intracellular gate-keepers of tissue glucocorticoid action. *Physiol. Rev.* **93**, 1139–1206 (2013).

37. R. Oakley, J. C. The Biology of the Glucocorticoid Receptor: New Signaling Mechanism in Health and Disease. *J allergy clin inmunol* **132**, 1033–1044 (2013).

38. Morgan, S. A., Hassan-Smith, Z. K., Doig, C. L., Sherlock, M. M., Stewart, P. M. & Lavery, G. G. Glucocorticoids and 11β-HSD1 are major regulators of intramyocellular protein metabolism. *J. Endocrinol.* **229**, 277–286 (2016).

39. Walker, E. A. & Stewart, P. M. 11β-hydroxysteroid dehydrogenase: Unexpected connections. *Trends Endocrinol. Metab.* **14**, 334–339 (2003).

40. Cain, D. W. & Cidlowski, J. A. Immune regulation by glucocorticoids. *Nat. Rev.*

Immunol. **17**, 233–247 (2017).

41. Reul, J. M. H. M. & De Kloet, E. R. Anatomical resolution of two types of corticosterone receptor sites in rat brain with in vitro autoradiography and computerized image analysis. *J. Steroid Biochem.* **24**, 269–272 (1986).

42. Morimoto, M., Morita, N., Ozawa, H., Yokoyama, K. & Kawata, M. Distribution of glucocorticoid receptor immunoreactivity and mRNA in the rat brain: An immunohistochemical and in situ hybridization study. *Neurosci. Res.* **26**, 235–269 (1996).

43. Aronsson, M., Fuxe, K., Dong, Y., Agnati, L. F., Okret, S. & Gustafsson, J. a. Localization of glucocorticoid receptor mRNA in the male rat brain by in situ hybridization. *Proc. Natl. Acad. Sci. U. S. A.* **85**, 9331–9335 (1988).

44. Cintra, A., Fuxe, K., Härfstrand, A., Agnati, L. F., Wikström, A. C., Okret, S., Vale, W. & Gustafsson, J. Å. Presence of glucocorticoid receptor immunoreactivity in corticotrophin releasing factor and in growth hormone releasing factor immunoreactive neurons of the rat di- and telencephalon. *Neurosci. Lett.* **77**, 25–30 (1987).

45. McEwen, B. S., De Kloet, E. R. & Rostene, W. Adrenal steroid receptors and actions in the nervous system. *Physiol. Rev.* **66**, 1121–1188 (1986).

46. Grad, I. & Picard, D. The glucocorticoid responses are shaped by molecular chaperones. *Mol. Cell. Endocrinol.* **275**, 2–12 (2007).

47. Pratt, W. B. & Toft, D. O. Steroid receptor interactions with heat shock protein and immunophilin chaperones. *Endocr. Rev.* **18**, 306–360 (1997).

48. Kirschke, E., Goswami, D., Southworth, D., Griffin, P. R. & Agard, D. A. Glucocorticoid receptor function regulated by coordinated action of the Hsp90 and Hsp70 chaperone cycles. *Cell* **157**, 1685–1697 (2014).

49. Kadmiel, M. & Cidlowski, J. A. Glucocorticoid receptor signaling in health and disease. *Trends Pharmacol. Sci.* **34**, 518–530 (2013).

50. Evans, R. M. The steroid and thyroid hormone receptor superfamily. *Science (80-.).* **240**, 889–895 (1988).

51. Herman, J. P., Mcklveen, J. M., Ghosal, S., Kopp, B., Wulsin, A., Makinson, R., Scheimann, J. & Myers, B. Regulation of the hypothalamic-pituitary-adrenocortical stress response. *Compr. Physiol.* **6**, 603–621 (2016).

52. Peckett, A. J., Wright, D. C. & Riddell, M. C. The effects of glucocorticoids on adipose tissue lipid metabolism. *Metabolism* **60**, 1500–1510 (2011).

53. Rhen, T. & Cidlowski, J. a. Antiinflammatory action of glucocorticoids--new

mechanisms for old drugs. *N. Engl. J. Med.* **353**, 1711–1723 (2005).

54. Tsigos, C. & Chrousos, G. P. Stress, obesity, and the metabolic syndrome: Soul and metabolism. *Ann. N. Y. Acad. Sci.* **1083**, (2006).

55. Hewagalamulage, S. D., Lee, T. K., Clarke, I. J. & Henry, B. A. Stress, cortisol, and obesity: a role for cortisol responsiveness in identifying individuals prone to obesity. *Domest. Anim. Endocrinol.* **56**, S112–S120 (2016).

56. Roy, M., Collier, B. & Roy, A. Hypothalamic-pituitary-adrenal axis dysregulation among diabetic outpatients. *Psychiatry Res.* **31**, 31–37 (1990).

57. Rutters, F., La Fleur, S., Lemmens, S., Born, J., Martens, M. & Adam, T. The Hypothalamic-Pituitary-Adrenal Axis, Obesity, and Chronic Stress Exposure: Foods and HPA Axis. *Curr. Obes. Rep.* **1**, 199–207 (2012).

58. Nicolaides, N. C., Charmandari, E., Chrousos, G. P. & Kino, T. Circadian endocrine rhythms: the hypothalamic-pituitary-adrenal axis and its actions. *Ann. N. Y. Acad. Sci.* **1318**, 71–80 (2014).

59. Berardelli, R., Karamouzis, I., D'Angelo, V., Zichi, C., Fussotto, B., Giordano, R., Ghigo, E. & Arvat, E. Role of mineralocorticoid receptors on the hypothalamus-pituitary-adrenal axis in humans. *Endocrine* **43**, 51–58 (2013).

60. McNeilly, A. D., Stewart, C. A., Sutherland, C. & Balfour, D. J. K. High fat feeding is associated with stimulation of the hypothalamic-pituitary-adrenal axis and reduced anxiety in the rat. *Psychoneuroendocrinology* **52**, 272–280 (2015).

61. Hryhorczuk, C., Décarie-Spain, L., Sharma, S., Daneault, C., Rosiers, C. Des, Alquier, T. & Fulton, S. Saturated high-fat feeding independent of obesity alters hypothalamus-pituitary-adrenal axis function but not anxiety-like behaviour. *Psychoneuroendocrinology* **83**, 142–149 (2017).

62. Moore, R. Y. Suprachiasmatic nucleus in sleep–wake regulation. *Sleep Med.* **8**, 27–33 (2007).

63. Kalsbeek, A., van der Spek, R., Lei, J., Endert, E., Buijs, R. M. & Fliers, E. Circadian rhythms in the hypothalamo–pituitary–adrenal (HPA) axis. *Mol. Cell. Endocrinol.* **349**, 20–29 (2012).

64. Chung, S., Lee, E. J., Cha, H. K., Kim, J., Kim, D., Son, G. H. & Kim, K. Cooperative roles of the suprachiasmatic nucleus central clock and the adrenal clock in controlling circadian glucocorticoid rhythm. *Sci. Rep.* **7**, 46404 (2017).

65. Herman, J. P., Prewitt, C. M. & Cullinan, W. E. Neuronal circuit regulation of the hypothalamo-pituitary-adrenocortical stress axis. *Crit. Rev. Neurobiol.* **10**, 371–394 (1996).

66. Froy, O. The relationship between nutrition and circadian rhythms in mammals. *Front. Neuroendocrinol.* **28**, 61–71 (2007).

67. Rudic, R. D., McNamara, P., Curtis, A.-M., Boston, R. C., Panda, S., Hogenesch, J. B. & FitzGerald, G. A. BMAL1 and CLOCK, Two Essential Components of the Circadian Clock, Are Involved in Glucose Homeostasis. *PLoS Biol.* **2**, e377 (2004).

68. Karlsson, B., Knutsson, A. & Lindahl, B. Is there an association between shift work and having a metabolic syndrome? Results from a population based study of 27 485 people. *Occup. Environ. Med.* **58**, 747–752 (2001).

69. Kalafatakis, K., Russell, G. M. & Lightman, S. L. Mechanisms in endocrinology: Does circadian and ultradian glucocorticoid exposure affect the brain? *Eur. J. Endocrinol.* **180**, R73–R89 (2019).

70. Oakley, R. H. & Cidlowski, J. A. Cellular processing of the glucocorticoid receptor gene and protein: new mechanisms for generating tissue-specific actions of glucocorticoids. *J. Biol. Chem.* **286**, 3177–3184 (2011).

71. Baschant, U. & Tuckermann, J. The role of the glucocorticoid receptor in inflammation and immunity. *J. Steroid Biochem. Mol. Biol.* **120**, 69–75 (2010).

72. De Bosscher, K. & Haegeman, G. Minireview: Latest Perspectives on Antiinflammatory Actions of Glucocorticoids. *Mol. Endocrinol.* **23**, 281–291 (2009).

73. Busillo, J. M. & Cidlowski, J. A. The five Rs of glucocorticoid action during inflammation: Ready, reinforce, repress, resolve, and restore. *Trends Endocrinol. Metab.* **24**, 109–119 (2013).

74. Nussinovitch, U., Freire de Carvalho, J., Maria R. Pereira, R. & Shoenfeld, Y. Glucocorticoids and the Cardiovascular System: State of the Art. *Curr. Pharm. Des.* **16**, 3574–3585 (2010).

75. Ren, R., Oakley, R. H., Cruz-Topete, D. & Cidlowski, J. A. Dual Role for Glucocorticoids in Cardiomyocyte Hypertrophy and Apoptosis. *Endocrinology* **153**, 5346–5360 (2012).

76. Pimenta, E., Wolley, M. & Stowasser, M. Adverse Cardiovascular Outcomes of Corticosteroid Excess. *Endocrinology* **153**, 5137–5142 (2012).

77. Rehman, Q. & Lane, N. E. Effect of glucocorticoids on bone density. *Med. Pediatr. Oncol.* **41**, 212–216 (2003).

78. Ambroggi, F., Turiault, M., Milet, A., Deroche-Gamonet, V., Parnaudeau, S., Balado, E., Barik, J., van der Veen, R., Maroteaux, G., Lemberger, T., Schütz, G., Lazar, M., Marinelli, M., Piazza, P. V. & Tronche, F. Stress and addiction: glucocorticoid receptor in dopaminoceptive neurons facilitates cocaine seeking. *Nat. Neurosci.* **12**, 247–249 (2009).

79. Desrivières, S., Lourdusamy, A., Müller, C., Ducci, F., Wong, C. P., Kaakinen, M., Pouta, A., Hartikainen, A.-L., Isohanni, M., Charoen, P., Peltonen, L., Freimer, N., Elliott, P., Jarvelin, M.-R. & Schumann, G. Glucocorticoid receptor (NR3C1) gene polymorphisms and onset of alcohol abuse in adolescents. *Addict. Biol.* **16**, 510–513 (2011).

80. Wei, Q., Fentress, H. M., Hoversten, M. T., Zhang, L., Hebda-Bauer, E. K., Watson, S. J., Seasholtz, A. F. & Akil, H. Early-Life Forebrain Glucocorticoid Receptor Overexpression Increases Anxiety Behavior and Cocaine Sensitization. *Biol. Psychiatry* **71**, 224–231 (2012).

81. Arnett, M. G., Kolber, B. J., Boyle, M. P. & Muglia, L. J. Behavioral insights from mouse models of forebrain- and amygdala-specific glucocorticoid receptor genetic disruption. *Mol. Cell. Endocrinol.* **336**, 2–5 (2011).

82. Quarta, C. *et al.* Molecular Integration of Incretin and Glucocorticoid Action Reverses Immunometabolic Dysfunction and Obesity. *Cell Metab.* **26**, 620–632 (2017).

83. Divertie, G. D., Jensen, M. D. & Miles, J. M. Stimulation of Lipolysis in Humans by Physiological Hypercortisolemia. *Diabetes* **40**, 1228–1260 (1991).

84. Xu, C., He, J., Jiang, H., Zu, L., Zhai, W., Pu, S. & Xu, G. Direct Effect of Glucocorticoids on Lipolysis in Adipocytes. *Mol. Endocrinol.* **23**, 1161–1170 (2009).

85. Gao, Z., Zhang, X., Zuberi, A., Hwang, D., Quon, M. J., Lefevre, M. & Ye, J. Inhibition of Insulin Sensitivity by Free Fatty Acids Requires Activation of Multiple Serine Kinases in 3T3-L1 Adipocytes. *Mol. Endocrinol.* **18**, 2024–2034 (2004).

86. Gathercole, L. L., Morgan, S. A., Bujalska, I. J., Hauton, D., Stewart, P. M. & Tomlinson, J. W. Regulation of Lipogenesis by Glucocorticoids and Insulin in Human Adipose Tissue. *PLoS One* **6**, e26223 (2011).

87. Minshull, M. & Strong, C. R. The stimulation of lipogenesis in white adipose tissue from fed rats by corticosterone. *Int. J. Biochem.* **17**, 529–532 (1985).

88. Lee, M.-J., Pramyothin, P., Karastergiou, K. & Fried, S. K. Deconstructing the roles of glucocorticoids in adipose tissue biology and the development of central obesity. *Biochim. Biophys. Acta - Mol. Basis Dis.* **1842**, 473–481 (2014).

89. Aso, Y., Yamamoto, R., Wakabayashi, S., Uchida, T., Takayanagi, K., Takebayashi, K., Okuno, T., Inoue, T., Node, K., Tobe, T., Inukai, T. & Nakano, Y. Comparison of serum high-molecular weight (HMW) adiponectin with total adiponectin concentrations in type 2 diabetic patients with coronary artery disease using a novel enzyme-linked immunosorbent assay to detect HMW adiponectin. *Diabetes* **55**, 1954–1960 (2006).

90. Fasshauer, M., Klein, J., Neumann, S., Eszlinger, M. & Paschke, R. Hormonal Regulation of Adiponectin Gene Expression in 3T3-L1 Adipocytes. *Biochem. Biophys. Res. Commun.* **290**, 1084–1089 (2002).

91. Papaspyrou-Rao, S., Schneider, S. H., Petersen, R. N. & Fried, S. K. Dexamethasone Increases Leptin Expression in Humans in Vivo. *J. Clin. Endocrinol. Metab.* **82**, 1635–1637 (1997).

92. Maffei, M., Halaas, J., Ravussin, E., Pratley, R. E., Lee, G. H., Zhang, Y., Fei, H., Kim, S., Lallone, R. & Ranganathan, S. Leptin levels in human and rodent: measurement of plasma leptin and ob RNA in obese and weight-reduced subjects. *Nat. Med.* **1**, 1155–1161 (1995).

93. Grunfeld, C., Baird, K., Obberghen, E. Van & Kahn, C. R. Glucocorticoid-Induced Insulin Resistance in Vitro: Evidence for Both Receptor and Postreceptor Defects. *Endocrinology* **109**, 1723–1730 (1981).

94. Olefsky, J. M. Effect of dexamethasone on insulin binding, glucose transport, and glucose oxidation of isolated rat adipocytes. *J. Clin. Invest.* **56**, 1499–1508 (1975).

95. Sakoda, H., Ogihara, T., Anai, M., Funaki, M., Inukai, K., Katagiri, H., Fukushima, Y., Onishi, Y., Ono, H., Fujishiro, M., Kikuchi, M., Oka, Y. & Asano, T. Dexamethasone-induced insulin resistance in 3T3-L1 adipocytes is due to inhibition of glucose transport rather than insulin signal transduction. *Diabetes* **49**, 1700–1708 (2000).

96. Weinstein, S. P., Wilson, C. M., Pritsker, A. & Cushman, S. W. Dexamethasone inhibits insulin-stimulated recruitment of GLUt4 to the cell surface in rat skeletal muscle. *Metabolism* **47**, 3–6 (1998).

97. Dimitriadis, G., Leighton, B., Parry-Billings, M., Sasson, S., Young, M., Krause, U., Bevan, S., Piva, T., Wegener, G. & Newsholme, E. A. Effects of glucocorticoid excess on the sensitivity of glucose transport and metabolism to insulin in rat skeletal muscle. *Biochem. J.* **321**, 707–712 (1997).

98. Coderre, L., Srivastava, A. K. & Chiasson, J.-L. Role of glucocorticoid in the regulation of glycogen metabolism in skeletal muscle. *Am. J. Physiol. - Endocrinol. Metab.* **260**, E927–E932 (1991).

99. Roden, M. Non-invasive studies of glycogen metabolism in human skeletal muscle using nuclear magnetic resonance spectroscopy. *Curr. Opin. Clin. Nutr. Metab. Care* **4**, 261–266 (2001).

100. Randle, P. J., Garland, P. B., Hales, C. N. & Newsholme, E. A. The glucose fatty-acid cycle. Its role in insulin sensitivity and the metabolic disturbances of diabetes mellitus. *Lancet* **1**, 785–789 (1963).

101. Roden, M. How Free Fatty Acids Inhibit Glucose Utilization in Human Skeletal

Muscle. *Physiology* **19**, 92–96 (2004).

102. Roden, M., Krssak, M., Stingl, H., Gruber, S., Hofer, A., Furnsinn, C., Moser, E. & Waldhausl, W. Rapid impairment of skeletal muscle glucose transport/phosphorylation by free fatty acids in humans. *Diabetes* **48**, 358–364 (1999).

103. Dresner, A., Laurent, D., Marcucci, M., Griffin, M. E., Dufour, S., Cline, G. W., Slezak, L. A., Andersen, D. K., Hundal, R. S., Rothman, D. L., Petersen, K. F. & Shulman, G. I. Effects of free fatty acids on glucose transport and IRS-1–associated phosphatidylinositol 3-kinase activity. *J. Clin. Invest.* **103**, 253–259 (1999).

104. Thompson, A. L. & Cooney, G. J. Acyl-CoA inhibition of hexokinase in rat and human skeletal muscle is a potential mechanism of lipid-induced insulin resistance. *Diabetes* **49**, 1761–1765 (2000).

105. Palmer, M. Gluconeogenesis. *University of Waterloo, Department of Chemistry* Available at: http://watcut.uwaterloo.ca/webnotes/Metabolism/Gluconeogenesis.html. (Accessed: 20th July 2019)

106. Kim, J., Tchernyshyov, I., Semenza, G. L. & Dang, C. V. HIF-1-mediated expression of pyruvate dehydrogenase kinase: A metabolic switch required for cellular adaptation to hypoxia. *Cell Metab.* **3**, 177–185 (2006).

107. Lam, T. K. T., Carpentier, A., Lewis, G. F., van de Werve, G., Fantus, I. G. & Giacca, A. Mechanisms of the free fatty acid-induced increase in hepatic glucose production. *Am. J. Physiol. Metab.* **284**, E863–E873 (2003).

108. Kuo, T., McQueen, A., Chen, T.-C. & Wang, J.-C. Regulation of Glucose Homeostasis by Glucocorticoids. *Adv. Exp. Med. Biol.* **872**, 99–126 (2015).

109. Sasaki, K., Cripe, T. P., Koch, S. R., Andreone, T. L., Petersen, D. D., Beale, E. G. & Granner, D. K. Multihormonal regulation of phosphoenolpyruvate carboxykinase gene transcription. The dominant role of insulin. *J. Biol. Chem.* **259**, 15242–15251 (1984).

110. Nordlie, R. C., Arion, W. J. & Glende, E. A. Liver Microsomal Glucose 6-Phosphatase, Inorganic Pyrophosphatase, and Pyrophosphate-Glucose Phosphotransferase. *J. Biol. Chem.* **240**, 3479–3484 (1965).

111. Connaughton, S., Chowdhury, F., Attia, R. R., Song, S., Zhang, Y., Elam, M. B., Cook, G. A. & Park, E. A. Regulation of pyruvate dehydrogenase kinase isoform 4 (PDK4) gene expression by glucocorticoids and insulin. *Mol. Cell. Endocrinol.* **315**, 159–167 (2010).

112. Sugden, M. C. & Holness, M. J. Recent advances in mechanisms regulating glucose oxidation at the level of the pyruvate dehydrogenase complex by PDKs. *Am. J.*

Physiol. Metab. **284**, E855–E862 (2003).

113. Wu, P., Blair, P. V, Sato, J., Jaskiewicz, J., Popov, K. M. & Harris, R. A. Starvation Increases the Amount of Pyruvate Dehydrogenase Kinase in Several Mammalian Tissues. *Arch. Biochem. Biophys.* **381**, 1–7 (2000).

114. Harris, R. A., Huang, B. & Wu, P. Control of pyruvate dehydrogenase kinase gene expression. *Adv. Enzyme Regul.* **41**, 269–288 (2001).

115. Mersmann, H. J. & Segal, H. L. Glucocorticoid control of the liver glycogen synthetase-activating system. *J. Biol. Chem.* **244**, 1701–1704 (1969).

116. Exton, J., Miller, T., Harper, S. & Park, C. Carbohydrate metabolism in perfused livers of adrenalectomized and steroid-replaced rats. *Am. J. Physiol.* **230**, 163–170 (1976).

117. Holland, W. L., Brozinick, J. T., Wang, L. P., Hawkins, E. D., Sargent, K. M., Liu, Y., Narra, K., Hoehn, K. L., Knotts, T. A., Siesky, A., Nelson, D. H., Karathanasis, S. K., Fontenot, G. K. K., Birnbaum, M. J. & Summers, S. A. Inhibition of Ceramide Synthesis Ameliorates Glucocorticoid-, Saturated-Fat-, and Obesity-Induced Insulin Resistance. *Cell Metab.* **5**, 167–179 (2007).

118. Chavez, J. A. & Summers, S. A. A ceramide-centric view of insulin resistance. *Cell Metab.* **15**, 585–594 (2012).

119. Manning, B. D. & Toker, A. Leading Edge Review AKT/PKB Signaling: Navigating the Network. *Cell* **169**, 381–405 (2017).

120. Moraitis, A. G., Block, T., Nguyen, D. & Belanoff, J. K. The role of glucocorticoid receptors in metabolic syndrome and psychiatric illness. *J. Steroid Biochem. Mol. Biol.* **165**, 114–120 (2017).

121. Weaver, J. U., Hitman, G. A. & Kopelman, P. G. An association between a BclI restriction fragment length polymorphism of the glucocorticoid receptor locus and hyperinsulinaemia in obese women. *J. Mol. Endocrinol.* **9**, 295–300 (1992).

122. Rosmond, R. & Holm, G. A 5-Year Follow-Up Study of 3 Polymorphisms in the Human Glucocorticoid Receptor Gene in Relation to Obesity, Hypertension, and Diabetes. *J. Cardiometab. Syndr.* **3**, 132–135 (2008).

123. Geelen, C. C., Van Greevenbroek, M. M., Van Rossum, E. F., Schaper, N. C., Nijpels, G., 't Hart, L. M., Schalkwijk, C. G., Ferreira, I., Van Der Kallen, C. J., Sauerwein, H. P., Dekker, J. M., Stehouwer, C. D. & Havekes, B. BclI Glucocorticoid Receptor Polymorphism Is Associated With Greater Body Fatness: The Hoorn and CODAM Studies. *J Clin Endocrinol Metab* **98**, E595–E599 (2013).

124. Ross, I. L., Levitt, N. S., Van Der Merwe, L., Schatz, D. A., Johannsson, G., Dandara, C., Pillay, T. S. & Blom, D. J. Investigation of glucocorticoid receptor

polymorphisms in relation to metabolic parameters in Addison's disease. *Eur. J. Endocrinol.* **168**, 403–412 (2013).

125. Martins, C. S., Elias, D., Colli, L. M., Couri, C. E., Souza, M. C. L. A., Moreira, A. C., Foss, M. C., Elias, L. L. K. & de Castro, M. HPA axis dysregulation, NR3C1 polymorphisms and glucocorticoid receptor isoforms imbalance in metabolic syndrome. *Diabetes. Metab. Res. Rev.* **33**, e2842 (2017).

126. Boullu-Ciocca, S., Paulmyer-Lacroix, O., Fina, F., Ouafik, L., Alessi, M.-C., Oliver, C. & Grino, M. Expression of the mRNAs Coding for the Glucocorticoid Receptor Isoforms in Obesity. *Obes. Res.* **11**, 925–929 (2003).

127. Constantinopoulos, P., Michalaki, M., Kottorou, A., Habeos, I., Psyrogiannis, A., Kalfarentzos, F. & Kyriazopoulou, V. Cortisol in tissue and systemic level as a contributing factor to the development of metabolic syndrome in severely obese patients. *Eur. J. Endocrinol.* **172**, 69–78 (2015).

128. Stahn, C. & Buttgereit, F. Genomic and nongenomic effects of glucocorticoids. *Nat. Clin. Pract. Rheumatol.* **4**, 525–533 (2008).

129. Löwenberg, M., Verhaar, A. P., van den Brink, G. R. & Hommes, D. W. Glucocorticoid signaling: a nongenomic mechanism for T-cell immunosuppression. *Trends Mol. Med.* **13**, 158–163 (2007).

130. Bartholome, B., Spies, C. M., Gaber, T., Schuchmann, S., Berki, T., Kunkel, D., Bienert, M., Radbruch, A., Burmester, G.-R., Lauster, R., Scheffold, A. & Buttgereit, F. Membrane glucocorticoid receptors (mGCR) are expressed in normal human peripheral blood mononuclear cells and up-regulated after in vitro stimulation and in patients with rheumatoid arthritis. *FASEB J.* **18**, 70–80 (2004).

131. Orchinik, M., Murray, T. F. & Moore, F. L. A corticosteroid receptor in neuronal membranes. *Science (80-.).* **252**, 1848–1851 (1991).

132. Revankar, C. M., Cimino, D. F., Sklar, L. A., Arterburn, J. B. & Prossnitz, E. R. A transmembrane intracellular estrogen receptor mediates rapid cell signaling. *Science (80-.).* **307**, 1625–1630 (2005).

133. Razandi, M., Pedram, A., Greene, G. L. & Levin, E. R. Cell Membrane and Nuclear Estrogen Receptors (ERs) Originate from a Single Transcript: Studies of ERα and ERβ Expressed in Chinese Hamster Ovary Cells. *Mol. Endocrinol.* **13**, 307–319 (1999).

134. Levin, E. R. & Hammes, S. R. Nuclear receptors outside the nucleus: extranuclear signalling by steroid receptors. *Nat. Rev. Mol. Cell Biol.* **17**, 783–797 (2016).

135. Belgardt, B. F., Okamura, T. & Brüning, J. C. Hormone and glucose signalling in POMC and AgRP neurons. *J. Physiol.* **587**, 5305–5314 (2009).

136. Paxinos, G. & Watson, C. *The rat brain in stereotaxic coordinates*. (Elsevier, 2007).

137. Jais, A. & Brüning, J. C. Hypothalamic inflammation in obesity and metabolic disease. *J. Clin. Invest.* **127**, 24–32 (2017).

138. Bernard, C. *Lecons de Physiologie Experimentale Applique a la Medicine Faites au College de France*. (Bailere et Fils, 1855).

139. Anand, B. K., Chhina, G. S., Sharma, K. N., Dua, S. & Singh, B. Activity of single neurons in the hypothalamic feeding centers: effect of glucose. *Am. J. Physiol. Content* **207**, 1146–1154 (1964).

140. Oomura, Y. & Yoshimatsu, H. Neural network of glucose monitoring system. *J. Auton. Nerv. Syst.* **10**, 359–372 (1984).

141. Lam, T. K. T., Gutierrez-Juarez, R., Pocai, A. & Rossetti, L. Regulation of Blood Glucose by Hypothalamic Pyruvate Metabolism. *Science (80-.).* **309**, 943–947 (2005).

142. Su, Y., Lam, T. K. T., He, W., Pocai, A., Bryan, J., Aguilar-Bryan, L. & Gutiérrez-Juárez, R. Hypothalamic leucine metabolism regulates liver glucose production. *Diabetes* **61**, 85–93 (2012).

143. Obici, S., Feng, Z., Morgan, K., Stein, D., Karkanias, G. & Rossetti, L. Central administration of oleic acid inhibits glucose production and food intake. *Diabetes* **51**, 271–275 (2002).

144. Chu, C. A., Sherck, S. M., Igawa, K., Sindelar, D. K., Neal, D. W., Emshwiller, M. & Cherrington, A. D. Effects of free fatty acids on hepatic glycogenolysis and gluconeogenesis in conscious dogs. *Am. J. Physiol. Metab.* **282**, E402–E411 (2002).

145. Lam, T. K. T., Pocai, A., Gutierrez-Juarez, R., Obici, S., Bryan, J., Aguilar-Bryan, L., Schwartz, G. J. & Rossetti, L. Hypothalamic sensing of circulating fatty acids is required for glucose homeostasis. *Nat. Med.* **11**, 320–327 (2005).

146. Woods, S. C., Lotter, E. C., McKay, L. D. & Porte, D. Chronic intracerebroventricular infusion of insulin reduces food intake and body weight of baboons. *Nature* **282**, 503–505 (1979).

147. Woods, S. C., Stein, L. J., McKay, L. D. & Porte Jr., D. Suppression of food intake by intravenous nutrients and insulin in the baboon. *Am.J.Physiol* **247**, R393–R401 (1984).

148. Schwartz, M. W., Figlewicz, D. P., Baskin, D. G., Woods, S. C. & Porte, D. Insulin in the brain: A hormonal regulator of energy balance. *Endocr. Rev.* **13**, 387–414 (1992).

149. Shah, R., Patel, M., Maahs, D. & Shah, V. Insulin delivery methods: Past, present

and future. *Int. J. Pharm. Investig.* **6**, 1–9 (2016).

150. Baskin, D. G., Figlewicz, D. P., Woods, S. C., Porte, D. & Dorsa, D. M. Insulin in the Brain. *Annu. Rev. Physiol.* **49**, 335–347 (1987).

151. Varela, L. & Horvath, T. L. Leptin and insulin pathways in POMC and AgRP neurons that modulate energy balance and glucose homeostasis. *EMBO Rep.* **13**, 1079–1086 (2012).

152. Könner, A. C., Janoschek, R., Plum, L., Jordan, S. D., Rother, E., Ma, X., Xu, C., Enriori, P., Hampel, B., Barsh, G. S., Kahn, C. R., Cowley, M. A., Ashcroft, F. M. & Brüning, J. C. Insulin Action in AgRP-Expressing Neurons Is Required for Suppression of Hepatic Glucose Production. *Cell Metab.* **5**, 438–449 (2007).

153. Lin, H. V., Plum, L., Ono, H., Gutiérrez-Juárez, R., Shanabrough, M., Borok, E., Horvath, T. L., Rossetti, L. & Accili, D. Divergent regulation of energy expenditure and hepatic glucose production by insulin receptor in agouti-related protein and POMC neurons. *Diabetes* **59**, 337–346 (2010).

154. Obici, S., Zhang, B. B., Karkanias, G. & Rossetti, L. Hypothalamic insulin signaling is required for inhibition of glucose production. *Nat. Med.* **8**, 1376–1382 (2002).

155. Pocai, A., Lam, T. K. T., Gutierrez-Juarez, R., Obici, S., Schwartz, G. J., Bryan, J., Aguilar-Bryan, L. & Rossetti, L. Hypothalamic K ATP channels control hepatic glucose production. *Nature* **434**, 1026–1031 (2005).

156. Ramnanan, C. J., Saraswathi, V., Smith, M. S., Donahue, E. P., Farmer, B., Farmer, T. D., Neal, D., Williams, P. E., Lautz, M., Mari, A., Cherrington, A. D. & Edgerton, D. S. Brain insulin action augments hepatic glycogen synthesis without suppressing glucose production or gluconeogenesis in dogs. *J. Clin. Invest.* **121**, 3713–3723 (2011).

157. Hoosein, N. M. & Gurd, R. S. Identification of glucagon receptors in rat brain. *Proc. Natl. Acad. Sci. U. S. A.* **81**, 4368–4372 (1984).

158. Mighiu, P. I., Yue, J. T. Y., Filippi, B. M., Abraham, M. A., Chari, M., Lam, C. K. L., Yang, C. S., Christian, N. R., Charron, M. J. & Lam, T. K. T. Hypothalamic glucagon signaling inhibits hepatic glucose production. *Nat. Med.* **19**, 766–772 (2013).

159. Inokuchi, A., Oomura, Y., Shimizu, N. & Yamamoto, T. Central action of glucagon in rat hypothalamus. *Am. J. Physiol.* **250**, R120–R126 (1986).

160. He, W., Lam, T. K. T., Obici, S. & Rossetti, L. Molecular disruption of hypothalamic nutrient sensing induces obesity. *Nat. Neurosci.* **9**, 227–233 (2006).

161. Parton, L. E., Ye, C. P., Coppari, R., Enriori, P. J., Choi, B., Zhang, C. Y., Xu, C., Vianna, C. R., Balthasar, N., Lee, C. E., Elmquist, J. K., Cowley, M. A. & Lowell,

B. B. Glucose sensing by POMC neurons regulates glucose homeostasis and is impaired in obesity. *Nature* **449**, 228–232 (2007).

162. Pocai, A., Lam, T. K. T., Obici, S., Gutierrez-Juarez, R., Muse, E. D., Arduini, A. & Rossetti, L. Restoration of hypothalamic lipid sensing normalizes energy and glucose homeostasis in overfed rats. *J. Clin. Invest.* **116**, 1081–1091 (2006).

163. Veyrat-Durebex, C., Deblon, N., Caillon, A., Andrew, R., Altirriba, J., Odermatt, A. & Rohner-Jeanrenaud, F. Central glucocorticoid administration promotes weight gain and increased 11β-hydroxysteroid dehydrogenase type 1 expression in white adipose tissue. *PLoS One* **7**, e34002 (2012).

164. Zakrzewska, K. E., Cusin, I., Stricker-Krongrad, A., Boss, O., Ricquier, D., Jeanrenaud, B. & Rohner-Jeanrenaud, F. Induction of obesity and hyperleptinemia by central glucocorticoid infusion in the rat. *Diabetes* **48**, 365–370 (1999).

165. Cusin, I., Rouru, J. & Rohner-Jeanrenaud, F. Intracerebroventricular glucocorticoid infusion in normal rats: Induction of parasympathetic-mediated obesity and insulin resistance. *Obes. Res.* **9**, 401–406 (2001).

166. Yi, C. X., Foppen, E., Abplanalp, W., Gao, Y., Alkemade, A., La Fleur, S. E., Serlie, M. J., Fliers, E., Buijs, R. M., Tschöp, M. H. & Kalsbeek, A. Glucocorticoid signaling in the arcuate nucleus modulates hepatic insulin sensitivity. *Diabetes* **61**, 339–345 (2012).

167. Blouet, C., Jo, Y.-H., Li, X. & Schwartz, G. J. Mediobasal Hypothalamic Leucine Sensing Regulates Food Intake through Activation of a Hypothalamus–Brainstem Circuit. *J. Neurosci.* **29**, 8302–8311 (2009).

168. Yue, J. T. Y., Abraham, M. A., Bauer, P. V., Lapierre, M. P., Wang, P., Duca, F. A., Filippi, B. M., Chan, O. & Lam, T. K. T. Inhibition of glycine transporter-1 in the dorsal vagal complex improves metabolic homeostasis in diabetes and obesity. *Nat. Commun.* **7**, 13501 (2016).

169. Yue, J. T. Y., Abraham, M. A., Lapierre, M. P., Mighiu, P. I., Light, P. E., Filippi, B. M. & Lam, T. K. T. A fatty acid-dependent hypothalamic-DVC neurocircuitry that regulates hepatic secretion of triglyceride-rich lipoproteins. *Nat. Commun.* **6**, 5970 (2015).

170. Sandoval, D. A., Bagnol, D., Woods, S. C., Alessio, D. A. D. & Seeley, R. J. Arcuate Glucagon-Like Peptide 1 Receptors Regulate Glucose Homeostasis but Not Food Intake. *Diabetes* **57**, 2046–2054 (2008).

171. Pocai, A., Morgan, K., Buettner, C., Gutierrez-Juarez, R., Obici, S. & Rossetti, L. Central leptin acutely reverses diet-induced hepatic insulin resistance. *Diabetes* **54**, 3182–3189 (2005).

172. Lamia, K. A., Papp, S. J., Yu, R. T., Barish, G. D., Uhlenhaut, N. H., Jonker, J. W.,

Downes, M. & Evans, R. M. Cryptochromes mediate rhythmic repression of the glucocorticoid receptor. *Nature* **480**, 552–556 (2011).

173. Coutinho, A. E. & Chapman, K. E. The anti-inflammatory and immunosuppressive effects of glucocorticoids, recent developments and mechanistic insights. *Mol. Cell. Endocrinol.* **335**, 2–13 (2011).

174. Cuevas-Ramos, D. & Fleseriu, M. Treatment of Cushing's disease: A mechanistic update. *J. Endocrinol.* **223**, R19–R39 (2014).

175. Wang, H., Lu, M., Yao, M. & Zhu, W. Effects of treatment with an Hsp90 inhibitor in tumors based on 15 phase II clinical trials. *Mol. Clin. Oncol.* **5**, 326–334 (2016).

176. Zuo, Y., Wang, J., Liao, F., Yan, X., Li, J., Huang, L. & Liu, F. Inhibition of Heat Shock Protein 90 by 17-AAG Reduces Inflammation via P2X7 Receptor/NLRP3 Inflammasome Pathway and Increases Neurogenesis After Subarachnoid Hemorrhage in Mice. *Front. Mol. Neurosci.* **11**, 1–16 (2018).

177. Ho, S. W., Tsui, Y. T. C., Wong, T. T., Cheung, S. K.-K., Goggins, W. B., Yi, L. M., Cheng, K. K. & Baum, L. Effects of 17-allylamino-17-demethoxygeldanamycin (17-AAG) in transgenic mouse models of frontotemporal lobar degeneration and Alzheimer's disease. *Transl. Neurodegener.* **2**, 2–24 (2013).

178. Côté, C. D., Rasmussen, B. A., Duca, F. A., Zadeh-Tahmasebi, M., Baur, J. A., Daljeet, M., Breen, D. M., Filippi, B. M. & Lam, T. K. T. Resveratrol activates duodenal Sirt1 to reverse insulin resistance in rats through a neuronal network. *Nat. Med.* **21**, 498–505 (2015).

179. Wang, J., Obici, S., Morgan, K., Barzilai, N., Feng, Z. & Rossetti, L. Overfeeding rapidly induces leptin and insulin resistance. *Diabetes* **50**, 2786–2791 (2001).

180. Morettini, M., Faelli, E., Perasso, L., Fioretti, S., Burattini, L., Ruggeri, P. & Di Nardo, F. IVGTT-based simple assessment of glucose tolerance in the Zucker fatty rat: Validation against minimal models. *PLoS One* **12**, (2017).

181. Patrono, C. & Peskar, B. A. (Bernhard A. . *Radioimmunoassay in Basic and Clinical Pharmacology*. (Springer Berlin Heidelberg, 1987).

182. Livak, K. J. & Schmittgen, T. D. Analysis of relative gene expression data using real-time quantitative PCR and the 2-ΔΔCT method. *Methods* **25**, 402–408 (2001).

183. Obici, S., Feng, Z., Karkanias, G., Baskin, D. G. & Rossetti, L. Decreasing hypothalamic insulin receptors causes hyperphagia and insulin resistance in rats. *Nat. Neurosci.* **5**, 566–572 (2002).

184. Morton, G. J., Gelling, R. W., Niswender, K. D., Morrison, C. D., Rhodes, C. J. & Schwartz, M. W. Leptin regulates insulin sensitivity via phosphatidylinositol-3-OH kinase signaling in mediobasal hypothalamic neurons. *Cell Metab.* **2**, 411–420

(2005).

185. Burmeister, M. A., Ayala, J. E., Smouse, H., Landivar-Rocha, A., Brown, J. D., Drucker, D. J., Stoffers, D. A., Sandoval, D. A., Seeley, R. J. & Ayala, J. E. The Hypothalamic Glucagon-Like Peptide 1 Receptor Is Sufficient but Not Necessary for the Regulation of Energy Balance and Glucose Homeostasis in Mice. *Diabetes* **66**, 372–384 (2017).

186. Muse, E. D., Lam, T. K. T., Scherer, P. E. & Rossetti, L. Hypothalamic resistin induces hepatic insulin resistance. *J. Clin. Invest.* **117**, 1670–1678 (2007).

187. Bentsen, M. A., Mirzadeh, Z. & Schwartz, M. W. Revisiting How the Brain Senses Glucose—And Why. *Cell Metab.* **29**, 11–17 (2019).

188. Dalvi, P. S., Chalmers, J. A., Luo, V., Han, D. Y., Wellhauser, L., Liu, Y., Tran, D. Q., Castel, J., Luquet, S., Wheeler, M. B. & Belsham, D. D. High fat induces acute and chronic inflammation in the hypothalamus: Effect of high-fat diet, palmitate and TNF-α on appetite-regulating NPY neurons. *Int. J. Obes.* **41**, 149–158 (2017).

189. Camm, E. J., Tijsseling, D., Richter, H. G., Adler, A., Hansell, J. A., Derks, J. B., Cross, C. M. & Giussani, D. A. Oxidative Stress in the Developing Brain: Effects of Postnatal Glucocorticoid Therapy and Antioxidants in the Rat. *PLoS One* **6**, e21142 (2011).

190. You, J.-M., Yun, S.-J., Nam, K. N., Kang, C., Won, R. & Lee, E. H. Mechanism of glucocorticoid-induced oxidative stress in rat hippocampal slice cultures. *Can. J. Physiol. Pharmacol.* **87**, 440–447 (2009).

191. Henstridge, D. C., Whitham, M. & Febbraio, M. A. Chaperoning to the metabolic party: The emerging therapeutic role of heat-shock proteins in obesity and type 2 diabetes. *Mol. Metab.* **3**, 781–793 (2014).

192. Chung, J., Nguyen, A.-K., Henstridge, D. C., Holmes, A. G., Chan, M. H. S., Mesa, J. L., Lancaster, G. I., Southgate, R. J., Bruce, C. R., Duffy, S. J., Horvath, I., Mestril, R., Watt, M. J., Hooper, P. L., Kingwell, B. A., Vigh, L., Hevener, A. & Febbraio, M. A. HSP72 protects against obesity-induced insulin resistance. *Proc. Natl. Acad. Sci. U. S. A.* **105**, 1739–1744 (2008).

193. Morino, S., Kondo, T., Sasaki, K., Adachi, H., Suico, M. A., Sekimoto, E., Matsuda, T., Shuto, T., Araki, E. & Kai, H. Mild Electrical Stimulation with Heat Shock Ameliorates Insulin Resistance via Enhanced Insulin Signaling. *PLoS One* **3**, e4068 (2008).

194. Gupte, A. A., Bomhoff, G. L., Swerdlow, R. H. & Geiger, P. C. Heat treatment improves glucose tolerance and prevents skeletal muscle insulin resistance in rats fed a high-fat diet. *Diabetes* **58**, 567–578 (2009).

195. Kondo, T., Sasaki, K., Matsuyama, R., Morino-Koga, S., Adachi, H., Suico, M. A.,

Kawashima, J., Motoshima, H., Furukawa, N., Kai, H. & Araki, E. Hyperthermia with mild electrical stimulation protects pancreatic β-cells from cell stresses and apoptosis. *Diabetes* **61**, 838–847 (2012).

196. Drew, B. G., Ribas, V., Le, J. A., Henstridge, D. C., Phun, J., Zhou, Z., Soleymani, T., Daraei, P., Sitz, D., Vergnes, L., Wanagat, J., Reue, K., Febbraio, M. A. & Hevener, A. L. HSP72 is a mitochondrial stress sexnsor critical for Parkin action, oxidative metabolism, and insulin sensitivity in skeletal muscle. *Diabetes* **63**, 1488–1505 (2014).

197. Jing, E., Sundararajan, P., Majumdar, I. D., Hazarika, S., Fowler, S., Szeto, A., Gesta, S., Mendez, A. J., Vishnudas, V. K., Sarangarajan, R. & Narain, N. R. Hsp90β knockdown in DIO mice reverses insulin resistance and improves glucose tolerance. *Nutr. Metab. (Lond).* **15**, 1–11 (2018).

198. Lee, J.-H., Gao, J., Kosinski, P. A., Elliman, S. J., Hughes, T. E., Gromada, J. & Kemp, D. M. Heat shock protein 90 (HSP90) inhibitors activate the heat shock factor 1 (HSF1) stress response pathway and improve glucose regulation in diabetic mice. *Biochem. Biophys. Res. Commun.* **430**, 1109–1113 (2013).

199. Li, Q. & Barres, B. A. Microglia and macrophages in brain homeostasis and disease. *Nat. Rev. Immunol.* **18**, 225–242 (2018).

200. Thaler, J. P. *et al.* Obesity is associated with hypothalamic injury in rodents and humans. *J. Clin. Invest.* **122**, 153–162 (2012).

201. Kreutzer, C. *et al.* Hypothalamic Inflammation in Human Obesity Is Mediated by Environmental and Genetic Factors. *Diabetes* **66**, 2407–2415 (2017).

202. Douglass, J. D., Dorfman, M. D., Fasnacht, R., Shaffer, L. D. & Thaler, J. P. Astrocyte IKKβ/NF-κB signaling is required for diet-induced obesity and hypothalamic inflammation. *Mol. Metab.* **6**, 366–373 (2017).

203. Degasperi, G. R., Romanatto, T., Denis, R. G. P., Araújo, E. P., Moraes, J. C., Inada, N. M., Vercesi, A. E. & Velloso, L. A. UCP2 protects hypothalamic cells from TNF-α-induced damage. *FEBS Lett.* **582**, 3103–3110 (2008).

204. Benzler, J., Ganjam, G. K., Pretz, D., Oelkrug, R., Koch, C. E., Legler, K., Stöhr, S., Culmsee, C., Williams, L. M. & Tups, A. Central Inhibition of IKKβ/NF-κB Signaling Attenuates High-Fat Diet–Induced Obesity and Glucose Intolerance. *Diabetes* **64**, 2015–2027 (2015).

205. Zheng, J., Ali, A. & Ramirez, V. D. Steroids conjugated to bovine serum albumin as tools to demonstrate specific steroid neuronal membrane binding sites. *J. Psychiatry Neurosci.* **21**, 187–197 (1996).

206. Hassel, B., Iversen, E. G. & Fonnum, F. Neurotoxicity of albumin in vivo. *Neurosci. Lett.* **167**, 29–32 (1994).

207. Madalena, K. M. & Lerch, J. K. The Effect of Glucocorticoid and Glucocorticoid Receptor Interactions on Brain, Spinal Cord, and Glial Cell Plasticity. *Neural Plast.* **2017**, 1–8 (2017).

208. Gass, P., Schröder, H., Prior, P. & Kiessling, M. Constitutive expression of heat shock protein 90 (HSP90) in neurons of the rat brain. *Neurosci. Lett.* **182**, 188–192 (1994).

209. Hideaki, I., Yohtalou, T., Yoshinobu, E. & Riki, O. Localization of HSP90 in rat brain. *Int. J. Biochem.* **25**, 93–99 (1993).

210. Douglass, J. D., Dorfman, M. D. & Thaler, J. P. Glia: silent partners in energy homeostasis and obesity pathogenesis. *Diabetologia* **60**, 226–236 (2017).

211. Chari, M., Yang, C. S., Lam, C. K. L., Lee, K., Mighiu, P., Kokorovic, A., Cheung, G. W. C., Lai, T. Y. Y., Wang, P. Y. T. & Lam, T. K. T. Glucose transporter-1 in the hypothalamic glial cells mediates glucose sensing to regulate glucose production in vivo. *Diabetes* **60**, 1901–1906 (2011).

212. García-Cáceres, C. *et al.* Astrocytic Insulin Signaling Couples Brain Glucose Uptake with Nutrient Availability. *Cell* **166**, 867–880 (2016).

213. Paeger, L., Pippow, A., Hess, S., Paehler, M., Klein, A. C., Husch, A., Pouzat, C., Brüning, J. C. & Kloppenburg, P. Energy imbalance alters Ca2+ handling and excitability of POMC neurons. *Elife* **6**, e25641 (2017).

214. Moraes, J. C., Coope, A., Morari, J., Cintra, D. E., Roman, E. A., Pauli, J. R., Romanatto, T., Carvalheira, J. B., Oliveira, A. L. R., Saad, M. J. & Velloso, L. A. High-Fat Diet Induces Apoptosis of Hypothalamic Neurons. *PLoS One* **4**, e5045 (2009).

215. Bernal-Mizrachi, C., Xiaozhong, L., Yin, L., Knutsen, R. H., Howard, M. J., Arends, J. J. A., DeSantis, P., Coleman, T. & Semenkovich, C. F. An Afferent Vagal Nerve Pathway Links Hepatic PPARα Activation to Glucocorticoid-Induced Insulin Resistance and Hypertension. *Cell Metab.* **5**, 91–102 (2007).

216. King, A. J. F. The use of animal models in diabetes research. *Br. J. Pharmacol.* **166**, 877–894 (2012).

217. Birrenkott, G. P. & Wiggins, M. E. Determination of Dexamethasone and Corticosterone Half-Lives in Male Broilers. *Poult. Sci.* **63**, 1064–1068 (1984).

218. He, Y., Yi, W., Suino-Powell, K., Zhou, X. E., Tolbert, W. D., Tang, X., Yang, J., Yang, H., Shi, J., Hou, L., Jiang, H., Melcher, K. & Xu, H. E. Structures and mechanism for the design of highly potent glucocorticoids. *Cell Res.* **24**, 713–726 (2014).

219. Bledsoe, R. K., Montana, V. G., Stanley, T. B., Delves, C. J., Apolito, C. J., McKee,

D. D., Consler, T. G., Parks, D. J., Stewart, E. L., Willson, T. M., Lambert, M. H., Moore, J. T., Pearce, K. H. & Xu, H. E. Crystal Structure of the Glucocorticoid Receptor Ligand Binding Domain Reveals a Novel Mode of Receptor Dimerization and Coactivator Recognition. *Cell* **110**, 93–105 (2002).

220. Cirulli, F., van Oers, H., De Kloet, E. R. & Levine, S. Differential influence of corticosterone and dexamethasone on schedule-induced polydipsia in adrenalectomized rats. *Behav. Brain Res.* **65**, 33–39 (1994).

221. National Library of Medicine HSDB Database. MIFEPRISTONE. Available at: https://toxnet.nlm.nih.gov/cgi-bin/sis/search/a?dbs+hsdb:@term+@DOCNO+6841. (Accessed: 22nd July 2019)

222. Heikinheimo, O. Clinical Pharmacokinetics of Mifepristone. *Clin. Pharmacokinet.* **33**, 7–17 (1997).

223. Song, L.-N., Coghlan, M. & Gelmann, E. P. Antiandrogen Effects of Mifepristone on Coactivator and Corepressor Interactions with the Androgen Receptor. *Mol. Endocrinol.* **18**, 70–85 (2004).

224. Castinetti, F., Conte-Devolx, B. & Brue, T. Medical Treatment of Cushing's Syndrome: Glucocorticoid Receptor Antagonists and Mifepristone. *Neuroendocrinology* **92**, 125–130 (2010).

225. Olster, D. H. & Blaustein, J. D. Immunocytochemical colocalization of progestin receptors and β-endorphin or enkephalin in the hypothalamus of female guinea pigs. *J. Neurobiol.* **21**, 768–780 (1990).

226. Warembourg, M. Uptake of 3H labeled synthetic progestin by rat brain and pituitary. A radioautography study. *Neurosci. Lett.* **9**, 329–332 (1978).

227. Issar, M., Sahasranaman, S., Buchwald, P. & Hochhaus, G. Differences in the glucocorticoid to progesterone receptor selectivity of inhaled glucocorticoids. *Eur. Respir. J.* **27**, 511–516 (2006).

228. Carey, M., Kehlenbrink, S. & Hawkins, M. Evidence for central regulation of glucose metabolism. *J. Biol. Chem.* **288**, 34981–34988 (2013).

229. Kishore, P., Boucai, L., Zhang, K., Li, W., Koppaka, S., Kehlenbrink, S., Schiwek, A., Esterson, Y. B., Mehta, D., Bursheh, S., Su, Y., Gutierrez-Juarez, R., Muzumdar, R., Schwartz, G. J. & Hawkins, M. Activation of KATP channels suppresses glucose production in humans. *J. Clin. Invest.* **121**, 4916–4920 (2011).

230. Prigeon, R. L., Quddusi, S., Paty, B. & D'Alessio, D. A. Suppression of glucose production by GLP-1 independent of islet hormones: a novel extrapancreatic effect. *Am. J. Physiol. - Endocrinol. Metab.* **285**, E701–E707 (2003).

231. Brashier, D. B. S., Sharma, A., Dahiya, N., Singh, S. & Khadka, A. Lorcaserin: A

novel antiobesity drug. *J. Pharmacol. Pharmacother.* **5**, 175–178 (2014).

232. Buse, J. B., Nauck, M., Forst, T., Sheu, W. H.-H., Shenouda, S. K., Heilmann, C. R., Hoogwerf, B. J., Gao, A., Boardman, M. K., Fineman, M., Porter, L. & Schernthaner, G. Exenatide once weekly versus liraglutide once daily in patients with type 2 diabetes (DURATION-6): a randomised, open-label study. *Lancet (London, England)* **381**, 117–124 (2013).

233. Sisley, S., Gutierrez-Aguilar, R., Scott, M., D'Alessio, D. A., Sandoval, D. A. & Seeley, R. J. Neuronal GLP1R mediates liraglutide's anorectic but not glucose-lowering effect. *J. Clin. Invest.* **124**, 2456–2463 (2014).

234. Secher, A., Jelsing, J., Baquero, A. F., Hecksher-Sørensen, J., Cowley, M. A., Dalbøge, L. S., Hansen, G., Grove, K. L., Pyke, C., Raun, K., Schäffer, L., Tang-Christensen, M., Verma, S., Witgen, B. M., Vrang, N. & Knudsen, L. B. The arcuate nucleus mediates GLP-1 receptor agonist liraglutide-dependent weight loss. *J. Clin. Invest.* **124**, 4473–4488 (2014).

235. De Kloet, E. R., Vreugdenhil, E., Oitzl, M. S. & Joëls, M. Brain corticosteroid receptor balance in health and disease. *Endocr. Rev.* **19**, 269–301 (1998).

236. Popoli, M., Yan, Z., McEwen, B. S. & Sanacora, G. The stressed synapse: The impact of stress and glucocorticoids on glutamate transmission. *Nat. Rev. Neurosci.* **13**, 22–37 (2012).